# University of Alberta

Influence of lipids (arachidonic acid and cholesterol) on calcium signalling in rodent pancreatic beta cells

by

Valerie Yeung-Yam-Wah

A thesis submitted to the Faculty of Graduate Studies and Research
in partial fulfillment of the requirements for the degree of

Doctor of Philosophy

Centre for Neuroscience


Fall 2010
Edmonton, Alberta

## EXAMINING COMMITTEE

Amy Tse, Centre for Neuroscience and Department of Pharmacology, University of Alberta

William F. Colmers, Centre for Neuroscience and Department of Pharmacology

Elena Posse de Chaves, Department of Pharmacology

Edward Karpinski, Department of Physiology

Andrew P. Braun, Department of Physiology and Pharmacology, University of Calgary

# DEDICATION

For Mom, Dad, Nick, and Julia

And for Owen

## ABSTRACT

$Ca^{2+}$ is an important mediator of stimulus-secretion coupling in β cells of the pancreatic islets, which secrete insulin in response to elevation in plasma glucose concentration. I studied the actions of two lipids, arachidonic acid (AA) and cholesterol, on enzymatically-dissociated single β cells of rat and mouse, using cytosolic $Ca^{2+}$ ($[Ca^{2+}]_i$) measurement in conjunction with whole-cell patch-clamp techniques.

AA, which is produced in the β cell upon stimulation with either glucose or acetylcholine, was found to induce a large increase in $[Ca^{2+}]_i$ that was dependent on both extracellular $Ca^{2+}$ entry and intracellular $Ca^{2+}$ release. Part of the AA-mediated extracellular $Ca^{2+}$ entry was due to $Ca^{2+}$ influx through the arachidonate-regulated $Ca^{2+}$ (ARC) channels, which have not previously been reported in β cells. The AA-mediated intracellular $Ca^{2+}$ release was a result of $Ca^{2+}$ mobilization from multiple inositol trisphosphate ($IP_3$)-sensitive intracellular stores, including the endoplasmic reticulum (ER) and an acidic $Ca^{2+}$ store that is probably the secretory granules. Therefore, in β cells, the AA-mediated $Ca^{2+}$ signal may amplify the $[Ca^{2+}]_i$ rise induced by insulin secretagogues.

Cholesterol is an integral component of cellular membranes and an important regulator of cellular functions. However, elevation of cholesterol level in the pancreatic islets reduces glucose-stimulated insulin secretion. I found that cholesterol overload impairs the glucose-stimulated $[Ca^{2+}]_i$ increase in β cells by two major mechanisms: the first is a decrease in glucose-stimulated ATP production, which is partly mediated by a decrease in glucose uptake, and the

second is the reduction of voltage-gated $Ca^{2+}$ current density. These effects of cholesterol may partly account for the decreased insulin secretion that develops in patients with type II diabetes, who typically exhibit hypercholesterolemia.

In summary, different lipids may mediate beneficial or detrimental effects on $Ca^{2+}$ regulation in rodent pancreatic β cells.

# TABLE OF CONTENTS

**Chapter 3**

**Chapter 4**



**Chapter 5**

## LIST OF FIGURES

# LIST OF ABBREVIATIONS

| | |
|---|---|
| AA | arachidonic acid |
| ABCA1 | ATP-binding cassette transporter subfamily A member 1 |
| ACAT | acyl-coenzyme A: acyltransferase |
| ACh | acetylcholine |
| ACoA | arachidonyl coenzyme A |
| ADP | adenosine diphosphate |
| ADPR | adenosine diphosphoribose |
| AM | acetoxymethyl ester |
| 2-APB | 2-aminoethoxydiphenyl borate |
| ApoA-I | apolipoprotein A-I |
| ApoE | apolipoprotein E |
| ARC | arachidonate-regulated $Ca^{2+}$ (channel) |
| ATP | adenosine 5'-triphosphate |
| β-$NAD^+$ | β-nicotinamide adenine dinucleotide |
| BHQ | tert-butylhydroquinone |
| BSA | bovine serum albumin |
| $[Ca^{2+}]_i$ | intracellular $Ca^{2+}$ concentration |
| cADPR | cyclic adenosine diphosphoribose |
| cAMP | cyclic adenosine monophosphate |
| CCE | capacitative $Ca^{2+}$ entry |
| CICR | $Ca^{2+}$-induced $Ca^{2+}$ release |
| CPA | cyclopiazonic acid |
| CRAC | $Ca^{2+}$-release-activated $Ca^{2+}$ (current) |
| DAG | diacylglycerol |
| DMEM | Dulbecco's modified Eagles' medium |
| DNAse | deoxyribonuclease |
| EDTA | ethylenediaminetetraacetic acid |
| EET | epoxyeicosatrienoic acid |
| EGTA | ethylene glycol-bis(β-aminoethyl ether)-N,N,N',N'-tetraacetic acid |

| | |
|---|---|
| Epac | exchange proteins directly associated with cAMP |
| ER | endoplasmic reticulum |
| ETYA | eicosatetraynoic acid |
| FKBP | FK506-binding proteins |
| FRET | fluorescent resonance energy transfer |
| G-6-P | glucose-6-phosphate |
| GI | gastrointestinal |
| GIP | gastric inhibitory peptide |
| GLP-1 | glucagon-like peptide 1 |
| GLUT | glucose transporter |
| GPN | glycyl-phenylalanyl β-naphthylamide |
| GPR40 | G-protein-coupled receptor 40 |
| GTP | guanosine triphosphate |
| HBSS | Hank's balanced salt solution |
| HDL | high-density lipoprotein |
| HETE | hydroxyeicosatetraenoic acid |
| HMG CoA | 3-hydroxy-3-methyl-glutaryl coenzyme A |
| IAPP | islet amyloid polypeptide |
| $IP_3$ | inositol trisphosphate |
| $IP_3R$ | inositol trisphosphate receptor |
| IRS | insulin receptor substrate |
| $K_{ATP}$ | ATP-sensitive $K^+$ channel |
| KRB | bicarbonate-buffered solution |
| LDL | low-density lipoprotein |
| LXRβ | liver X receptor β |
| MAP | mitogen-activated protein |
| MβCD | methyl-β-cyclodextrin |
| NAADP | nicotinic acid adenine dinucleotide phosphate |
| 2-NBDG | 2-[*N*-(7-nitrobenz-2-oxa-1,3-diazol-4-yl)amino]-2-deoxy-d-glucose |
| NCX | $Na^+/Ca^{2+}$ exchanger |
| NMR | normal Ringer's solution |

| | |
|---|---|
| NPY | neuropeptide Y |
| NSF | N-ethylmaleimide-sensitive factor |
| OA | oleic acid |
| PACAP | pituitary adenylate-cyclase-activating peptide |
| PI3-kinase | phosphatidylinositol 3-kinase |
| $PIP_2$ | phosphatidylinositol 4,5-bisphosphate |
| PKA | protein kinase A |
| PKC | protein kinase C |
| $PLA_2$ | phospholipase $A_2$ |
| PLC | phospholipase C |
| PMCA | plasma membrance $Ca^{2+}$-ATPase |
| RyR | ryanodine receptor |
| SERCA | sarco/endoplasmic reticulum $Ca^{2+}$-ATPase |
| siRNA | small interfering RNA |
| SLCA2 | solute carrier family 2 |
| SNAP-25 | 25-kDa synaptosomal-associated protein |
| SNARE | soluble NSF attachment protein receptor |
| SOCE | store-operated $Ca^{2+}$ entry |
| SPCA | secretory pathway $Ca^{2+}$-ATPase |
| SREBP | sterol-regulatory-element binding protein |
| STIM | stromal interacting molecule |
| SUR | sulfonylurea |
| TEA | tetraethylammonium |
| TPC | two-pore channel |
| TRP | transient receptor potential |
| TRPM2 | transient receptor potential channel, melastatin subfamily type 2 |
| VAMP | vesicle-associated membrane protein |
| VGCC | voltage-gated $Ca^{2+}$ channel |
| VIP | vasoactive intestinal peptide |
| VLDL | very-low-density lipoprotein |
| VMH | ventromedial hypothalamus |

# Chapter 1

# General introduction

## 1.1 Pancreatic islet histology and physiology, and diabetes mellitus

The pancreas consists of two functionally and anatomically distinct parts: the exocrine pancreas, which produces digestive enzymes that are secreted into the duodenum via the pancreatic duct, and the endocrine pancreas, which produces a variety of endocrine factors that are secreted into the circulation. The endocrine pancreas is composed of the islets of Langerhans, which are named after the German pathologist Paul Langerhans, who discovered the structures in 1869. The islets, which are distributed throughout the endocrine pancreas, comprise a number of different cell types that secrete hormones that are essential for the regulation of glucose homeostasis in the body.

### *1.1.1 Types of pancreatic cells*

Three major different cell types have been reported in the mammalian pancreatic islets: the α cells, the β cells, and the δ cells. The β cells, which secrete insulin, make up the majority of the pancreatic islet mass (~67% in the rat (1) and ~53% in the human (2)). The immediate effect of insulin is to lower the level of plasma glucose. Its mechanisms of action are discussed in further detail in Section 1.1.4. Islet amyloid polypeptide (IAPP; also known as amylin) and C-peptide are co-secreted with insulin from β cells. IAPP, which reduces food intake, delays gastric emptying, and suppresses glucagon secretion, is used therapeutically as an anti-diabetic agent to reduce postprandial glucose load (3). However, negative effects of IAPP on diabetes have also been reported. A study of IAPP knockout mice showed that IAPP may have a negative feedback effect on

insulin secretion (4). Accumulation of IAPP oligomers in islets was shown to cause formation of fibrils, which are thought to be a pathological feature of type II diabetes (5). C-peptide, which is a byproduct of insulin synthesis, is shown to increase glucose uptake in muscle, as well as to regulate activity of $Na^+/K^+$-ATPase (which is downregulated in diabetes) (6). The α cells secrete glucagon and make up ~24% of the islet cells in the rat and ~39% in humans (1;2). Glucagon, like insulin, is involved in regulation of plasma glucose, but its actions are opposite to those of insulin: it stimulates release of glucose from the liver, by facilitating glycogenolysis and gluconeogenesis. The somatostatin-secreting δ cells make up ~6% of the islet cells in the rat and ~10% in humans (1;2). Somatostatin is generally an inhibitory hormone (for example, it inhibits secretion of hormones from the gastrointestinal tract and the exocrine pancreas), though the primary function of somatostatin secreted from islet cells is the local inhibition of β cells and α cells (7;8).

### *1.1.2 Non-glucose factors that influence the secretion of islet hormones*

While secretion of insulin and glucagon are primarily regulated by changes in plasma glucose concentration, they can also be modulated by other factors, including neurotransmitters and peptides released from parasympathetic and sympathetic nerves, amino acids, and hormones secreted in a paracrine, autocrine, or endocrine manner.

The pancreas receives innervation from the autonomic nervous system, including both parasympathetic and sympathetic fibres, which are under the

control of the ventromedial hypothalamus (VMH). It has been shown in humans, as well as in other mammals, that stimulation of vagus nerve results in lowering of plasma glucose level (9). Parasympathetic nerves secrete a number of neurotransmitters, including acetylcholine (ACh), which stimulates the β cells directly via $M_3$ muscarinic receptors. These nerve endings also release a number of peptides that have been shown to stimulate insulin secretion, including vasoactive intestinal peptide (VIP) (10) and pituitary adenylate cyclase activating peptide (PACAP) (11). On the other hand, electrical stimulation of the splanchnic nerve triggers noradrenaline release and results in inhibition of insulin secretion (12). This inhibitory effect is mediated directly, via stimulation of the α-adrenoceptors on β cells, and also indirectly, via stimulation of glucagon secretion from α cells. In addition, the sympathetic terminals release neuropeptide Y (NPY), which suppresses glucose-stimulated insulin secretion (13).

Amino acids have also been shown to promote glucose-stimulated insulin secretion, possibly via metabolism and ATP production. Arginine, a cationic amino acid, can cause membrane depolarization in β cells, which in turn activates voltage-gated $Ca^{2+}$ channels, (VGCCs) and triggers insulin secretion (14).

The hormones secreted by islet cells can modulate secretion of other islet hormones in a paracrine fashion. For example, insulin suppresses the secretion of glucagon, while glucagon downregulates the secretion of insulin and somatostatin (15), and IAPP inhibits secretion of glucagon and somatostatin (8). Insulin and IAPP can also act in an autocrine fashion: insulin secretion is stimulated by insulin (16), but inhibited by IAPP (8). Secretion of insulin and glucagon can also

be regulated in an endocrine fashion by gastrointestinal (GI) hormones, including gastrin, glucagon-like-peptide 1 (GLP-1), and gastric inhibitory peptide (GIP). GLP-1 and GIP are secreted by cells in the GI tract in response to nutrient ingestion. These incretin hormones can stimulate insulin secretion and inhibit glucagon secretion via specific G-protein-coupled-receptors. For example, GLP-1 acts through the GLP-1 receptor that is coupled to $G_s$. Thus, binding of GLP-1 results in activation of adenylate cyclase and formation of cyclic adenosine monophosphate (cAMP), which in turn activates protein kinase A (PKA)- and exchange proteins directly associated with cAMP (Epac)-mediated signal transduction pathways (17). In insulin-secreting cells, GLP-1 has been found to inhibit ATP-sensitive $K^+$ ($K_{ATP}$) channels (18) and to stimulate $Ca^{2+}$ release from endoplasmic reticulum (ER) (19;20).

### *1.1.3 Stimulation of insulin secretion by glucose*

The major mechanism by which glucose triggers insulin release from β cells (the $K_{ATP}$-dependent pathway) is well-characterized (Figure 1-1, page 13). An increase in plasma glucose concentration, such as that following a meal, can initiate insulin secretion. The elevation in plasma glucose increases the rate of uptake by the glucose transporter, resulting in greater transport of glucose into the β cell. The glucose transporter (GLUT) family consists of at least 14 members, of which the best-studied members are GLUT1, GLUT2, GLUT3, GLUT4, and GLUT5. The GLUT family is also known as the solute carrier family 2 (SLCA2), and its members are responsible for facilitated diffusion of hexoses. The various

isoforms differ in both their affinity for hexoses and their tissue distribution. GLUT2 is the most important isoform in the context of insulin secretion, since rat β cells (21;22) and human islets (23) express primarily GLUT2. Glucose-stimulated insulin secretion in islets from GLUT2-null mice (which show no change in glucokinase expression) was drastically reduced, indicating that GLUT2 is crucial for insulin secretion (24). GLUT2, which is constitutively expressed on the cell surface (25;26), is a specialized glucose transporter, due to its high Michaelis-Menten constant ($K_m$; which reflects the inverse of the affinity for substrate) for glucose (15-20 mM). GLUT2 thus has a low affinity for glucose, and the rate of glucose uptake through this transporter is proportional to plasma glucose concentration. In contrast to GLUT2, other GLUT isoforms (such as GLUT1 and GLUT4) have a high affinity for glucose (with a $K_m$ of 2-10 mM), and thus are saturated even at low glucose concentrations (27). When glucose is transported into the cell, it undergoes glycolysis. The rate-limiting step in glycolysis is the first step, which involves the phosphorylation of glucose by glucokinase, to yield glucose-6-phosphate (G-6-P). Glucokinase (also known as type IV hexokinase) is a member of the hexokinase family and has a high $K_m$ (low affinity) for glucose (15-20 mM). Thus, when plasma glucose is high (>5 mM), glucose is phosphorylated by glucokinase, and when plasma glucose is low (<5 mM), there is little phosphorylation of glucose. β cells have low expression levels of the high-affinity hexokinase isoforms (types I, II, and III). After phosphorylation of glucose by glucokinase, glucose-6-phosphate undergoes a number of steps to yield pyruvate. Pyruvate is then converted to acetyl-CoA,

which enters the citric acid cycle that fuels mitochondrial ATP production. The increase in cytosolic ATP/ADP ratio then inhibits $K_{ATP}$ channels (28). The $K_{ATP}$ channel is found in β cells from all species, including humans, and in all insulin-secreting cell lines. This channel is an inward rectifier that is open at resting membrane potential (about -70mV in the β cell) and is crucial in coupling cell metabolism to membrane excitability. The $K_{ATP}$ channel is made up of two different types of subunits, the Kir6.2 subunit and the sulfonylurea (SUR) subunit. The $K_{ATP}$ channel is an octameric complex, with each Kir subunit (four make up the pore of the channel) being associated with one SUR subunit (29). Regulation of channel activity is complex and depends on a balance between inhibition by ATP at the Kir subunit and stimulation by Mg-ADP at the SUR subunit (30). Upon stimulation of the β cell by glucose, the elevation in cytosolic ATP/ADP ratio causes the closure of $K_{ATP}$ channels, resulting in membrane depolarization and activation of VGCCs. An increase in intracellular $Ca^{2+}$ concentration ($[Ca^{2+}]_i$) due to VGCC-mediated extracellular $Ca^{2+}$ entry in turn triggers the exocytosis of insulin-containing dense-core secretory granules.

In addition to the triggering of the $K_{ATP}$-dependent pathway described above, an amplifying $K_{ATP}$-independent pathway has also been implicated in the action of glucose and other insulin secretagogues (31). Various second messengers have been postulated to be involved in the amplifying pathway, including PKA and protein kinase C (PKC), and multiple cellular targets have been implicated. For instance, PKA has been shown to enhance voltage-gated $Ca^{2+}$ current in β cells

(32), while both PKA and PKC have been shown to increase the size of the readily releasable pool of insulin granules (33).

### *1.1.4 Physiological actions of insulin*

There are multiple actions of insulin in the body, though its immediate effect is to lower plasma glucose concentration. Insulin acts on muscle, liver, and adipose tissue, to promote glucose uptake (through facilitative GLUTs), storage, and utilization (via glycogen synthesis and glucose oxidation). Insulin also upregulates triglyceride synthesis in adipocytes, and protein synthesis in muscle cells. Other than its effects on nutrient metabolism, insulin is known to act as a potent growth factor (34) and an activator of nitric oxide synthase (35). The actions of insulin are mediated by plasma membrane insulin receptors. Insulin receptors are expressed to some degree in all cells, but are very highly expressed in muscle, liver, and adipose cells. Upon binding of insulin molecules, insulin receptors, which have intrinsic tyrosine kinase activity, first transphosphorylate and then phosphorylate a number of downstream effectors. For example, in muscle, the insulin receptor substrate 1 (IRS-1) is the major mediator of insulin's effects on glucose metabolism. Phosphorylation of tyrosine residues on IRS-1 induces association with (and thus activation of) phosphatidylinositol (PI)-3 kinase, leading to the stimulation of glucose transport, including the translocation of GLUT4 from intracellular compartments to the plasma membrane (36). On the other hand, the growth- and proliferation- promoting effects of insulin are

mediated by the mitogen-activated protein (MAP) kinase pathway in vascular smooth muscle cells (34).

### *1.1.5 Diabetes mellitus*

Diabetes mellitus is characterized by the elevation of plasma glucose (hyperglycemia) and is classified as either type I or type II. Type I diabetes, which accounts for ~10% of all cases of diabetes, is associated with selective autoimmune destruction of the β cells, which leads to a deficit in insulin secretion. Type II diabetes, on the other hand is characterized by both the development of peripheral resistance to insulin and the reduction in the ability of glucose to stimulate insulin secretion. In the early phase of the disease, insulin receptors in myocytes, hepatocytes and adipocytes become less sensitive to insulin stimulation, resulting in a reduction in glucose uptake and elevation of plasma glucose level. Genetic and environmental factors, as well as obesity, can contribute to the development of insulin resistance. In response to the decreased tissue sensitivity to insulin, the pancreatic islets compensate by increasing insulin secretion. Initially, there is an expansion of β cell mass (37) and enhancement of β cell sensitivity to glucose (38). When insulin secretion fails to meet its demand, the persistent elevation of plasma glucose (glucotoxicity) leads to β cell dysfunction and destruction. In patients with type 2 diabetes, the islets display a number of functional defects, including reduction in mRNA expression of GLUT2 and glucokinase, increase in oxidative stress, reduction of glucose-stimulated insulin secretion (23) and decrease in β cell mass (39).

## 1.2 Importance of lipids in β cell function

In addition to glucose and amino acids, the level of free fatty acids also influences insulin secretion from β cells. For example, acute stimulation of β cells with a low concentration of palmitate, the most abundant saturated fatty acid in plasma, was shown to increase voltage-gated $Ca^{2+}$ current, as well as the size of the readily releasable pool of insulin granules (40). Some of the stimulatory actions of fatty acids may be mediated by GPR40, a G-protein-coupled receptor which is expressed on β cells and is activated by fatty acids such as oleate, palmitate and arachidonic acid (AA) (41). AA has been suggested to be an important second messenger in the $K_{ATP}$-independent amplifying pathway during glucose stimulation. AA can trigger $[Ca^{2+}]_i$ rise and insulin secretion even in the presence of a substimulatory glucose concentration (42-44). Furthermore, AA accumulates in islets upon stimulation with either glucose (45) or ACh (46), and inhibitors of phospholipase $A_2$ ($PLA_2$) suppress glucose-stimulated insulin secretion in rat (47;48) and human (49) islets. These observations are consistent with the notion that AA may be an important modulator of insulin secretion.

While some lipids may have important role in cellular signalling in β cells, chronic elevation of fatty acids is detrimental to β cell function. The dysfunction of β cells and reduction in β cell mass that characterize type II diabetes are often accompanied by dyslipidemia: in humans, the major changes that occur are hypertriglyceridemia, a decrease in high-density lipoprotein (HDL) cholesterol in plasma, and alterations in low-density lipoprotein (LDL) metabolism (50). Although the elevation in plasma triglycerides is thought to contribute to the

development of β cell dysfunction and to cell death (51), the impact of the changes in HDL and LDL cholesterol on glucose-stimulated insulin secretion is unclear. The alterations in both HDLs and LDLs could contribute to elevation of cellular cholesterol in diabetes. HDLs are thought to play a protective role in terms of cellular cholesterol, because they mediate reverse cholesterol transport (transport of cholesterol from tissues to the liver, where it is packaged for excretion). On the other hand, the primary function of LDLs is to transport cholesterol into the tissues: LDLs are taken up by cells via LDL receptors on the cell surface, and their cholesterol is stored in intracellular pools. Incubation of human and mouse islets with high concentrations of LDLs led to a decrease in glucose-stimulated insulin secretion, and the observed effects were dependent on LDL receptor, suggesting that cholesterol derived from LDLs may be responsible for the adverse effects (52). Thus, changes in LDL metabolism that occur in diabetes may lead to cholesterol-mediated β cell dysfunction.

### 1.3 Objectives of my thesis

The role of lipids in β cell function is complex. Whether a specific lipid is beneficial or detrimental to the β cell depends on the type of lipid and the duration of exposure. This thesis examines the roles of two lipids, AA and cholesterol, in the cellular signaling of rodent pancreatic β cells. As described above, AA has been shown to trigger a rise in $[Ca^{2+}]_i$ even at basal glucose concentrations (42), suggesting that it may have an important role in the $Ca^{2+}$ signalling of β cells. Part of the AA-mediated $Ca^{2+}$ signal is dependent on extracellular $Ca^{2+}$ influx

(44), but the mechanism of $Ca^{2+}$ entry is not completely understood. Project 1 of my thesis is a study on the mechanism underlying the AA-mediated extracellular $Ca^{2+}$ entry in rat pancreatic β cells (Chapter 3).

In addition to the triggering of extracellular $Ca^{2+}$ influx, AA causes release of $Ca^{2+}$ from intracellular stores (42;53;54). AA-mediated $Ca^{2+}$ signals have been reported to be mediated by ryanodine receptors (55) and to be dependent on $Ca^{2+}$ release from ER (43). However, β cells contain multiple intracellular stores, including the inositol trisphosphate ($IP_3$)-sensitive store, the ryanodine-sensitive stores, the mitochondria, and stores that are associated with acidic organelles. Project 2 of my thesis describes the contribution of different intracellular $Ca^{2+}$ stores to the AA-induced intracellular $Ca^{2+}$ release (Chapter 4).

Cholesterol homeostasis in cells is tightly regulated and is under the control of a complex network. Disrupting any component of that network can lead to drastic changes in cellular cholesterol levels, and this in turn can cause changes in cellular function. In whole animals, transgenic mice have demonstrated the importance of cholesterol in the maintenance of normal insulin secretion. For example, pancreatic islets from mice deficient in apolipoprotein E (apoE) showed elevated cholesterol and reduced glucose-stimulated insulin secretion (56). ApoE is a constituent of chylomicrons, very-low-density lipoproteins (VLDLs), and HDLs, and it binds to LDL receptors on peripheral cells. In islets and insulin-secreting cell lines, lowering cellular cholesterol from the normal level has variable effects on insulin secretion (56-60). However, elevation of cellular cholesterol in insulin-secreting cell lines has been shown to impair glucose-

induced insulin secretion (56;59). Thus, the actions of cholesterol on glucose-stimulated insulin secretion are complex, and cholesterol may affect multiple steps in the stimulus-secretion pathway. Project 3 of my thesis describes the multiple effects of short-term cholesterol elevations in single mouse β cells (Chapter 5). Some of these mechanisms may underlie the impairment of glucose-stimulated insulin secretion mediated by high levels of cholesterol.

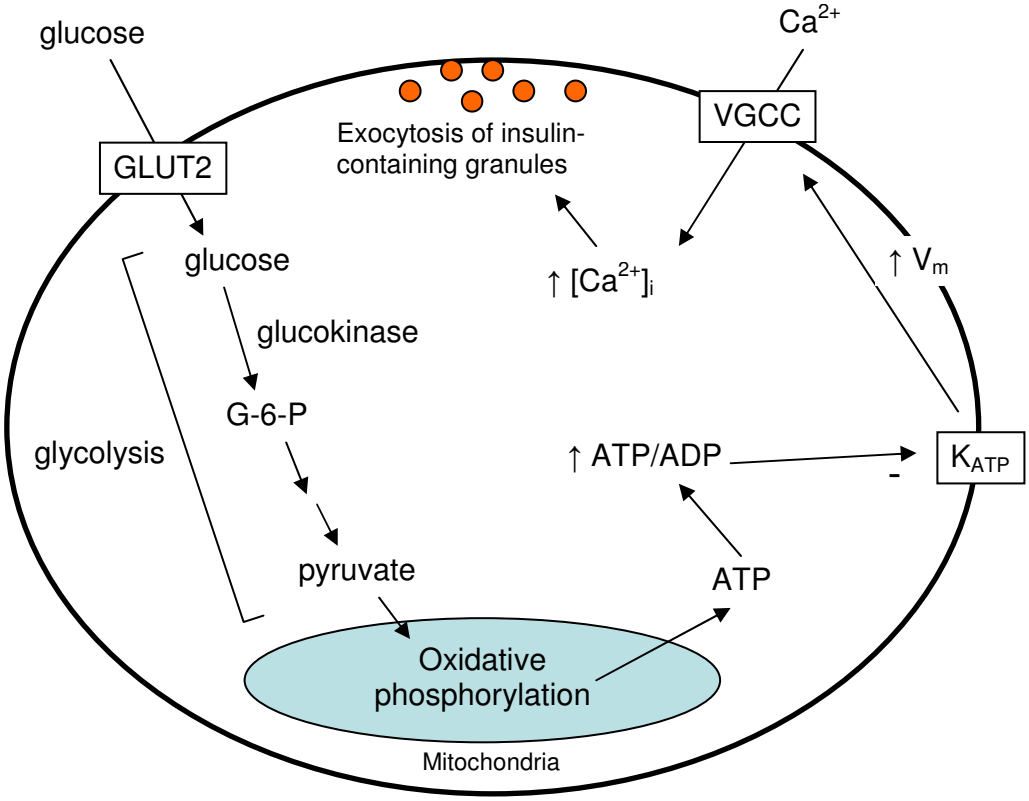


**Figure 1-1**: Major pathways of glucose-stimulated insulin secretion. Glucose uptake into the β cell is mediated via GLUT2. Glucose then undergoes glycolysis, resulting in mitochondrial ATP production. The increase in cytosolic ATP/ADP ratio then closes $K_{ATP}$ channels, resulting in depolarization, VGCC activation and triggering of exocytosis.

## References


1. Pipeleers,DG, Pipeleers-Marichal,MA: A method for the purification of single A, B and D cells and for the isolation of coupled cells from isolated rat islets. *Diabetologia* 20:654-663, 1981
2. Cabrera,O, Berman,DM, Kenyon,NS, Ricordi,C, Berggren,PO, Caicedo,A: The unique cytoarchitecture of human pancreatic islets has implications for islet cell function. *Proc Natl Acad Sci U S A* 103:2334-2339, 2006
3. Ryan,GJ, Jobe,LJ, Martin,R: Pramlintide in the treatment of type 1 and type 2 diabetes mellitus. *Clin Ther* 27:1500-1512, 2005
4. Gebre-Medhin,S, Mulder,H, Pekny,M, Westermark,G, Tornell,J, Westermark,P, Sundler,F, Ahren,B, Betsholtz,C: Increased insulin secretion and glucose tolerance in mice lacking islet amyloid polypeptide (amylin). *Biochem Biophys Res Commun* 250:271-277, 1998
5. Marzban,L, Park,K, Verchere,CB: Islet amyloid polypeptide and type 2 diabetes. *Exp Gerontol* 38:347-351, 2003
6. Hills,CE, Brunskill,NJ: Cellular and physiological effects of C-peptide. *Clin Sci (Lond)* 116:565-574, 2009
7. Kanno,T, Gopel,SO, Rorsman,P, Wakui,M: Cellular function in multicellular system for hormone-secretion: electrophysiological aspect of studies on alpha-, beta- and delta-cells of the pancreatic islet. *Neurosci Res* 42:79-90, 2002
8. Wang,F, Adrian,TE, Westermark,GT, Ding,X, Gasslander,T, Permert,J: Islet amyloid polypeptide tonally inhibits beta-, alpha-, and delta-cell secretion in isolated rat pancreatic islets. *Am J Physiol* 276:E19-E24, 1999
9. Ahren,B: Autonomic regulation of islet hormone secretion--implications for health and disease. *Diabetologia* 43:393-410, 2000
10. Havel,PJ, Dunning,BE, Verchere,CB, Baskin,DG, O'Dorisio,T, Taborsky,GJ, Jr.: Evidence that vasoactive intestinal polypeptide is a parasympathetic neurotransmitter in the endocrine pancreas in dogs. *Regul Pept* 71:163-170, 1997
11. Filipsson,K, Sundler,F, Ahren,B: PACAP is an islet neuropeptide which contributes to glucose-stimulated insulin secretion. *Biochem Biophys Res Commun* 256:664-667, 1999
12. Kurose,T, Seino,Y, Nishi,S, Tsuji,K, Taminato,T, Tsuda,K, Imura,H: Mechanism of sympathetic neural regulation of insulin, somatostatin, and glucagon secretion. *Am J Physiol* 258:E220-E227, 1990
13. Skoglund,G, Gross,R, Ahren,B, Loubatieres-Mariani,MM: Different mechanisms are involved in neuropeptide Y-induced pancreatic vasoconstriction and inhibition of insulin secretion. *Eur J Pharmacol* 236:69-74, 1993
14. Sener,A, Best,LC, Yates,AP, Kadiata,MM, Olivares,E, Louchami,K, Jijakli,H, Ladriere,L, Malaisse,WJ: Stimulus-secretion coupling of arginine-induced insulin release: comparison between the cationic amino acid and its methyl ester. *Endocrine* 13:329-340, 2000
15. Brunicardi,FC, Kleinman,R, Moldovan,S, Nguyen,TH, Watt,PC, Walsh,J, Gingerich,R: Immunoneutralization of somatostatin, insulin, and glucagon causes alterations in islet cell secretion in the isolated perfused human pancreas. *Pancreas* 23:302-308, 2001
16. Aspinwall,CA, Lakey,JR, Kennedy,RT: Insulin-stimulated insulin secretion in single pancreatic beta cells. *J Biol Chem* 274:6360-6365, 1999
17. Doyle,ME, Egan,JM: Mechanisms of action of glucagon-like peptide 1 in the pancreas. *Pharmacol Ther* 113:546-593, 2007

18. Light,PE, Manning Fox,JE, Riedel,MJ, Wheeler,MB: Glucagon-like peptide-1 inhibits pancreatic ATP-sensitive potassium channels via a protein kinase A- and ADP-dependent mechanism. *Mol Endocrinol* 16:2135-2144, 2002
19. Tsuboi,T, da,S, X, Holz,GG, Jouaville,LS, Thomas,AP, Rutter,GA: Glucagon-like peptide-1 mobilizes intracellular Ca2+ and stimulates mitochondrial ATP synthesis in pancreatic MIN6 beta-cells. *Biochem J* 369:287-299, 2003
20. Kang,G, Joseph,JW, Chepurny,OG, Monaco,M, Wheeler,MB, Bos,JL, Schwede,F, Genieser,HG, Holz,GG: Epac-selective cAMP analog 8-pCPT-2'-O-Me-cAMP as a stimulus for Ca2+-induced Ca2+ release and exocytosis in pancreatic beta-cells. *J Biol Chem* 278:8279-8285, 2003
21. Heimberg,H, De,VA, Pipeleers,D, Thorens,B, Schuit,F: Differences in glucose transporter gene expression between rat pancreatic alpha- and beta-cells are correlated to differences in glucose transport but not in glucose utilization. *J Biol Chem* 270:8971-8975, 1995
22. Sato,Y, Ito,T, Udaka,N, Kanisawa,M, Noguchi,Y, Cushman,SW, Satoh,S: Immunohistochemical localization of facilitated-diffusion glucose transporters in rat pancreatic islets. *Tissue Cell* 28:637-643, 1996
23. Del,GS, Lupi,R, Marselli,L, Masini,M, Bugliani,M, Sbrana,S, Torri,S, Pollera,M, Boggi,U, Mosca,F, Del,PS, Marchetti,P: Functional and molecular defects of pancreatic islets in human type 2 diabetes. *Diabetes* 54:727-735, 2005
24. Guillam,MT, Dupraz,P, Thorens,B: Glucose uptake, utilization, and signaling in GLUT2-null islets. *Diabetes* 49:1485-1491, 2000
25. Thorens,B, Gerard,N, Deriaz,N: GLUT2 surface expression and intracellular transport via the constitutive pathway in pancreatic beta cells and insulinoma: evidence for a block in trans-Golgi network exit by brefeldin A. *J Cell Biol* 123:1687-1694, 1993
26. Hou,JC, Williams,D, Vicogne,J, Pessin,JE: The glucose transporter 2 undergoes plasma membrane endocytosis and lysosomal degradation in a secretagogue-dependent manner. *Endocrinology* 150:4056-4064, 2009
27. Kahn,BB: Facilitative glucose transporters: regulatory mechanisms and dysregulation in diabetes. *J Clin Invest* 89:1367-1374, 1992
28. Ashcroft,FM, Harrison,DE, Ashcroft,SJ: Glucose induces closure of single potassium channels in isolated rat pancreatic beta-cells. *Nature* 312:446-448, 1984
29. Clement,JP, Kunjilwar,K, Gonzalez,G, Schwanstecher,M, Panten,U, Aguilar-Bryan,L, Bryan,J: Association and stoichiometry of K(ATP) channel subunits. *Neuron* 18:827-838, 1997
30. Hopkins,WF, Fatherazi,S, Peter-Riesch,B, Corkey,BE, Cook,DL: Two sites for adenine-nucleotide regulation of ATP-sensitive potassium channels in mouse pancreatic beta-cells and HIT cells. *J Membr Biol* 129:287-295, 1992
31. Henquin,JC: Pathways in beta-cell stimulus-secretion coupling as targets for therapeutic insulin secretagogues. *Diabetes* 53 Suppl 3:S48-S58, 2004
32. Ammala,C, Ashcroft,FM, Rorsman,P: Calcium-independent potentiation of insulin release by cyclic AMP in single beta-cells. *Nature* 363:356-358, 1993
33. Wan,QF, Dong,Y, Yang,H, Lou,X, Ding,J, Xu,T: Protein kinase activation increases insulin secretion by sensitizing the secretory machinery to Ca2+. *J Gen Physiol* 124:653-662, 2004
34. Wang,CC, Goalstone,ML, Draznin,B: Molecular mechanisms of insulin resistance that impact cardiovascular biology. *Diabetes* 53:2735-2740, 2004
35. Scherrer,U, Randin,D, Vollenweider,P, Vollenweider,L, Nicod,P: Nitric oxide release accounts for insulin's vascular effects in humans. *J Clin Invest* 94:2511-2515, 1994

36. Pessin,JE, Saltiel,AR: Signaling pathways in insulin action: molecular targets of insulin resistance. *J Clin Invest* 106:165-169, 2000
37. Butler,AE, Janson,J, Bonner-Weir,S, Ritzel,R, Rizza,RA, Butler,PC: Beta-cell deficit and increased beta-cell apoptosis in humans with type 2 diabetes. *Diabetes* 52:102-110, 2003
38. Polonsky,KS: Dynamics of insulin secretion in obesity and diabetes. *Int J Obes Relat Metab Disord* 24 Suppl 2:S29-S31, 2000
39. Marchetti,P, Dotta,F, Lauro,D, Purrello,F: An overview of pancreatic beta-cell defects in human type 2 diabetes: implications for treatment. *Regul Pept* 146:4-11, 2008
40. Olofsson,CS, Salehi,A, Holm,C, Rorsman,P: Palmitate increases L-type Ca2+ currents and the size of the readily releasable granule pool in mouse pancreatic beta-cells. *J Physiol* 557:935-948, 2004
41. Itoh,Y, Kawamata,Y, Harada,M, Kobayashi,M, Fujii,R, Fukusumi,S, Ogi,K, Hosoya,M, Tanaka,Y, Uejima,H, Tanaka,H, Maruyama,M, Satoh,R, Okubo,S, Kizawa,H, Komatsu,H, Matsumura,F, Noguchi,Y, Shinohara,T, Hinuma,S, Fujisawa,Y, Fujino,M: Free fatty acids regulate insulin secretion from pancreatic beta cells through GPR40. *Nature* 422:173-176, 2003
42. Band,AM, Jones,PM, Howell,SL: Arachidonic acid-induced insulin secretion from rat islets of Langerhans. *J Mol Endocrinol* 8:95-101, 1992
43. Woolcott,OO, Gustafsson,AJ, Dzabic,M, Pierro,C, Tedeschi,P, Sandgren,J, Bari,MR, Nguyen,KH, Bianchi,M, Rakonjac,M, Radmark,O, Ostenson,CG, Islam,MS: Arachidonic acid is a physiological activator of the ryanodine receptor in pancreatic beta-cells. *Cell Calcium* 39:529-537, 2006
44. Ramanadham,S, Gross,R, Turk,J: Arachidonic acid induces an increase in the cytosolic calcium concentration in single pancreatic islet beta cells. *Biochem Biophys Res Commun* 184:647-653, 1992
45. Wolf,BA, Pasquale,SM, Turk,J: Free fatty acid accumulation in secretagogue-stimulated pancreatic islets and effects of arachidonate on depolarization-induced insulin secretion. *Biochemistry* 30:6372-6379, 1991
46. Konrad,RJ, Jolly,YC, Major,C, Wolf,BA: Carbachol stimulation of phospholipase A2 and insulin secretion in pancreatic islets. *Biochem J* 287 ( Pt 1):283-290, 1992
47. Konrad,RJ, Jolly,YC, Major,C, Wolf,BA: Inhibition of phospholipase A2 and insulin secretion in pancreatic islets. *Biochim Biophys Acta* 1135:215-220, 1992
48. Loweth,AC, Scarpello,JH, Morgan,NG: A specific inhibitor of cytosolic phospholipase A2 activity, AACOCF3, inhibits glucose-induced insulin secretion from isolated rat islets. *Biochem Biophys Res Commun* 218:423-427, 1996
49. Persaud,SJ, Muller,D, Belin,VD, Kitsou-Mylona,I, Asare-Anane,H, Papadimitriou,A, Burns,CJ, Huang,GC, Amiel,SA, Jones,PM: The role of arachidonic acid and its metabolites in insulin secretion from human islets of langerhans. *Diabetes* 56:197-203, 2007
50. Howard,BV: Insulin resistance and lipid metabolism. *Am J Cardiol* 84:28J-32J, 1999
51. Cnop,M: Fatty acids and glucolipotoxicity in the pathogenesis of Type 2 diabetes. *Biochem Soc Trans* 36:348-352, 2008
52. Rutti,S, Ehses,JA, Sibler,RA, Prazak,R, Rohrer,L, Georgopoulos,S, Meier,DT, Niclauss,N, Berney,T, Donath,MY, von,EA: Low- and high-density lipoproteins modulate function, apoptosis, and proliferation of primary human and murine pancreatic beta-cells. *Endocrinology* 150:4521-4530, 2009
53. Metz,SA, Draznin,B, Sussman,KE, Leitner,JW: Unmasking of arachidonate-induced insulin release by removal of extracellular calcium. Arachidonic acid

mobilizes cellular calcium in rat islets of Langerhans. *Biochem Biophys Res Commun* 142:251-258, 1987
54. Metz,SA: Exogenous arachidonic acid promotes insulin release from intact or permeabilized rat islets by dual mechanisms. Putative activation of Ca2+ mobilization and protein kinase C. *Diabetes* 37:1453-1469, 1988
55. Woolcott,OO, Gustafsson,AJ, Dzabic,M, Pierro,C, Tedeschi,P, Sandgren,J, Bari,MR, Nguyen,KH, Bianchi,M, Rakonjac,M, Radmark,O, Ostenson,CG, Islam,MS: Arachidonic acid is a physiological activator of the ryanodine receptor in pancreatic beta-cells. *Cell Calcium* 39:529-537, 2006
56. Hao,M, Head,WS, Gunawardana,SC, Hasty,AH, Piston,DW: Direct effect of cholesterol on insulin secretion: a novel mechanism for pancreatic beta-cell dysfunction. *Diabetes* 56:2328-2338, 2007
57. Xia,F, Xie,L, Mihic,A, Gao,X, Chen,Y, Gaisano,HY, Tsushima,RG: Inhibition of cholesterol biosynthesis impairs insulin secretion and voltage-gated calcium channel function in pancreatic beta-cells. *Endocrinology* 149:5136-5145, 2008
58. Xia,F, Gao,X, Kwan,E, Lam,PP, Chan,L, Sy,K, Sheu,L, Wheeler,MB, Gaisano,HY, Tsushima,RG: Disruption of pancreatic beta-cell lipid rafts modifies Kv2.1 channel gating and insulin exocytosis. *J Biol Chem* 279:24685-24691, 2004
59. Hao,M, Bogan,JS: Cholesterol regulates glucose-stimulated insulin secretion through phosphatidylinositol 4,5-bisphosphate. *J Biol Chem* 284:29489-29498, 2009
60. Vikman,J, Jimenez-Feltstrom,J, Nyman,P, Thelin,J, Eliasson,L: Insulin secretion is highly sensitive to desorption of plasma membrane cholesterol. *FASEB J* 23:58-67, 2009

# Chapter 2

# Materials and methods

## 2.1 Animals

Male Sprague-Dawley rats (8-10 weeks) were obtained from the Bioscience Animal facility at the University of Alberta. Male apolipoprotein E (apoE)-deficient mice (*ApoE*$^{-/-}$) and their wild-type background controls (C57BL/6J) (10-14 weeks old) were purchased from Jackson Laboratory (Bar Harbor, ME, USA). All rats and mice were housed and treated according to the standards set by the Canadian Council on Animal Care. All procedures received prior approval from the Health Sciences Animal Policy and Welfare Committee of the University of Alberta. Rats and mice were housed two and four per cage, respectively, under a 12-hour light/dark cycle at room temperature, and were provided with food and water *ad libitum*.

## 2.2 Cell preparation and short-term culture

Animals were euthanized in accordance with the standards of the Canadian Council on Animal Care. Ice-cold Hank's balanced salt solution (HBSS; see Section 2.10) was injected into the pancreatic duct and the pancreata were then surgically removed. The tissue was cut up into small pieces with surgical scissors and then dissociated enzymatically with HBSS containing collagenase (type V, 0.9 mg/mL for mice and 1.2 mg/mL for rats) and DNAse (type II, 5 μg/mL) by shaking vigorously for 10 mins at 37$^{o}$C. The tissue mixture was filtered through a mesh screen to remove lymph nodes, and the filtrate was centrifuged at 2000 RPM for 1 min (at room temperature). Following centrifugation, the tissue pellet

was suspended in RPMI medium (which is named for Roswell Park Memorial Institute, where it was developed) and the islets were hand-picked under a dissecting microscope with a fire-polished Pasteur pipette and kept in standard culture conditions in RPMI medium for 2 hours before dissociation to obtain single islet cells. Islets were put in chelation buffer (see Section 2.10), then centrifuged at 2000 RPM for 4 mins (at room temperature). The supernatant was removed and the islets were enzymatically dissociated with trypsin (0.0075 g/mL) and DNAse (type II, 20 mg/mL) in chelation buffer for 5 mins at 37$^{o}$C, followed by trituration with a fire-polished Pasteur pipette. Following a second centrifugation, the tissue pellet was washed three times with Dulbecco's modified Eagle medium (DMEM) containing 0.1% bovine serum albumin (DMEM-BSA). Finally, the tissue pellet was diluted in DMEM-BSA and single islets cells were then plated on glass coverslips coated with poly-L-lysine (0.1 mg/mL). Cells were allowed to attach for 30-60 mins before the addition of 2 mL of RPMI culture medium (containing 11 mM glucose, 10% fetal bovine serum, 50 μg/ml streptomycin and 50 IU/ml penicillin) to each culture dish. Experiments were performed in cells maintained in standard culture conditions (37$^{o}$C, 5% $CO_2$) for 24-48 hours.

Depending on the experiments, single live β cells were identified from the mixed islet cell cultures with the following procedures. First, it has been shown that among the different types of islet cells, β cells have the largest size (1). Therefore, single β cells can be identified by their larger cell size. Second, stimulation with glucose (20 mM) or the $K_{ATP}$ channel blocker, tolbutamide (100

μM) are known to cause a rise in intracellular $Ca^{2+}$ concentration ($[Ca^{2+}]_i$) in β cells. Therefore, individual β cells can also be identified by their $Ca^{2+}$ response to glucose or tolbutamide.

### 2.3 Measurement of $[Ca^{2+}]_i$

In experiments involving measurements of $Ca^{2+}$ signal at physiological temperature (35-37$^oC$), $[Ca^{2+}]_i$ was monitored with digital imaging using a Tillvision imaging system equipped with a Polychrome II high-speed monochromator (Applied Scientific Instruments, Eugene, OR, USA). Details were as described in our previous study (2). Briefly, cells were loaded with fura-2/AM (acetoxymethyl ester; 2.5 μM) for 10 minutes at 37$^oC$. Following the removal of fura-2, cells were incubated with standard bath solution at physiological temperature for 5-10 min before recording. In all experiments, cells were constantly perfused with bath solution. Fura-2 was excited sequentially by 340 and 380 nm light delivered from a Xenon lamp via a 40X, 1.3 NA UV fluor oil objective lens (Olympus, Carsen Group, Markham, ON, Canada). Fluorescent images were collected at 510 nm for 15-20 ms every 10 s by a Peltier-cooled CCD camera. Since the cells were loaded with AM dyes, there was no correction for cell autofluorescence in the digital imaging experiments. The ratio of fluorescence, R (340nm/380nm) from individual cells was analyzed with Tillvision Software 3.02 (Till Photonics, Applied Scientific Instruments, Eugene, OR, USA) on an IBM-compatible computer, and $[Ca^{2+}]_i$ was calculated as described below.

For experiments involving simultaneous measurement of $[Ca^{2+}]_i$ and electrophysiology, the rig was equipped for indo-1 fluorescence measurement. Therefore, in these experiments, cells were loaded with indo-1/AM (2.5 μM for 15 min at 37°C) or indo-$K^+$ salt (100 μM loaded via the whole-cell pipette). Measurement of $[Ca^{2+}]_i$ was performed at room temperature (20-23°C). Indo-1 was excited by 365 nm light from a HBO 100W Hg lamp via a 40X, 1.3 NA UV fluor oil objective lens (Nikon, Melville, NY, USA). Emission fluorescence at 405 ± 35 nm and 495 ± 45 nm was collected with two photomultiplier tubes (Hamamatsu H3460-04) for 20 ms at 0.5 s or 1 s intervals. The output of the photomultiplier tubes was converted to TTL pulses and counted by a CYCTM-10 counter card (Cyber Research Inc., Branford, CT, USA) installed in an IBM-compatible PC. For experiments involving whole-cell loading of indo-1, the fluorescence of the pipette and the cell before establishment of whole-cell configuration was used for background subtraction. The ratio of fluorescence, R (400nm/500nm), was used to calculate $[Ca^{2+}]_i$ as described below.

Fluorescence ratios of indo-1 and fura-2 were analyzed according to the equation: $[Ca^{2+}]_i = K^* (R-R_{min})/(R_{max}-R)$ (3). $R_{min}$ is the fluorescence ratio of $Ca^{2+}$-free indicator, while $R_{max}$ is the fluorescence ratio of $Ca^{2+}$-bound indicator. K* is a constant determined empirically. Calibrations for indo-1 or fura-2 measurements were determined from single cells dialyzed (via a whole-cell pipette) with one of three pipette solutions. $R_{min}$ was measured in cells loaded with (mM): 52 K-aspartate, 10 KCl, 50 K-EGTA, 50 K-Hepes, and 0.1 fura-2 or indo-1; pH 7.4. $R_{max}$ was measured in cells loaded with (mM): 136 K-aspartate,

15 $CaCl_2$, 50 K-Hepes, and 0.1 fura-2 or indo-1; pH 7.4. K* was calculated from the equation above using R values obtained from cells loaded with (mM): 60 K-aspartate, 50 K-Hepes, 20 K-EGTA, 15 $CaCl_2$, and 0.1 fura-2 or indo-1; pH 7.4, which has a calculated free $Ca^{2+}$ concentration of 212 nM at 22°C (4). For all fura-2 measurements shown in Chapters 3, 4, and 5, the values for $R_{min}$, $R_{max}$, and K* were 0.13, 3.4, and 2.72 μM, respectively. For all indo-1 measurements shown in Chapters 3 and 4, the values for $R_{min}$, $R_{max}$, and K* were 0.3, 2.9, and 1.77 μM, respectively.

## 2.4 Electrophysiology

In all experiments involving electrophysiology, single cells were voltage-clamped at room temperature (20-23°C) with the whole-cell patch-clamp technique. Membrane potentials or currents were recorded with an EPC-9 amplifier (HEKA Elektronik, Lambrecht/Pfalz, Germany) that was controlled by an IBM-compatible PC and the data acquisition program Patchmaster (HEKA Elektronik, Lambrecht/Pfalz, Germany). The recording pipettes were made from hematocrit glass (VWR Scientific Canada Ltd., London, ON, Canada) and the resistance was 2-4 MΩ after filling with the pipette solution. A -10 mV correction for junction potential was applied throughout.

## 2.5 Measurement of $Ca^{2+}$ influx using $Mn^{2+}$ quench technique

Cells were loaded with indo-1/AM as described above, and bathed in an extracellular solution containing 0.2 mM $MnCl_2$. $Mn^{2+}$ can enter the cell via any $Ca^{2+}$-permeable pathway and bind to indo-1, thus quenching its fluorescence. Since the indo-1 fluorescence at 405 nm (F405) is not sensitive to changes in $[Ca^{2+}]_i$ (near the isosbestic wavelength of indo-1), a reduction in F405 reflects $Mn^{2+}$ entering the cell through a $Ca^{2+}$-permeable pathway, and thus $Ca^{2+}$ entry into the cell. All experiments were performed at 35-37$^{o}$C.

## 2.6 Cholesterol manipulation

Mouse islet cells were cultured (as detailed in Section 2.2) for 24-48 hours before cholesterol manipulations were performed. To elevate cellular cholesterol, islet cells were incubated with soluble cholesterol (1 mg cholesterol/mL) in RPMI (for imaging, voltage-clamp, and glucose uptake experiments) or bicarbonate-buffered solution (for ATP assay) for 1 hour at 37$^{o}$C. The molar ratio of cholesterol to methyl-β-cyclodextrin (MβCD) in the soluble cholesterol preparation (obtained from Sigma) was ~1:6; thus, MβCD acted as a cholesterol donor (5). Untreated islet cells that were cultured for the same amount of time and that underwent mock transfer procedures were used as controls. To examine whether the effect of exogenous soluble cholesterol was indeed related to elevation of cellular cholesterol, islet cells were treated with soluble cholesterol (1 mg cholesterol/mL) plus 10 or 20 mM MβCD in RPMI (for imaging, voltage-

clamp, and glucose uptake experiments) or bicarbonate-buffered solution (for ATP assay) for 1 hour at 37°C. For cholesterol extraction in islet cells from *ApoE*$^{-/-}$ mice, single islet cells were incubated with the 3-hydroxy-3-methyl-glutaryl-coenzyme A (HMG CoA) reductase inhibitor, lovastatin (5 μM) overnight at 37°C, followed by lovastatin (5 μM) plus MβCD (10 mM) for 1 hour at 37°C.

### 2.7 Measurement of glucose uptake

Three groups of mouse islet cells were employed: control, cholesterol overload and treatment with cholesterol plus excessive MβCD (as outlined in Section 2.6). Following cholesterol manipulation, single mouse islet cells were washed thoroughly with standard bath solution and then incubated with 20 mM glucose plus the fluorescent glucose analog, 2-[*N*-(7-nitrobenz-2-oxa-1,3-diazol-4-yl) amino]-2-deoxy-d-glucose (2-NBDG; 200 μM) as well as fura 2/AM (2.5 μM) for 10 minutes at 37°C. Cells were then washed with standard bath solution for 5 mins at room temperature, and the 2-NBDG fluorescence of individual cells at 520-560 nm (excitation at 485 nm) was collected and analyzed with Tillvision Software 3.02 (Till Photonics, Applied Scientific Instruments). The average fluorescence of cells that were never exposed to 2-NBDG was employed for background subtraction. Following the measurement of 2-NBDG fluorescence, the islet cells were challenged with tolbutamide (100 μM). Only cells exhibiting a $Ca^{2+}$ response to tolbutamide (identified as β cells) were included for analysis.

## 2.8 Measurement of cellular ATP

Three groups of mouse islet cells were employed (with an equal number of mouse islets in each group): control, cholesterol overload and treatment with cholesterol plus excessive MβCD (as outlined in Section 2.6). Following cholesterol manipulation, cells were washed thoroughly and incubated in a bicarbonate-buffered solution (KRB) containing 3 mM glucose for 20-50 minutes. Cells were then exposed to KRB containing either 3 mM or 20mM glucose for 40 minutes. Cells were collected from the glass cover slips by flushing with a glass pipette. The cells were then centrifuged at 2000 RPM for 4 mins at room temperature, and the cell pellet was resuspended in KRB. Cells were lysed using the proprietary cell-lysing buffer and cellular ATP was measured immediately using the luciferase assay (all buffers supplied in the ATP bioluminescent somatic cell assay kit from Sigma (Saint Louis, Missouri, USA)). In the luciferase assay, light is produced according to the following reactions:

$$\text{ATP} + \text{luciferin} \xrightarrow{\text{Firefly luciferase}} \text{adenyl luciferin} + \text{PPi}$$

$$\text{Adenyl-luciferin} + O_2 \longrightarrow \text{oxyluciferin} + \text{AMP} + \text{light}$$

Light output was measured in a tube-based luminometer (Berthold Technologies, Bad Wildbad, Germany). Signal was integrated for 3 s for each tube.

## 2.9 Statistical analysis

Functions in the Microcal Origin program 8 (Microcal Software) were employed for all statistical and curve fitting procedures. Amplitudes of $Ca^{2+}$

signals obtained with fura-2 or indo-1 were analyzed as single-point measurements (basal $Ca^{2+}$ subtracted from peak response; Chapters 3, 4, and 5). The rate of $Mn^{2+}$ quench was calculated from the slopes of the linear fit to individual segments of the indo-1 fluorescence at 405 nm (in Chapter 3). The inactivation of $I_{Ca}$ was estimated by fitting the decay of the current signal with a single exponential (in Chapter 5). Statistical difference was determined by a paired Student's *t*-test, or by an independent Student's *t*-test for comparisons of values between two different populations of cells. Any difference with $p < 0.05$ was considered statistically significant, and is marked with an asterisk (*) in the figures. All values shown are means $\pm$ SEM.

### 2.10 Chemicals and buffered solutions

Arachidonic acid (AA; purchased as sodium arachidonate), adenosine 5'-triphosphate (ATP), bafilomycin A1, bovine serum albumin (BSA), caffeine, soluble cholesterol, cyclosporin A, diazoxide, EGTA, eicosatetraynoic acid (ETYA), glycyl-phenylalanyl β-naphthylamide (GPN), methyl-β-cyclodextrin (MβCD), nicotinic acid adenine dinucleotide phosphate (NAADP), penicillin G, poly-L-lysine, streptomycin, tetraethylammonium chloride (TEA), tolbutamide, and all enzymes (including collagenase type, DNAse type II, and trypsin type) were obtained from Sigma (Oakville, ON, Canada). Fura-2/AM, indo-1/AM, indo-$K^+$ salt, and 2-NBDG were obtained from Molecular Probes. Fetal bovine serum, RPMI 1640, and DMEM were obtained from Gibco (Grand Island, NY,

USA). Adenophostin A, ryanodine, and thapsigargin were obtained from Calbiochem (San Diego, CA, USA).

Stock solutions of sodium arachidonate or ETYA were made in $H_2O$ or DMSO, respectively. On the same day as the experiment, the stock was dissolved in the appropriate bath solution at a concentration of 0.1%.

HBSS contained (in mM): 136.9 NaCl, 5.4 KCl, 5.6 glucose, 4.2 $NaHCO_3$, 1.3 $CaCl_2$, 0.8 $MgSO_4$, 0.4 $KH_2PO_4$, and 0.44 $Na_2HPO_4$. Chelation buffer contained: 124 NaCl, 5.4 KCl, 1 $NaH_2PO_4$, 14.3 $NaHCO_3$, 10 Hepes, 2.8 glucose, and 3 EDTA (all in mM), plus 7.5 μg/mL DNAse II and 0.5% BSA. DMEM-BSA consisted of DMEM (5.5 mM glucose) supplemented with 0.1% BSA. Cell culture medium consisted of RPMI 1640 (11 mM glucose) supplemented with 10% fetal bovine serum and 1% penicillin V/streptomycin. The standard bath solution (NMR) contained (in mM): 5 $CaCl_2$, 1 $MgCl_2$, 10 Hepes, 150 NaCl, 2.5 KCl, and 3 glucose. The $Ca^{2+}$-free bath solution contained (in mM): 3 $MgCl_2$, 10 Hepes, 150 NaCl, 2.5 KCl, 3 glucose, and 1 EGTA. The bicarbonate-buffered solution (KRB) contained (in mM): 120 NaCl, 4.8 KCl, 1.2 $MgCl_2$, 1 $Na_2HPO_4$, 24 $NaHCO_3$, 2.5 $CaCl_2$, 3 glucose, supplemented with 1 mg/mL BSA. During glucose challenge, the glucose concentration in the standard bath solution or KRB was increased from 3 to 20 mM and no compensation was made for the difference in osmolarity. Unless otherwise stated, the standard whole-cell pipette solution contained (in mM): 120 aspartic acid, 20 TEACl, 20 Hepes, 2.5 $MgCl_2$, 0.1 GTP, and 5 ATP, and was titrated with Cs-OH. During measurement of ARC current, 10 mM EGTA was added to the standard whole-cell pipette solution. For

measurement of $K^+$ current, the whole-cell pipette solutions contained (in mM): 120 K-aspartate, 20 Hepes, 20 KCl, 2.5 $MgCl_2$, 0.1 GTP, and 5 ATP.

## References


1. Pipeleers,DG, In't Veld,PA, Van de Winkel,M, Maes,E, Schuit,FC, Gepts,W: A new in vitro model for the study of pancreatic A and B cells. *Endocrinology* 117:806-816, 1985
2. Hughes,E, Lee,AK, Tse,A: Dominant role of sarcoendoplasmic reticulum Ca2+-ATPase pump in Ca2+ homeostasis and exocytosis in rat pancreatic beta-cells. *Endocrinology* 147:1396-1407, 2006
3. Grynkiewicz,G, Poenie,M, Tsien,RY: A new generation of Ca2+ indicators with greatly improved fluorescence properties. *J Biol Chem* 260:3440-3450, 1985
4. Blinks,JR, Wier,WG, Hess,P, Prendergast,FG: Measurement of Ca2+ concentrations in living cells. *Prog Biophys Mol Biol* 40:1-114, 1982
5. Zidovetzki,R, Levitan,I: Use of cyclodextrins to manipulate plasma membrane cholesterol content: evidence, misconceptions and control strategies. *Biochim Biophys Acta* 1768:1311-1324, 2007

# Chapter 3

## Arachidonic acid stimulates extracellular $Ca^{2+}$ entry in rat pancreatic β cells via activation of the noncapacitative arachidonate-regulated $Ca^{2+}$ (ARC) channels

## 3.1 Introduction

### *3.1.1 Generation of AA and its metabolites*

AA is a 20-carbon endogenous polyunsaturated fatty acid that acts as a second messenger in many cells. AA can be synthesized by two pathways (see Figure 3-1). The first pathway involves the direct cleavage of membrane phospholipids by phospholipase $A_2$ ($PLA_2$). Three isoforms of $PLA_2$ are expressed in β cells: the secretory form ($sPLA_2$) (1), the $Ca^{2+}$-independent form ($iPLA_2$) (2), and the $Ca^{2+}$-dependent cytosolic form ($cPLA_2$) (3;4). The second pathway involves the cleavage of membrane phospholipids by phospholipase C (PLC), yielding diacylglycerol (DAG), which is then converted to AA by DAG lipase.

AA is the precursor for a number of intracellular messengers and can be metabolized by four groups of enzymes: cyclooxygenases (yielding prostaglandins and thromboxanes), lipoxygenases (yielding leukotrienes and hydroxyeicosatetraenoic acids (HETEs)), cytochrome P450 enzymes (which generate epoxyeicosatrienoic acids (EETs)), and peroxidation by free radicals (which yields isoprostanes) (5). Many of the products of AA metabolism are biologically active and some of the effects of AA on insulin secretion were suggested to be mediated by its metabolites, as detailed in Sections 3.1.2 and 3.1.3.

### *3.1.2 Role of AA in insulin secretion*

Upon stimulation with glucose, the concentrations of AA in rat islets can be as high as 35 μM (6). Glucose stimulation of rat islets also caused accumulation of

AA metabolites, including 12-HETE (a lipoxygenase product) (7) and prostaglandin $E_2$ (a cyclooxygenase product). ACh, a physiological stimulator of insulin secretion, also caused AA accumulation in rat islets (8). The generation of AA and its metabolites during glucose or cholinergic stimulation raises the possibility that AA may have a role in modulating insulin secretion. Consistent with this, inhibitors of $PLA_2$ reduced glucose-stimulated insulin secretion in rat (3;9) and human islets (10). However, the role of AA metabolites on insulin secretion is controversial; glucose-stimulated insulin secretion in isolated rat islets was partially inhibited by lipoxygenase inhibitors but potentiated by cyclooxygenase inhibitors (11).

### *3.1.3 Actions of AA on $Ca^{2+}$ signals and insulin secretion*

At a low glucose concentration, exogenous AA has been reported to cause a biphasic increase in $[Ca^{2+}]_i$ in isolated rat β cells (12), and to induce insulin secretion in rat islets (13) and human islets (10). There is some evidence suggesting that AA may potentiate insulin secretion without affecting the $Ca^{2+}$ signal. Intracellular application of either exogenous $cPLA_2$ or exogenous AA in isolated mouse β cells increased the depolarization-induced exocytotic response without increasing $[Ca^{2+}]_i$ (14). Thus, AA may modify the secretory response downstream of the $Ca^{2+}$ signal.

Nevertheless, insulin secretion is $Ca^{2+}$-dependent. Therefore, the stimulatory action of AA is closely related to the ability of AA to trigger $[Ca^{2+}]_i$ rise. The mechanism by which AA stimulates $[Ca^{2+}]_i$ rise in low glucose is not well

understood. There appear to be two components to the AA-induced $[Ca^{2+}]_i$ rise: an extracellular $Ca^{2+}$ entry component and an intracellular $Ca^{2+}$ release component. A number of different mechanisms mediating each of the two components have been suggested, and they may be associated with AA itself or with one of its many metabolites.

AA is known to activate extracellular $Ca^{2+}$ influx (12) but the mechanism of $Ca^{2+}$ entry is controversial. Exogenous $PLA_2$ or exogenous AA was reported to suppress the opening of $K_{ATP}$ channels in excised inside-out patches from the HIT cell line (15). However, the same study reported that AA, acting via a metabolite generated by the cyclooxygenase pathway, increased the opening of $K_{ATP}$ channels. Thus, it remains unclear whether AA causes depolarization via closure of $K_{ATP}$ channels. On the other hand, exogenous application of $sPLA_2$ was shown to reduce $K_{ATP}$ current in single mouse β cells (16). AA has also been reported to modulate the delayed rectifier channel Kv2.1 in INS-1 cells (17). While these results seem to suggest that AA may induce membrane depolarization and activation of VGCCs, VGCC inhibitors caused only a partial reduction of the AA-induced $[Ca^{2+}]_i$ rise (12;18), suggesting the involvement of a VGCC-independent pathway in the AA-mediated extracellular $Ca^{2+}$ entry.

One possible mechanism for the AA-mediated VGCC-independent pathway is the fatty-acid-sensitive GPR40 receptors. Itoh *et al.* reported that in MIN6 cells, long-chain fatty acids, including AA, increased both $[Ca^{2+}]_i$ and insulin secretion via activation of GPR40 in the presence of a high concentration of glucose (19). Another study has also shown that oleic acid (OA), which is a more potent

activator of GPR40 than AA, potentiated the glucose-induced $[Ca^{2+}]_i$ rise in isolated rat β cells (20). However, the same study showed that OA did not affect $[Ca^{2+}]_i$ at a low glucose concentration. Consistent with this, insulin secretion in rat islets at a low glucose concentration was unaffected by exogenous OA (13). It is therefore unlikely that the effects of AA at a low glucose concentration are mediated by GPR40.

AA has also been implicated as an activator of transient receptor potential (TRP) channels (21;22). TRP channels are postulated to underlie capacitative calcium entry (CCE) (23), the mechanism whereby depletion of intracellular ER $Ca^{2+}$ stores activates extracellular $Ca^{2+}$ influx (24). CCE is also known as store-operated $Ca^{2+}$ entry (SOCE) or the $Ca^{2+}$-release-activated $Ca^{2+}$ (CRAC) current. Since insulin-secreting cells have been shown to express TRP channels (25) and CCE-mediated extracellular $Ca^{2+}$ entry has been described in β cells (26;27), it is possible that AA may activate extracellular $Ca^{2+}$ entry via CCE activation. On the other hand, it is also possible that AA may trigger $Ca^{2+}$ entry through the arachidonate-regulated $Ca^{2+}$ (ARC) channel (discussed in further detail below).

### *3.1.4 The ARC channel*

The ARC channel was first reported in 2000 by Mignen *et al*. in HEK293 cells (28). They had found that AA activated a noncapacitative inward current which was accompanied by a $[Ca^{2+}]_i$ rise in HEK293 cells. To date, the ARC channel has been described in a variety of cell lines, including HeLa, COS, RBL-1, DT40 (29), Saos-2 (30), and SY5Y (31) cell lines, as well as in parotid and

pancreatic acinar cells (32). The activation of ARC channel does not require the emptying of intracellular $Ca^{2+}$ stores and it is insensitive to the CCE blocker, 2-APB (29). Instead, its activation is dependent on low doses (<10 μM) of exogenous AA or endogenous generation of AA via agonist stimulation, but is not sensitive to other fatty acids, such as palmitic acid and OA (29). The ARC current is highly $Ca^{2+}$-selective, has a very positive reversal potential (+60 mV), is inwardly rectifying, and is inhibited by $La^{3+}$ (28) or $Gd^{3+}$ (29). Furthermore, the site of action of AA on the ARC channel is intracellular and does not require AA metabolism (29).

Until very recently, little was known about the molecular composition of the ARC channel. New evidence now shows that the ARC channel is made up of proteins belonging to the stromal interacting molecule (STIM) and Orai families. The STIM family of proteins was first identified in a limited RNAi-based screen in Drosophila S2 cells (33), and STIM1 is expressed in both ER and plasma membrane (34;35). In HEK293 cells, knockdown of STIM1 expression using small interfering RNA (siRNA) against STIM1 caused a partial reduction of ARC current, while overexpressing STIM1 caused an increase in ARC current (36). Thus, STIM1 appears to be a key regulator of $Ca^{2+}$ entry through ARC channels. However, the identity of the pore-forming protein was a mystery until the identification of Orai proteins in a genome-wide RNA-interference-based screen in *Drosophila* cells. Three human homologs of *Drosophila* Orai (Orai1, Orai2, and Orai3) were identified (37). Overexpression of either Orai1 or Orai3, but not Orai2, caused an increase in ARC currents. Conversely, transfection with siRNA

against either Orai1 or Orai3 resulted in partial inhibition of ARC currents (38). Therefore, both Orai1 and Orai3 are necessary components of the ARC channel. Note that it has also been shown that CCE channels are also composed of Orai1 and STIM1 proteins (39). Therefore, ARC channels cannot be detected simply on the basis of STIM1 or Orai expression.

## 3.2 Results

### *3.2.1 The AA-mediated $[Ca^{2+}]_i$ rise in rat β cells did not involve activation of GPR40 receptors or AA metabolism*

An example of a glucose-mediated $[Ca^{2+}]_i$ rise in a rat β cell is shown in Figure 3-2A. The elevation of the glucose concentration in the bath solution from 3 to 20 mM triggered a $[Ca^{2+}]_i$ rise. When the cell was subsequently challenged with AA (15 μM in 3 mM extracellular glucose), a robust $[Ca^{2+}]_i$ rise was evoked. This concentration of AA was around the midpoint of the reported range of AA accumulation (up to 35 μM) in rat pancreatic islets during glucose stimulation (40). In 44 rat β cells (identified by the presence of glucose-mediated $Ca^{2+}$ signals), the mean amplitude of the AA (15 μM)- triggered $[Ca^{2+}]_i$ rise was 488 ± 33 nM (Figure 3-2D). Since the orphan G-protein-coupled receptor, GPR40, was found to be abundantly expressed in rat pancreatic islets, and AA was reported to activate rat GPR40 receptors with an $EC_{50}$ of 8 μM (19), we tested whether a potent agonist of GPR40 receptor, OA ($EC_{50}$ of ~3 μM), could mimic the action of AA in the presence of a low glucose concentration. As shown in Figure 3-2B, OA (10 μM in 3 mM glucose) did not trigger any appreciable

$[Ca^{2+}]_i$ rise but subsequent exposure of AA to the same cell evoked a robust $Ca^{2+}$ signal. In 30 cells, the mean increase in basal $[Ca^{2+}]_i$ triggered by OA was negligible when compared with that evoked by AA (Figure 3-2D). This is in agreement with results from Fujiwara *et al*.: in rat β cells, OA could trigger a $[Ca^{2+}]_i$ rise in the presence of 11.2 mM glucose, but not in the presence of 2.8 mM glucose (41). Thus, the AA-mediated $[Ca^{2+}]_i$ rise in the presence of 3 mM glucose did not involve activation of GPR40 receptors.

AA is rapidly metabolized in the cell into a variety of eicosanoid products. To test whether the effect of AA on $[Ca^{2+}]_i$ is due to one of the AA metabolites, we examined the actions of eicosatetraynoic acid (ETYA), a non-metabolizable analog of AA that is a blocker of lipoxygenase, cycloxygenase and P450 pathways for AA metabolism (42). Figure 3-2C shows the application of ETYA (30 μM) evoked a robust $[Ca^{2+}]_i$ rise. The mean increase in $[Ca^{2+}]_i$ evoked by 15 or 30 μM ETYA was smaller but comparable to those evoked by 15 μM AA (Figure 3-2D). Thus, the actions of AA on $[Ca^{2+}]_i$ in β cells did not require AA metabolism.

### *3.2.2 The AA-mediated $Ca^{2+}$ intracellular $Ca^{2+}$ release was accompanied by VGCC-independent extracellular $Ca^{2+}$ entry*

Previous studies have shown that AA stimulated $Ca^{2+}$ release from intracellular stores (43;44). Consistent with this, we found that in the absence of extracellular $Ca^{2+}$, AA evoked a transient $[Ca^{2+}]_i$ rise. In the example shown in Figure 3-3A, individual cells were voltage clamped at -70 mV in the presence of

5 mM extracellular $Ca^{2+}$. Upon switching to a $Ca^{2+}$-free extracellular solution (which also contained 1 mM of the $Ca^{2+}$ chelator, EGTA), the basal $[Ca^{2+}]_i$ declined by ~0.08 μM. Following the application of AA (5 μM in the $Ca^{2+}$-free solution), $[Ca^{2+}]_i$ rose to ~0.7 μM, reflecting $Ca^{2+}$ release from intracellular stores. Note that despite the continuous presence of AA in the $Ca^{2+}$-free solution, the AA-mediated $Ca^{2+}$ signal started to decline after it reached a peak and $[Ca^{2+}]_i$ returned to the basal level within ~40 s, indicating the termination of intracellular $Ca^{2+}$ release. To examine whether the AA-mediated intracellular $Ca^{2+}$ release was followed by any VGCC-independent extracellular $Ca^{2+}$ entry, we changed the extracellular solution from $Ca^{2+}$-free to one containing 5 mM $Ca^{2+}$ and the same concentration of AA. Upon addition of extracellular $Ca^{2+}$, $[Ca^{2+}]_i$ rose gradually to ~0.6 μM, reflecting influx of extracellular $Ca^{2+}$. This extracellular $Ca^{2+}$ influx was AA-dependent because $[Ca^{2+}]_i$ returned to the basal level following the removal of AA (Figure 3-3A). Figure 3-3B summarized the results obtained from 6 cells recorded with the same experimental protocol as in Figure 3-3A. In these cells, the mean amplitude of the $Ca^{2+}$ signal triggered by AA (5 μM) in the $Ca^{2+}$-free extracellular solution was 0.35 ± 0.13 μM (Figure 3-3B). Following the termination of intracellular $Ca^{2+}$ release, the addition of 5 mM extracellular $Ca^{2+}$ in the continued presence of AA elevated $[Ca^{2+}]_i$ by 0.91 ± 0.29 μM. On the other hand, switching the extracellular solution from one containing 5 mM $Ca^{2+}$ to a $Ca^{2+}$-free solution under control conditions (i.e. without any AA) decreased basal $[Ca^{2+}]_i$ by 90 ± 20 nM (Figure 3-3B), whose magnitude is ~10-fold smaller than the change of basal $[Ca^{2+}]_i$ induced by the addition of $Ca^{2+}$ in the presence of AA.

These observations suggest that the AA-mediated $Ca^{2+}$ signal can be separated into two components: $Ca^{2+}$ release from intracellular stores and the activation of extracellular $Ca^{2+}$ entry. Since in our experiment, cells were voltage-clamped at -70 mV (below the threshold for VGCC activation in β cells), the AA-mediated extracellular $Ca^{2+}$ influx was independent of VGCC activation.

### *3.2.3 The AA-mediated extracellular $Ca^{2+}$ entry was not due to CCE*

Our observations above indicate that the AA-mediated intracellular $Ca^{2+}$ release is followed by the activation of a VGCC-independent extracellular $Ca^{2+}$ influx. Since depletion of intracellular $Ca^{2+}$ stores is known to activate CCE in β cells (26;45), it is possible that the AA-mediated extracellular $Ca^{2+}$ entry is due to CCE. On the other hand, it is also possible that the AA-mediated extracellular $Ca^{2+}$ entry is due to direct activation of ARC channels as reported previously in other cell types (46). To distinguish between these possibilities, we employed the $Mn^{2+}$ quench technique to investigate the AA-mediated extracellular $Ca^{2+}$ entry. We measured $Mn^{2+}$ quench instead of $[Ca^{2+}]_i$ here because 2-aminoethoxydiphenyl borate (2-APB), an inhibitor of CCE, could affect $Ca^{2+}$ signals. For example, 2-APB has been shown to affect $Ca^{2+}$ release from $IP_3$ stores, mitochondrial $Ca^{2+}$ uptake, and plasma membrane $Ca^{2+}$ pump (47;48). In the $Mn^{2+}$ quenching experiment, cells were loaded with indo-1 AM. To hyperpolarize β cells, we included the $K_{ATP}$ channel opener, diazoxide (0.2 mM), in the extracellular solution. When the cell was exposed to $Mn^{2+}$ (0.2 mM), there was a gradual reduction of fluorescence at 405 nm (F405; near the $Ca^{2+}$-

independent wavelength of indo-1), reflecting a basal leak of $Mn^{2+}$ into the cell (Figure 3-4A). When the cell was stimulated with AA (15 μM), there was an acceleration in the rate of decrease of F405, reflecting an increase in the entry of $Mn^{2+}$ via the opening of channels which are permeable to divalent cations. As shown in Figure 3-4A, $La^{3+}$ (50 μM), which is a potent inhibitor of VGCCs and CCE as well as ARC channels (23;46), abolished the reduction in F405. In 7 cells examined, AA (15 μM) increased the basal rate of $Mn^{2+}$ quench by ~3-fold and $La^{3+}$ reduced the rate of $Mn^{2+}$ quench (Figure 3-4B). Since diazoxide was present in the bath solution to hyperpolarize the cells and we have already shown in the experiment above (Figure 3-2) that the AA-mediated extracellular $Ca^{2+}$ influx was independent of VGCC activation, it is unlikely that the effect of $La^{3+}$ on the $Mn^{2+}$ quench was solely due to VGCC inhibition. Thus, the result in Figure 3-4 suggests that the AA-mediated extracellular $Ca^{2+}$ influx might be due to the activation of CCE or ARC channels. We have shown previously that depletion of intracellular $Ca^{2+}$ stores increased the rate of $Mn^{2+}$ quench in rat β cells and this effect could be inhibited by 2-APB (50 μM), the CCE blocker (26). Since ARC channels are known to be inhibited by $La^{3+}$ (50–100 μM) but are insensitive to 2-APB (46), we can distinguish between the involvement of these two channels with 2-APB. Figure 3-5A shows that the rate of $Mn^{2+}$ quench in AA was not slowed by 2-APB (50 μM). In 7 cells examined, 2-APB did not affect the AA-mediated increase in the mean rate of $Mn^{2+}$ quench (Figure 3-5B). These observations suggest ARC channels are involved in the AA-mediated extracellular $Ca^{2+}$ entry.

### *3.2.4 AA activated ARC channels*

An important feature of the ARC channel is that AA acts on the intracellular face of the membrane to activate ARC channels (29). Therefore, we examined whether intracellular dialysis of arachidonyl-coenzyme A (ACoA; an analog of AA with a large negatively charged head group that prevents the molecule from crossing the plasma membrane (29)) could activate $[Ca^{2+}]_i$ rise. In this experiment, individual cells were voltage-clamped at -70 mV. Because of the large size of ACoA (MW = 1060), the rate of diffusion of ACoA from the pipette into the cell is expected to be slow. Using the equation of Pusch and Neher: $\tau = (0.6 \pm 0.17)R_A M^{1/3}(r/7.68)^3$ (where $\tau$ is the diffusion time constant, $R_A$ is the pipette resistance, M is molecular weight of the substance and r is the cell radius (49)) and when $R_A$ = 14 MΩ and r = 10 μm, we estimated that the diffusion of ACoA into a β cell would have a time constant of 188 ± 53 s. In order to obtain a measurable response within a few minutes of whole-cell dialysis, we included a high concentration (30 μM) of ACoA in the pipette solution. Following the establishment of whole-cell configuration, both indo-1 and ACoA diffused from the pipette into the cytosol. Because $[Ca^{2+}]_i$ measurement is based on the ratio of fluorescence (see Section 2.3), only a low concentration of cytosolic indo-1 is needed. Since indo-1 has a smaller MW than ACoA (838 versus 1060), we were able to measure basal $[Ca^{2+}]_i$ before a sufficient amount of ACoA was dialyzed into the cell. As shown in the example in Figure 3-6A, at ~20 s after whole-cell dialysis, sufficient indo-1 had entered the cell for a reliable measurement of $[Ca^{2+}]_i$. $[Ca^{2+}]_i$ stayed near the basal level for ~3 min before it gradually rose to

~1.7 μM, reflecting that sufficient concentration of ACoA had entered the cell to activate $[Ca^{2+}]_i$ rise. Note that the ACoA-mediated $Ca^{2+}$ signal was abolished upon the removal of extracellular $Ca^{2+}$, indicating that the $[Ca^{2+}]_i$ rise required extracellular $Ca^{2+}$ influx. Similar results were observed in 8 cells (summarized in Figure 3-6B) and the mean $[Ca^{2+}]_i$ rise evoked by ACoA (30 μM) was 2.2 ± 0.5 μM, which was ~2-fold larger than that evoked by 5 μM AA (Figure 3-3B). The large $[Ca^{2+}]_i$ rise evoked by ACoA was probably due to the high concentration of ACoA (30 μM) employed here. Nevertheless, in view of the high concentration of AA (up to 35 μM) in rat pancreatic islets during glucose stimulation (40), it is possible that such amplitude of ARC-mediated $[Ca^{2+}]_i$ rise may occur at physiological conditions. On the other hand, extracellular application of the same concentration of ACoA did not affect basal $[Ca^{2+}]_i$ (Figure 3-6C). Thus, AA acts on an intracellular site to activate extracellular $Ca^{2+}$ influx.

Since intracellular dialysis of ACoA triggered robust $[Ca^{2+}]_i$ rise in β cells, we further examined whether ACoA could evoke any measurable macroscopic ARC current. In this experiment, EGTA (10 mM) was added to the whole-cell pipette solution to prevent any contamination of $Ca^{2+}$-activated currents. Individual cells were voltage-clamped at -70 mV and 30 μM ACoA was dialysed into the cell. Figure 3-7A shows a representative example of the activation of an inward current at -70 mV when a cell was dialysed with ACoA. The current amplitude at -70 mV was measured every 10 s and the first data point in Figure 3-7A was obtained at ~90 s after the establishment of the whole-cell configuration. Initially, the holding current remained at ~-12 pA, which probably reflects the basal leak of the cell. At

~230 s after whole-cell dialysis, there was a gradual increase in the holding current. The current reached a peak at ~500 s after whole-cell dialysis and the mean current amplitude was ~−23 pA. To examine whether the ACoA-evoked inward current was due to the activation of ARC channels, we tested the sensitivity of this current to $La^{3+}$. As shown in Figure 3-7A, following the bath application of $La^{3+}$ (50 μM), the holding current returned to the basal level. To obtain the average cell density of ARC current, we measured the $La^{3+}$-sensitive component of the ACoA-mediated increase in holding current at -70 mV in individual cells and normalized the value to cell capacitance. As shown in Figure 3-7B, the macroscopic ARC current density averaged from 12 cells was 1.7 ± 0.3 pA/pF. Although the inclusion of EGTA in the whole-cell pipette in this experiment may result in $Ca^{2+}$ store depletion and activation of CCE, we found that whole-cell dialysis of EGTA (10 mM) alone did not result in any appreciable increase in inward current. In 6 cells examined, the increase in inward current (at -70 mV) after 7–8 min of whole-cell dialysis of EGTA was only 0.1 ± 0.2 pA/pF. Thus, the increase in inward current observed with intracellular dialysis of ACoA (Figure 3-7) was primarily due to the activation of ARC channels.

### 3.3 Discussion

The activation of the highly $Ca^{2+}$-permeable ARC channels by AA was first described in HEK293 cells transfected with the $M_3$ muscarinic receptors (m3-HEK293 cells) (28;50). Subsequently, ARC channels were described in the non-excitable parotid and pancreatic acinar cells (32). For excitable cells, ARC

channels have been described only in SH-SY5Y neuroblastoma cells (31). Our current study shows that the AA-triggered extracellular $Ca^{2+}$ entry in rat β cells share many common features with the activation of ARC channels. First, ARC current is known to be activated by low concentrations of AA (2–8 μM) but not by other fatty acids such as palmitic acid and OA (29). We found that OA (10 μM) did not trigger any $Ca^{2+}$ signal in rat β cells (Figure 3-2B) but AA at concentrations as low as 5 μM could trigger robust $[Ca^{2+}]_i$ rise that was partially dependent on the presence of extracellular $Ca^{2+}$ (Figure 3-3). Second, the activation of ARC channels was not dependent on AA metabolism and could be activated by the non-metabolizable AA analog, ETYA (29). Similarly, our results show that ETYA could activate $[Ca^{2+}]_i$ rise in rat β cells (Figure 3-2D). Third, the macroscopic ARC current exhibited strong inward rectification and significant current could be detected at negative potentials (28). In our study, when β cells were voltage clamped at -70 mV to prevent activation of VGCC, AA was able to trigger robust extracellular $Ca^{2+}$ influx (Figure 3-3). Fourth, intracellular ACoA was reported to activate the ARC channel (29). We found that whole-cell dialysis of ACoA into β cells triggered robust extracellular $Ca^{2+}$ entry (Figure 3-6). Fifth, ARC channel was inhibited by $La^{3+}$ but unaffected by 2-APB (29). In our study, the AA-mediated acceleration in $Mn^{2+}$ quench in β cells was abolished by $La^{3+}$ (Figure 3-4) but unaffected by 2-APB (Figure 3-5). A similar inhibition of AA-mediated increase in $Mn^{2+}$ quench by $La^{3+}$ was reported in m3-HEK293 cells (51). Moreover, the ACoA-evoked inward current in β cell was abolished by $La^{3+}$ (Figure 3-7A). Lastly, the macroscopic ARC current was small in magnitude; the

ARC current density at -80 mV in different cell types (activated by 8 μM AA) ranged from 0.5 to 1.4 pA/pF (29). Consistent with this, the mean current density evoked by intracellular ACoA in rat β cells at -70 mV was ~1.7 pA/pF. Thus, our findings demonstrate that ARC channels can play a significant role in the regulation of extracellular $Ca^{2+}$ entry in rat β cells.

In nonexcitable cells, it has been suggested that the generation of AA during agonist stimulation which in turn activates ARC channels have important roles in the modulation of the frequency of the agonist-induced $[Ca^{2+}]_i$ oscillations (46). Glucose stimulation has been reported to evoke $[Ca^{2+}]_i$ oscillations in rodent β cells but the oscillatory $Ca^{2+}$ signal was primarily driven by fluctuations in membrane potentials, which in turn caused periodic activation of VGCCs (52;53). Since AA may affect multiple ion channels in the β cells, including the delayed rectifiers (17) and $K_{ATP}$ channels (15) and there is no specific blocker of ARC channels, it would be difficult to determine whether the $Ca^{2+}$ entry mediated via ARC channels affects the frequency of the glucose-mediated $Ca^{2+}$ signals. Nevertheless, our findings here indicate that the activation of ARC channels is an important component of the AA-mediated $Ca^{2+}$ signals in pancreatic β cells. Since insulin secretion is $Ca^{2+}$-dependent and AA is known to stimulate insulin secretion, it is possible that the ARC-mediated extracellular $Ca^{2+}$ influx contributes to the actions of AA on insulin secretion.

A version of this chapter has been published in Cell Calcium (Jan;47(1):77-83 (2010)).

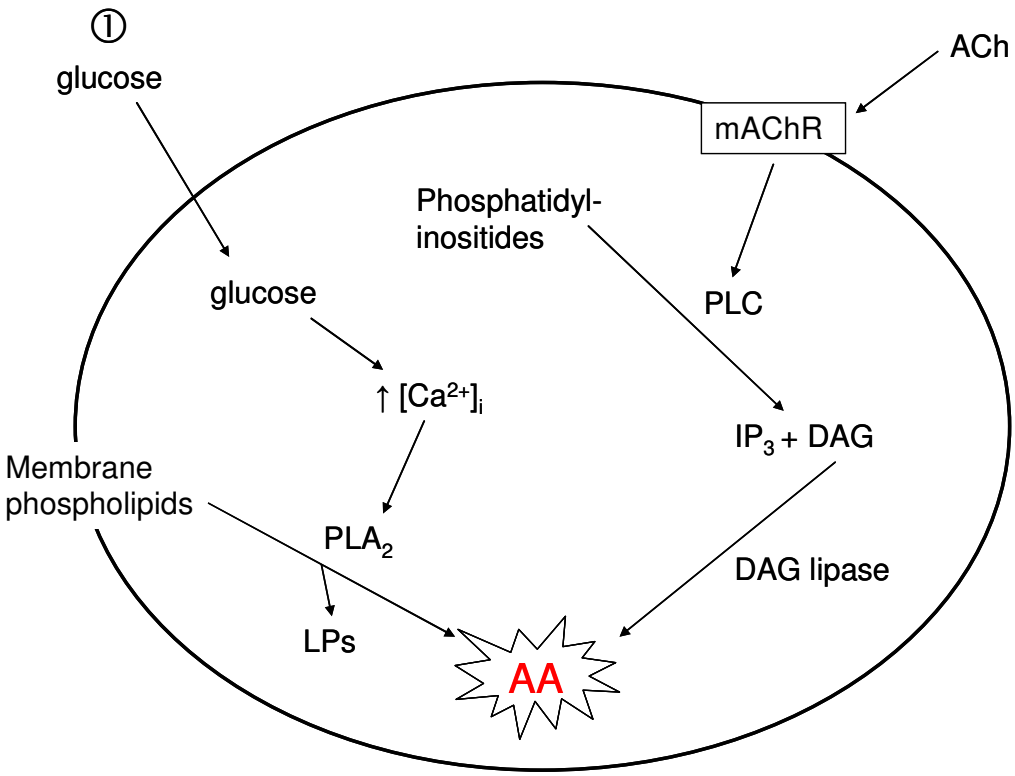


**Figure 3-1**: AA can be generated in the β cell by two pathways. The first (①) is the direct cleavage of membrane phospholipids by phospholipase $A_2$ ($PLA_2$) to yield AA and lysophospholipids (LPs). The second pathway (②) involves cleavage of membrane phospholipids by phospholipase C (PLC), yielding diacylglycerol (DAG) and inositol trisphosphate ($IP_3$), followed by production of AA through the action of DAG lipase.

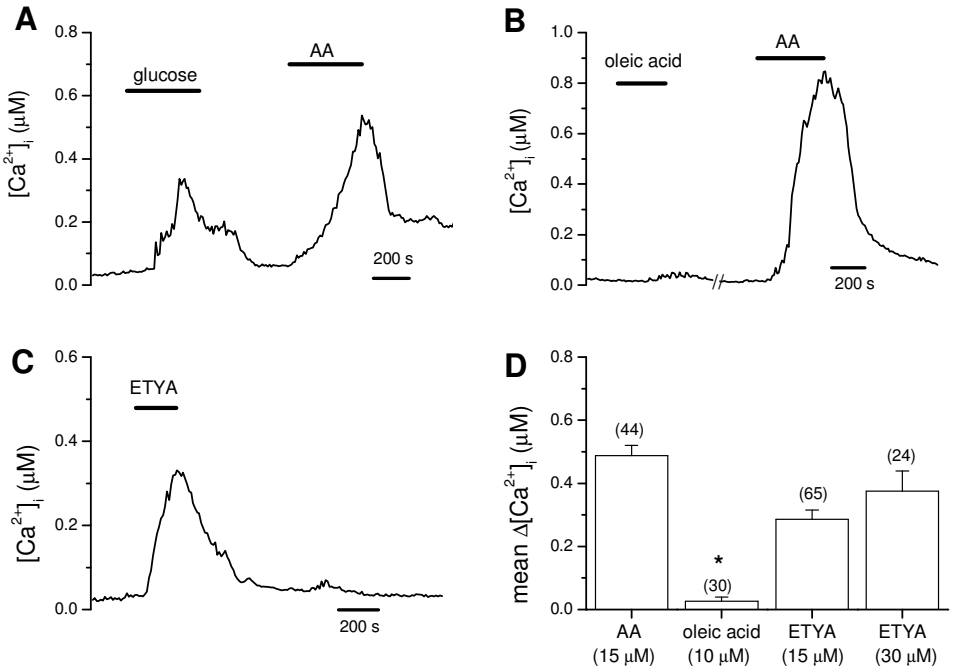


**Figure 3-2**: The AA-mediated $[Ca^{2+}]_i$ rise in rat β cell did not involve activation of GPR40 receptors or AA metabolism. (***A***) AA (15 μM) induced $[Ca^{2+}]_i$ rise in a β cell which was identified by its $Ca^{2+}$ response to glucose (20 mM). (***B***) Oleic acid (10 μM), a more potent agonist of GPR40 receptors than AA, failed to trigger any major $[Ca^{2+}]_i$ rise but subsequent exposure of AA (15 μM) to the same cell was able to trigger a robust rise in $[Ca^{2+}]_i$. (***C***) The action of AA on $[Ca^{2+}]_i$ could be mimicked by ETYA (30 μM), a non-metabolizable analog of AA. (***D***) The mean increase in $[Ca^{2+}]_i$ evoked by AA, oleic acid and ETYA. The effect of oleic acid was significantly smaller than that of AA. Cells were recorded from 2-4 batches of islet cells and * denotes significant difference from the AA-mediated $[Ca^{2+}]_i$ rise.

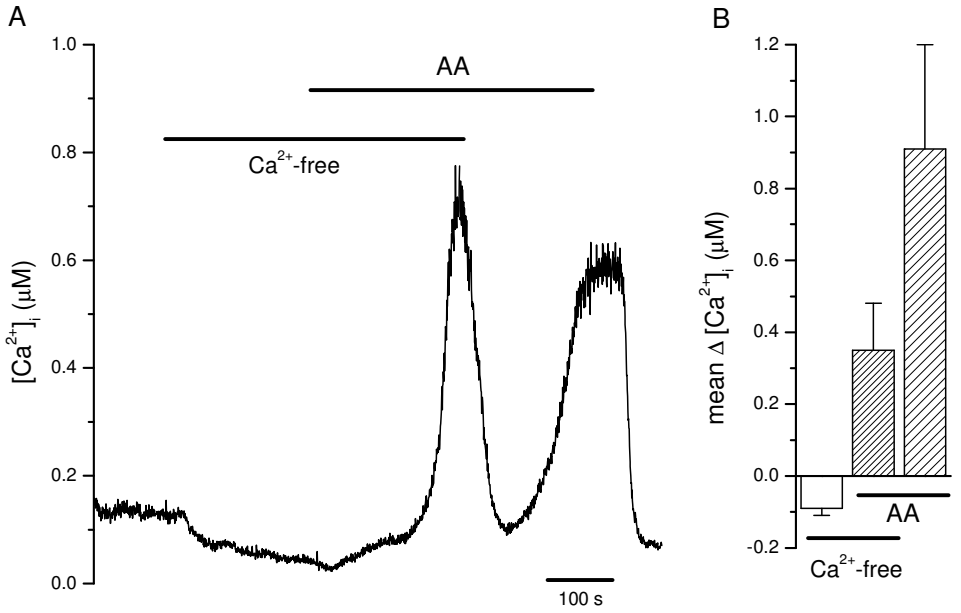


**Figure 3-3**: The AA-mediated $Ca^{2+}$ signal comprised an intracellular $Ca^{2+}$ release component and a VGCC-independent extracellular $Ca^{2+}$ entry component. (***A***) The removal of extracellular $Ca^{2+}$ ($Ca^{2+}$-free bath solution) resulted in a decrease in basal $[Ca^{2+}]_i$. In the absence of extracellular $Ca^{2+}$, application of AA (5 μM) evoked a transient $[Ca^{2+}]_i$ rise which decayed to the basal level within ~40 s. The addition of extracellular $Ca^{2+}$ in the continued presence of AA triggered a slow $[Ca^{2+}]_i$ rise which persisted until AA was removed from the bath. The cell was voltage-clamped at -70 mV. (***B***) Summary of the mean amplitude of the AA (5 μM)-mediated $[Ca^{2+}]_i$ rise in the $Ca^{2+}$-free extracellular solution, the mean amplitude of the AA-mediated rise due to extracellular $Ca^{2+}$ entry and the mean change in $[Ca^{2+}]_i$ when the bath solution was switched from one containing 5 mM $Ca^{2+}$ to a $Ca^{2+}$-free solution. Values were averaged from 6 cells (3 batches) voltage-clamped at -70 mV.

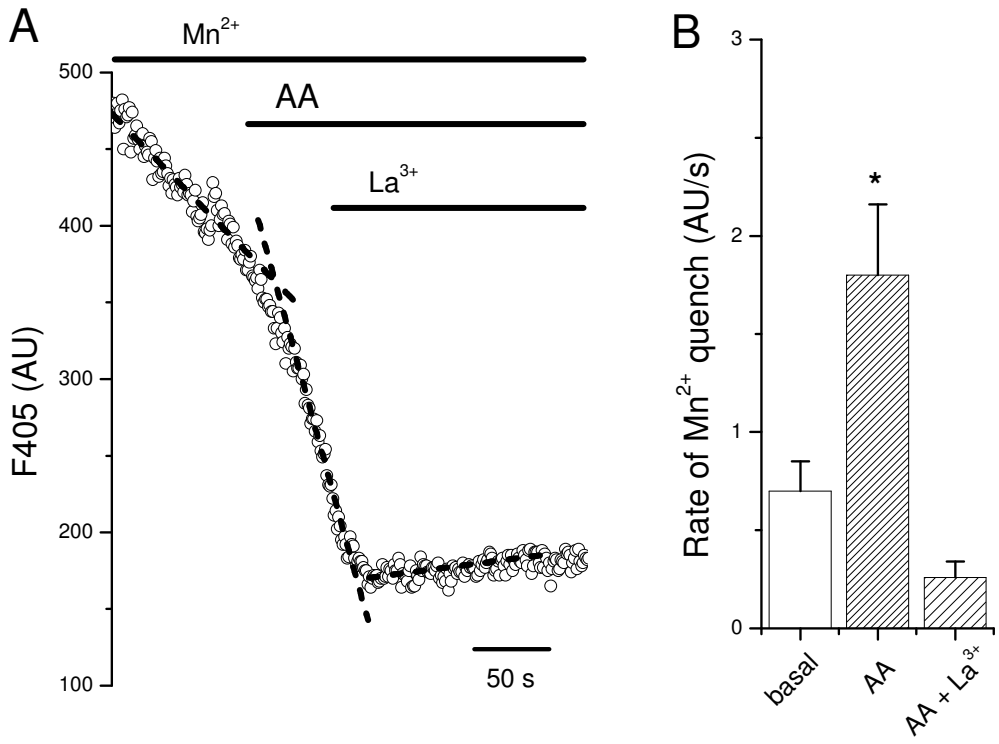


**Figure 3-4**: The AA-mediated increase in the rate of $Mn^{2+}$ quench was inhibited by $La^{3+}$. (***A***) Application of AA (15 μM) accelerated the rate of decrease of indo-1 fluorescence at 405 nm (F405; expressed in arbitrary units (AU)). The cell was loaded with indo-1 AM and bathed in diazoxide (0.2 mM). When exposed to $Mn^{2+}$ (0.2 mM), there was a gradual reduction of F405 (quench). The rate of $Mn^{2+}$ quench was estimated from the slope of the linear fits (dashed lines) to different segments in the plot of the F405. Note that in the presence of AA, the rate of $Mn^{2+}$ quench was faster. The decrease in F405 was completely abolished by $La^{3+}$ (50 μM). In this experiment, a perfusion pipette was placed near the cell for rapid solution exchange. (***B***) Summary of the rate of $Mn^{2+}$ quench in control (basal), in AA (15 μM) and in AA + $La^{3+}$ (50 μM). Values were averaged from 7 cells (2 batches) and * denotes significant difference from the basal rate.

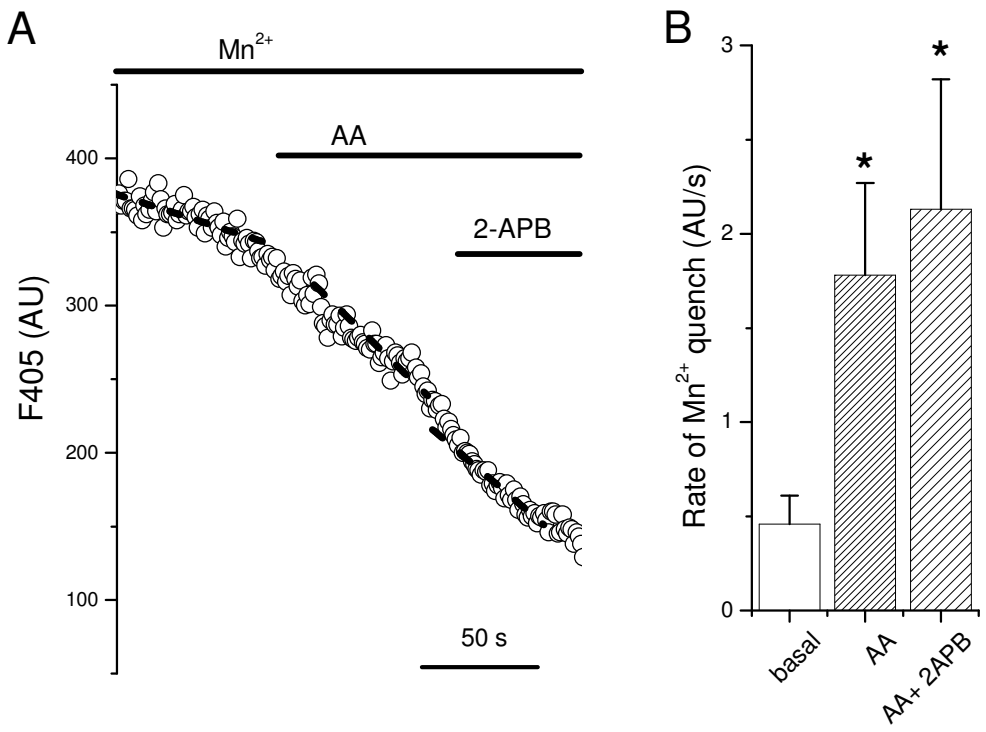


**Figure 3-5**: Inhibitor of CCE could not reduce the AA-mediated increase in the rate of $Mn^{2+}$ quench. (***A***) The increase in the rate of $Mn^{2+}$ quench by AA (15 μM) was not affected by the application of 2-APB (50 μM). In this experiment, a perfusion pipette was placed near the cell for rapid solution exchange. (***B***) Summary of the rate of $Mn^{2+}$ quench in control (basal), in AA (15 μM) and in AA + 2-APB (50 μM). Values were averaged from 7 cells (3 batches) and * denotes significant difference from the basal rate.

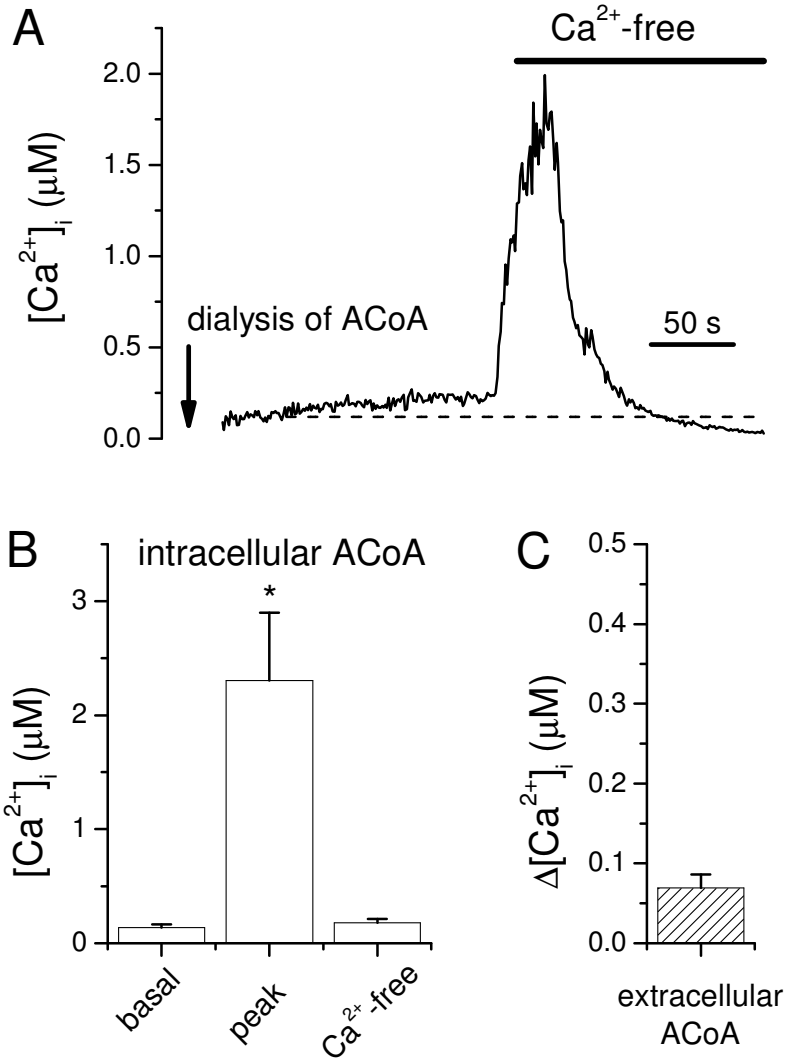


**Figure 3-6**: Activation of ARC channels by ACoA at an intracellular site. (***A***) Whole-cell dialysis of ACoA (30 μM) triggered a robust $[Ca^{2+}]_i$ rise which was abolished by the removal of extracellular $Ca^{2+}$. The $[Ca^{2+}]_i$ trace started at ~20 s after the establishment of whole-cell. The basal $[Ca^{2+}]_i$ (averaged from 60 to 90 s after whole-cell) was denoted in a dashed line. (***B***) Summary of the effect of whole-cell dialysis of ACoA (30 μM) from 8 cells (3 batches). $[Ca^{2+}]_i$ was measured at ~60 s after the establishment of whole-cell (basal), at the peak amplitude of the $Ca^{2+}$-signal (peak) and after the removal of extracellular $Ca^{2+}$ ($Ca^{2+}$-free). * denotes significant difference from the basal value. (***C***) Extracellular application of ACoA (30 μM) triggered a negligible $[Ca^{2+}]_i$ rise (average value from 27 cells in 2 batches).

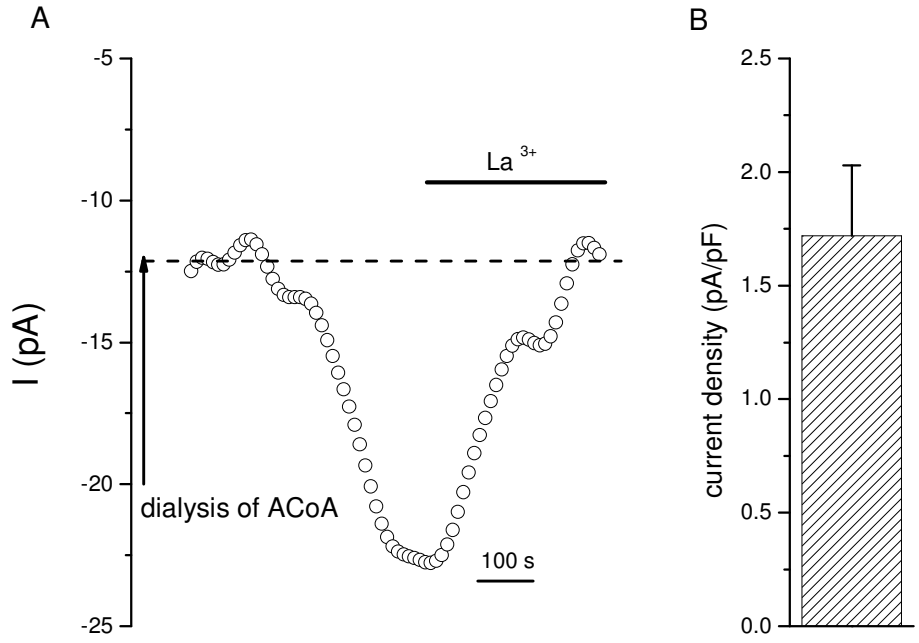


**Figure 3-7**: Activation of ARC current by intracellular ACoA. (***A***) Whole-cell dialysis of ACoA (30 μM) evoked an inward current when the cell was voltage clamped at -70 mV. The current trace started at ~90 s after the establishment of whole-cell. Each data point was the amplitude of the holding current at -70 mV measured every 10 s. The level of the basal holding current (averaged from 10 to 180 s after whole-cell) is denoted by a dashed line. Bath application of $La^{3+}$ (50 μM) abolished the ACoA-mediated increase in current. (***B***) The ARC current density averaged from 12 cells (2 batches) dialysed with ACoA (30 μM). The $La^{3+}$-sensitive component of the holding current at -70 mV from individual cells was normalized to cell capacitance.

## References


1. Loweth,AC, Scarpello,JH, Morgan,NG: Phospholipase A2 expression in human and rodent insulin-secreting cells. *Mol Cell Endocrinol* 112:177-183, 1995
2. Song,K, Zhang,X, Zhao,C, Ang,NT, Ma,ZA: Inhibition of Ca2+-independent phospholipase A2 results in insufficient insulin secretion and impaired glucose tolerance. *Mol Endocrinol* 19:504-515, 2005
3. Loweth,AC, Scarpello,JH, Morgan,NG: A specific inhibitor of cytosolic phospholipase A2 activity, AACOCF3, inhibits glucose-induced insulin secretion from isolated rat islets. *Biochem Biophys Res Commun* 218:423-427, 1996
4. Jones,PM, Burns,CJ, Belin,VD, Roderigo-Milne,HM, Persaud,SJ: The role of cytosolic phospholipase A(2) in insulin secretion. *Diabetes* 53 Suppl 1:S172-S178, 2004
5. *Basic and Clinical Pharmacology*. New York, McGraw-Hill, 2001,
6. Wolf,BA, Pasquale,SM, Turk,J: Free fatty acid accumulation in secretagogue-stimulated pancreatic islets and effects of arachidonate on depolarization-induced insulin secretion. *Biochemistry* 30:6372-6379, 1991
7. Metz,SA: Glucose increases the synthesis of lipoxygenase-mediated metabolites of arachidonic acid in intact rat islets. *Proc Natl Acad Sci U S A* 82:198-202, 1985
8. Konrad,RJ, Jolly,YC, Major,C, Wolf,BA: Carbachol stimulation of phospholipase A2 and insulin secretion in pancreatic islets. *Biochem J* 287 ( Pt 1):283-290, 1992
9. Konrad,RJ, Jolly,YC, Major,C, Wolf,BA: Inhibition of phospholipase A2 and insulin secretion in pancreatic islets. *Biochim Biophys Acta* 1135:215-220, 1992
10. Persaud,SJ, Muller,D, Belin,VD, Kitsou-Mylona,I, Asare-Anane,H, Papadimitriou,A, Burns,CJ, Huang,GC, Amiel,SA, Jones,PM: The role of arachidonic acid and its metabolites in insulin secretion from human islets of langerhans. *Diabetes* 56:197-203, 2007
11. Yamamoto,S, Ishii,M, Nakadate,T, Nakaki,T, Kato,R: Modulation of insulin secretion by lipoxygenase products of arachidonic acid. Relation to lipoxygenase activity of pancreatic islets. *J Biol Chem* 258:12149-12152, 1983
12. Ramanadham,S, Gross,R, Turk,J: Arachidonic acid induces an increase in the cytosolic calcium concentration in single pancreatic islet beta cells. *Biochem Biophys Res Commun* 184:647-653, 1992
13. Band,AM, Jones,PM, Howell,SL: Arachidonic acid-induced insulin secretion from rat islets of Langerhans. *J Mol Endocrinol* 8:95-101, 1992
14. Juhl,K, Hoy,M, Olsen,HL, Bokvist,K, Efanov,AM, Hoffmann,EK, Gromada,J: cPLA2alpha-evoked formation of arachidonic acid and lysophospholipids is required for exocytosis in mouse pancreatic beta-cells. *Am J Physiol Endocrinol Metab* 285:E73-E81, 2003
15. Eddlestone,GT: ATP-sensitive K channel modulation by products of PLA2 action in the insulin-secreting HIT cell line. *Am J Physiol* 268:C181-C190, 1995
16. Juhl,K, Efanov,AM, Olsen,HL, Gromada,J: Secretory phospholipase A2 is released from pancreatic beta-cells and stimulates insulin secretion via inhibition of ATP-dependent K+ channels. *Biochem Biophys Res Commun* 310:274-279, 2003
17. Jacobson,DA, Weber,CR, Bao,S, Turk,J, Philipson,LH: Modulation of the pancreatic islet beta-cell-delayed rectifier potassium channel Kv2.1 by the polyunsaturated fatty acid arachidonate. *J Biol Chem* 282:7442-7449, 2007
18. Ramanadham,S, Turk,J: omega-Conotoxin inhibits glucose- and arachidonic acid-induced rises in intracellular [Ca2+] in rat pancreatic islet beta-cells. *Cell Calcium* 15:259-264, 1994

19. Itoh,Y, Kawamata,Y, Harada,M, Kobayashi,M, Fujii,R, Fukusumi,S, Ogi,K, Hosoya,M, Tanaka,Y, Uejima,H, Tanaka,H, Maruyama,M, Satoh,R, Okubo,S, Kizawa,H, Komatsu,H, Matsumura,F, Noguchi,Y, Shinohara,T, Hinuma,S, Fujisawa,Y, Fujino,M: Free fatty acids regulate insulin secretion from pancreatic beta cells through GPR40. *Nature* 422:173-176, 2003
20. Fujiwara,K, Maekawa,F, Yada,T: Oleic acid interacts with GPR40 to induce Ca2+ signaling in rat islet beta-cells: mediation by PLC and L-type Ca2+ channel and link to insulin release. *Am J Physiol Endocrinol Metab* 289:E670-E677, 2005
21. Watanabe,H, Vriens,J, Prenen,J, Droogmans,G, Voets,T, Nilius,B: Anandamide and arachidonic acid use epoxyeicosatrienoic acids to activate TRPV4 channels. *Nature* 424:434-438, 2003
22. Chyb,S, Raghu,P, Hardie,RC: Polyunsaturated fatty acids activate the Drosophila light-sensitive channels TRP and TRPL. *Nature* 397:255-259, 1999
23. Putney,JW, Jr.: Pharmacology of capacitative calcium entry. *Mol Interv* 1:84-94, 2001
24. Putney,JW: Capacitative calcium entry: from concept to molecules. *Immunol Rev* 231:10-22, 2009
25. Qian,F, Huang,P, Ma,L, Kuznetsov,A, Tamarina,N, Philipson,LH: TRP genes: candidates for nonselective cation channels and store-operated channels in insulin-secreting cells. *Diabetes* 51 Suppl 1:S183-S189, 2002
26. Hughes,E, Lee,AK, Tse,A: Dominant role of sarcoendoplasmic reticulum Ca2+-ATPase pump in Ca2+ homeostasis and exocytosis in rat pancreatic beta-cells. *Endocrinology* 147:1396-1407, 2006
27. Dyachok,O, Gylfe,E: Store-operated influx of $Ca^{2+}$ in pancreatic beta-cells exhibits graded dependence on the filling of the endoplasmic reticulum. *J Cell Sci* 114:2179-2186, 2001
28. Mignen,O, Shuttleworth,TJ: I(ARC), a novel arachidonate-regulated, noncapacitative Ca(2+) entry channel. *J Biol Chem* 275:9114-9119, 2000
29. Mignen,O, Thompson,JL, Shuttleworth,TJ: Ca2+ selectivity and fatty acid specificity of the noncapacitative, arachidonate-regulated Ca2+ (ARC) channels. *J Biol Chem* 278:10174-10181, 2003
30. Holmes,AM, Roderick,HL, McDonald,F, Bootman,MD: Interaction between store-operated and arachidonate-activated calcium entry. *Cell Calcium* 41:1-12, 2007
31. Yoo,AS, Cheng,I, Chung,S, Grenfell,TZ, Lee,H, Pack-Chung,E, Handler,M, Shen,J, Xia,W, Tesco,G, Saunders,AJ, Ding,K, Frosch,MP, Tanzi,RE, Kim,TW: Presenilin-mediated modulation of capacitative calcium entry. *Neuron* 27:561-572, 2000
32. Mignen,O, Thompson,JL, Yule,DI, Shuttleworth,TJ: Agonist activation of arachidonate-regulated Ca2+-selective (ARC) channels in murine parotid and pancreatic acinar cells. *J Physiol* 564:791-801, 2005
33. Roos,J, DiGregorio,PJ, Yeromin,AV, Ohlsen,K, Lioudyno,M, Zhang,S, Safrina,O, Kozak,JA, Wagner,SL, Cahalan,MD, Velicelebi,G, Stauderman,KA: STIM1, an essential and conserved component of store-operated Ca2+ channel function. *J Cell Biol* 169:435-445, 2005
34. Liou,J, Kim,ML, Heo,WD, Jones,JT, Myers,JW, Ferrell,JE, Jr., Meyer,T: STIM is a Ca2+ sensor essential for Ca2+-store-depletion-triggered Ca2+ influx. *Curr Biol* 15:1235-1241, 2005
35. Manji,SS, Parker,NJ, Williams,RT, Van,SL, Pearson,RB, Dziadek,M, Smith,PJ: STIM1: a novel phosphoprotein located at the cell surface. *Biochim Biophys Acta* 1481:147-155, 2000

36. Mignen,O, Thompson,JL, Shuttleworth,TJ: STIM1 regulates Ca2+ entry via arachidonate-regulated Ca2+-selective (ARC) channels without store depletion or translocation to the plasma membrane. *J Physiol* 579:703-715, 2007
37. Gwack,Y, Srikanth,S, Feske,S, Cruz-Guilloty,F, Oh-Hora,M, Neems,DS, Hogan,PG, Rao,A: Biochemical and functional characterization of Orai proteins. *J Biol Chem* 282:16232-16243, 2007
38. Mignen,O, Thompson,JL, Shuttleworth,TJ: Both Orai1 and Orai3 are essential components of the arachidonate-regulated Ca2+-selective (ARC) channels. *J Physiol* 586:185-195, 2008
39. Hewavitharana,T, Deng,X, Soboloff,J, Gill,DL: Role of STIM and Orai proteins in the store-operated calcium signaling pathway. *Cell Calcium* 42:173-182, 2007
40. Ramanadham,S, Gross,RW, Han,X, Turk,J: Inhibition of arachidonate release by secretagogue-stimulated pancreatic islets suppresses both insulin secretion and the rise in beta-cell cytosolic calcium ion concentration. *Biochemistry* 32:337-346, 1993
41. Fujiwara,K, Maekawa,F, Yada,T: Oleic acid interacts with GPR40 to induce Ca2+ signaling in rat islet beta-cells: mediation by PLC and L-type Ca2+ channel and link to insulin release. *Am J Physiol Endocrinol Metab* 289:E670-E677, 2005
42. Tobias,LD, Hamilton,JG: The effect of 5,8,11,14-eicosatetraynoic acid on lipid metabolism. *Lipids* 14:181-193, 1979
43. Wolf,BA, Turk,J, Sherman,WR, McDaniel,ML: Intracellular Ca2+ mobilization by arachidonic acid. Comparison with myo-inositol 1,4,5-trisphosphate in isolated pancreatic islets. *J Biol Chem* 261:3501-3511, 1986
44. Woolcott,OO, Gustafsson,AJ, Dzabic,M, Pierro,C, Tedeschi,P, Sandgren,J, Bari,MR, Nguyen,KH, Bianchi,M, Rakonjac,M, Radmark,O, Ostenson,CG, Islam,MS: Arachidonic acid is a physiological activator of the ryanodine receptor in pancreatic beta-cells. *Cell Calcium* 39:529-537, 2006
45. Bootman,MD, Collins,TJ, Mackenzie,L, Roderick,HL, Berridge,MJ, Peppiatt,CM: 2-aminoethoxydiphenyl borate (2-APB) is a reliable blocker of store-operated Ca2+ entry but an inconsistent inhibitor of InsP3-induced Ca2+ release. *FASEB J* 16:1145-1150, 2002
46. Shuttleworth,TJ, Thompson,JL, Mignen,O: ARC channels: a novel pathway for receptor-activated calcium entry. *Physiology (Bethesda )* 19:355-361, 2004
47. Missiaen,L, Callewaert,G, De,SH, Parys,JB: 2-Aminoethoxydiphenyl borate affects the inositol 1,4,5-trisphosphate receptor, the intracellular Ca2+ pump and the non-specific Ca2+ leak from the non-mitochondrial Ca2+ stores in permeabilized A7r5 cells. *Cell Calcium* 29:111-116, 2001
48. Peppiatt,CM, Collins,TJ, Mackenzie,L, Conway,SJ, Holmes,AB, Bootman,MD, Berridge,MJ, Seo,JT, Roderick,HL: 2-Aminoethoxydiphenyl borate (2-APB) antagonises inositol 1,4,5-trisphosphate-induced calcium release, inhibits calcium pumps and has a use-dependent and slowly reversible action on store-operated calcium entry channels. *Cell Calcium* 34:97-108, 2003
49. Pusch,M, Neher,E: Rates of diffusional exchange between small cells and a measuring patch pipette. *Pflugers Arch* 411:204-211, 1988
50. Mignen,O, Shuttleworth,TJ: Permeation of monovalent cations through the non-capacitative arachidonate-regulated Ca2+ channels in HEK293 cells. Comparison with endogenous store-operated channels. *J Biol Chem* 276:21365-21374, 2001
51. Shuttleworth,TJ, Thompson,JL: Muscarinic receptor activation of arachidonate-mediated Ca2+ entry in HEK293 cells is independent of phospholipase C. *J Biol Chem* 273:32636-32643, 1998

52. Antunes,CM, Salgado,AP, Rosario,LM, Santos,RM: Differential patterns of glucose-induced electrical activity and intracellular calcium responses in single mouse and rat pancreatic islets. *Diabetes* 49:2028-2038, 2000
53. Manning Fox,JE, Gyulkhandanyan,AV, Satin,LS, Wheeler,MB: Oscillatory membrane potential response to glucose in islet beta-cells: a comparison of islet-cell electrical activity in mouse and rat. *Endocrinology* 147:4655-4663, 2006

# Chapter 4

## Arachidonic acid stimulates intracellular $Ca^{2+}$ release from $IP_3$-sensitive acidic and ER stores in rat pancreatic β cells

## 4.1 Introduction

### *4.1.1 Regulation of $Ca^{2+}$ release and uptake in ER*

Multiple functional $Ca^{2+}$ stores exist in β cells, including the ER and a novel $Ca^{2+}$ store associated with an acidic organelle. Although reports about the characteristics of the acidic $Ca^{2+}$ store are still emerging, the mechanisms underlying $Ca^{2+}$ release and $Ca^{2+}$ uptake from the ER are relatively well-studied. $Ca^{2+}$ release from the ER is mediated by two types of receptors, inositol 1,4,5-trisphosphate receptors ($IP_3Rs$) and ryanodine receptors (RyRs). $IP_3Rs$ have a ligand-binding domain, which contains a binding site for $IP_3$; a regulatory domain, which contains binding sites for $Ca^{2+}$; and a pore-forming (channel) domain. Activation of $IP_3Rs$ requires $IP_3$, which is produced by agonist stimulation of G-protein-coupled receptors that are associated with phospholipase C (PLC), such as the $M_1$ and $M_3$ muscarinic receptors (1) and $P_2Y$ receptors (2). PLC catalyzes the hydrolysis of phosphatidylinositol-4.5-bisphosphate ($PIP_2$), producing $IP_3$ and diacylglycerol (DAG). $IP_3$ then binds to the $IP_3R$ channels, releasing $Ca^{2+}$. $IP_3$-mediated $Ca^{2+}$ release via $IP_3R$ is modulated by cytosolic $Ca^{2+}$. Its effects are biphasic: at nanomolar [$Ca^{2+}$], the open probability of the channel is increased, but at micromolar [$Ca^{2+}$], the open probability of the channel is decreased (3). $IP_3Rs$, of which there are three mammalian isoforms ($IP_3R1$, $IP_3R2$, and $IP_3R3$), have been detected in mouse (4), rat (5) and human islets (6), as well as insulin-secreting cell lines (7). The three $IP_3R$ isoforms differ in their binding affinities for $IP_3$ and for $Ca^{2+}$; $IP_3R3$, for example, has the lowest affinity for $IP_3$ and the highest affinity for $Ca^{2+}$ (8;9). Although all three isoforms are

expressed to some extent in all cell types, one isoform may predominate. RINm5f cells, for example, preferentially express $IP_3R3$ (10). RyRs are cation-selective channels made up of four pore-forming subunits and four associated molecules known as FK506-binding proteins (FKBPs). The FKBPs stabilize the pore-forming subunits and facilitate channel gating (11). Three isoforms of RyR (RyR1, RyR2, and RyR3) have been identified. Expression of both RyR2 and RyR3 (but not RyR1, which is present mainly in skeletal muscle) has been reported in mouse (12), rat (13), and human islets (13;14), although some studies have failed to find any evidence of RyR receptor activity in β cells (e.g. in mouse (15)). Physiologically, RyRs can be activated by cytosolic $Ca^{2+}$ and by cyclic adenosine diphosphoribose (cADPR) (11;12;16;17). The activation of RyR by $Ca^{2+}$ is biphasic: at nanomolar [$Ca^{2+}$], RyR is activated by $Ca^{2+}$, but at millimolar [$Ca^{2+}$], it is inhibited by $Ca^{2+}$ (18). It has been shown that cADPR, which is a metabolite of β-nicotinamide adenine dinucleotide (β-$NAD^+$), acts only on nonskeletal isoforms of RyR (i.e. RyR2 and RyR3). There is disagreement as to whether cADPR acts directly at the receptor or through an accessory protein such as FKBP (11;16;17). RyRs are so named because they can be activated by low concentrations of ryanodine (<1 μM), a plant alkaloid, but high concentrations of ryanodine (>10 μM) have an inhibitory effect on RyR (19). Due to their regulation by $Ca^{2+}$, both $IP_3Rs$ and RyRs may mediate $Ca^{2+}$-induced $Ca^{2+}$ release (CICR) in β cells, wherein $Ca^{2+}$ promotes its own release from intracellular $Ca^{2+}$ stores (13;20;21). One important function of CICR in β cells is the amplification of $Ca^{2+}$-dependent exocytosis. In INS-1 cells, for example, CICR produces a

global increase in $[Ca^{2+}]_i$ that recruits secretory granules and results in more synchronized granule release, and thus enhances $Ca^{2+}$-dependent exocytosis (22).

Uptake of $Ca^{2+}$ into the ER is primarily under the control of the sarco/endoplasmic reticulum $Ca^{2+}$-ATPase (SERCA) pump, a P-type ATPase that is inhibited by thapsigargin, tert-butylhydroquinone (BHQ), or cyclopiazonic acid (CPA). Of the four isoforms of SERCA that have been described (SERCA1, SERCA2a, SERCA2b, and SERCA3), only two, SERCA2b and SERCA3, are expressed in rat and human islets (23). Activity of SERCA2b, but not SERCA3, is critical for normal $Ca^{2+}$ handling in β cells. In MIN6 cells, ablating expression of SERCA2b (by injection of targeted antisense oligonucleotides) decreased the amount of $Ca^{2+}$ releasable from the ER, while ablating SERCA3 expression had no effect on the size of the ER $Ca^{2+}$ store (24). Although the β cell has several mechanisms for $Ca^{2+}$ clearance, it has been shown that SERCA pumps are dominant. For example, in mouse (25) and rat (26) β cells, inhibitors of SERCA pumps have been shown to cause a dramatic slowing in the rate of cytosolic $Ca^{2+}$ removal, indicating that SERCA is the principal mechanism of cytosolic $Ca^{2+}$ clearance in β cells.

### *4.1.2 Evidence for an acidic $Ca^{2+}$ store in β cells*

In many cell types, there is mounting evidence that $Ca^{2+}$ can be released from intracellular stores that are associated with acidic organelles. The organelles known to have an acidic pH (<7) are the lysosomes, endosomes and the secretory granules (27). In general, the acidic stores are defined as $Ca^{2+}$ stores that are

sensitive to bafilomycin A1 or glycyl-phenylalanyl-β-naphthylamide (GPN). Bafilomycin A1 reduces the activity of the V-type (vacuolar) $H^+$-ATPase and thus disrupts the pH gradient in acidic organelles (28). GPN is a substrate of the lysosomal hydrolase cathepsin C. The accumulation of GPN inside the lysosomes leads to their osmotic swelling and collapse (29). Although GPN is typically used to lyse lysosomes, it has also been shown to cause lysis of secretory granules (30). Thus, at present, there is no specific pharmacological agent to differentiate between $Ca^{2+}$ release from the different acidic organelles. Nicotinic acid adenine dinucleotide phosphate (NAADP), which was originally discovered to mobilize $Ca^{2+}$ from a lysosome-related organelle in sea urchin eggs (31), has been postulated to be the messenger for the triggering of $Ca^{2+}$ release from acidic stores. In mammalian cells, NAADP displays a bell-shaped concentration-response curve; that is, at low concentrations (~100 nM) it releases $Ca^{2+}$ from the lysosomal stores, but at high concentrations (~100 μM), it inhibits $Ca^{2+}$ release (32;33). NAADP was recently shown to gate the two-pore channels (TPCs) in endosomal and lysosomal membranes (34). However, other NAADP-sensitive $Ca^{2+}$-permeable channels, such as the transient receptor potential channel, melastatin subfamily type 2 (TRPM2), have been detected on the lysosomal compartments of INS-1 cells (35). Other than the lysosomal and endosomal compartments, NAADP has also been reported to release $Ca^{2+}$ from the secretory granules in permeabilized pancreatic acinar cells (36), as well as permeabilized MIN6 cells (37).

NAADP was reported to trigger a $Ca^{2+}$ signal in human β cells, and NAADP at high concentration was found to reduce insulin-induced $[Ca^{2+}]_i$ rise (33). In MIN6 cells, glucose stimulation caused an increase in cellular [NAADP] and application of intracellular NAADP causes $[Ca^{2+}]_i$ rise (32). The glucose-stimulated $[Ca^{2+}]_i$ rise in MIN6 cells was reduced by a high concentration (100 μM) of NAADP (32), suggesting the possible involvement of a NAADP-sensitive store in glucose-mediated $Ca^{2+}$ signaling. However, the significance of NAADP-mediated $Ca^{2+}$ signaling in β cells remains controversial. In mouse β cells, intracellular application of NAADP caused only a very small rise (< 80 nM) in basal $[Ca^{2+}]_i$ (30). Application of intracellular NAADP also failed to affect the organellar $[Ca^{2+}]$ in the organelles of permeabilized mouse β cells (15). Nevertheless, there is some evidence suggesting the presence of an acidic $Ca^{2+}$ store in β cells. In mouse β cells, ~92% of the organelle $Ca^{2+}$ was found to be present in an acidic store that could be mobilized by a combination of $Ca^{2+}$ ionophore and protonophore (15). $Ca^{2+}$ release from a GPN-sensitive acidic $Ca^{2+}$ store could be detected in mouse β cells during the decay phase of the $Ca^{2+}$ signal following a large $Ca^{2+}$ load (30 s of stimulation with high KCl) (30). GLP-1-induced potentiation of glucose-stimulated insulin secretion was ablated by pretreatment with GPN or bafilomycin A1 (38).

Several studies have raised the possibility that the secretory granule is the functional acidic $Ca^{2+}$ store in β cells. In mouse β cells, the size of the readily releasable pool of granules was reduced by GPN treatment (30). In rat β cells, the amount of exocytosis evoked by exogenous ATP (possibly via $P_2Y$ receptors) was

drastically reduced by the combined treatment of $Ca^{2+}$ ionophore and protonophore (39). The secretory granules collectively constitute a large source of $Ca^{2+}$ and their $Ca^{2+}$ content has been estimated to be 30-90 μM (40). While the $Ca^{2+}$ in secretory granules is known to contribute to the packaging and processing of intravesicular content (41-43), there is increasing evidence that the $Ca^{2+}$ in granules may be mobilized under physiological conditions. In chromaffin cells, for example, $Ca^{2+}$ release from isolated chromaffin granules can be triggered with $IP_3$, suggesting the presence of $IP_3R$ on chromaffin granules (44-46). A functional $Ca^{2+}$ store associated with secretory granules was demonstrated by Blondel *et al*. in βTC3 cells overexpressing $IP_3$ receptor subtype 3 ($IP_3R3$) (47). A follow-up immunohistochemistry study "demonstrated" that $IP_3R3$ was localized to secretory granules of rat islets (48), but the antibody used in that study was subsequently shown to have cross-reactivity with insulin (49). However, a later study revealed the presence of $IP_3Rs$ in the secretory granules of mouse pancreatic β cells (4). In rat β cells, exocytosis induced by activation of $P_2Y$ receptors was blocked by 2-APB (an $IP_3R$ inhibitor) in combination with ionomycin and monensin, indicating that there may be an $IP_3$-sensitive store associated with the secretory granules (39). In permeabilized MIN6 cells, $IP_3$ failed to release $Ca^{2+}$ from aequorin-labelled secretory granules (40), but either ryanodine or intracellular NAADP could trigger $Ca^{2+}$ release from the granules (37;40). In permeabilized acinar cells, however, $Ca^{2+}$ release from the secretory granules can be activated by NAADP, cADPR or $IP_3$ (36). Thus, depending on

the cell type, $Ca^{2+}$ release from secretory granules can be triggered via the activation of $IP_3$, ryanodine or NAADP receptors.

In MIN6 cells with aequorin-targeted secretory granules, Mitchell *et al*. found that $Ca^{2+}$ accumulates in the granules upon stimulation of the cells with glucose or other nutrient insulin secretagogues (40), suggesting that $Ca^{2+}$ uptake into the secretory granules may play a role in maintaining $Ca^{2+}$ homeostasis. The mechanism of $Ca^{2+}$ uptake into the secretory granules is not well understood. The secretory pathway $Ca^{2+}$-ATPase (SPCA) is postulated to be important for $Ca^{2+}$ accumulation in secretory granules. Two human isoforms of SPCA, SPCA1 and SPCA2, have been identified. SPCA1 is postulated to be a housekeeping enzyme, whereas SPCA2 may have a role in the regulated secretory pathway (50). SPCA1 immunoreactivity has been identified in ER, Golgi, and dense-core-granule-associated membranes in β-cell-derived cell lines (51). SPCA1 is relatively insensitive to the SERCA pump inhibitor thapsigargin (e.g. $K_d$ of ~28 μM), but SPCA2 has a $K_d$ of ~ 2μM for thapsigargin (50). It is controversial whether the $Ca^{2+}$ uptake into the secretory granules is sensitive to thapsigargin. In MIN6 cells, $Ca^{2+}$ uptake into the secretory granules could not be inhibited by the conventional SERCA pump inhibitors thapsigargin or CPA (40). However, in both chromaffin and PC12 cells, $Ca^{2+}$ accumulation in the granules was reduced by SERCA pump inhibitors (52;53).

### *4.1.3 Effects of AA on intracellular $Ca^{2+}$ release*

In addition to triggering extracellular $Ca^{2+}$ influx, AA causes release of $Ca^{2+}$ from intracellular stores (54-56). AA elicited $Ca^{2+}$ efflux from ER in permeabilized rat islets (57), and from isolated sarcoplasmic reticulum (58). Woolcott *et al*. demonstrated in INS-1 cells that the $[Ca^{2+}]_i$ rise induced by AA (150 μM) in the presence of extracellular $Ca^{2+}$ was abolished by pretreatment with thapsigargin or when ryanodine receptors were inhibited by treatment with caffeine and a high concentration of ryanodine (59). However, the study by Woolcott *et al*. did not differentiate between the intracellular $Ca^{2+}$ release component and the extracellular $Ca^{2+}$ entry component of the AA-mediated response, and activation of RyRs in INS-1 cells has been reported to activate TRP channels on the plasma membrane resulting in depolarization (60). Thus, it is unclear whether the inhibitory action of ryanodine on the AA response was due to an inhibition of $Ca^{2+}$ release from RyR stores or a suppression of the TRP-mediated depolarization. Since β cells may have multiple intracellular $Ca^{2+}$ stores, including the acidic $Ca^{2+}$ stores, $IP_3$-sensitive ER stores and ryanodine-sensitive stores, this chapter of my thesis endeavours to characterize the involvement of the different $Ca^{2+}$ stores in the AA-induced intracellular $Ca^{2+}$ release. We found that the AA-mediated intracellular $Ca^{2+}$ release was attenuated by the disruption of acidic $Ca^{2+}$ stores and the emptying of the $IP_3$-sensitive stores essentially abolished the AA response. Our findings indicate that the ~70% of the AA-mediated intracellular $Ca^{2+}$ release arises from the mobilization of $Ca^{2+}$ from

an acidic store that is gated by $IP_3R$ (possibly the secretory granules) and the remaining ~30% comes from an $IP_3$-sensitive ER store.

## 4.2 Results

### *4.2.1 AA causes intracellular $Ca^{2+}$ release in rat $\beta$ cells in a dose-dependent manner*

Previous studies have shown that AA stimulated $Ca^{2+}$ release from intracellular stores in insulin-secreting cells (57;59). Consistent with this, we found that in the absence of extracellular $Ca^{2+}$, exogenous AA (15 μM) evoked a transient $[Ca^{2+}]_i$ rise. In the example shown in Figure 4-1A, individual cells were voltage-clamped at -70 mV in the presence of 5 mM extracellular $Ca^{2+}$. Upon switching to a $Ca^{2+}$-free extracellular solution (which also contained 1 mM of the $Ca^{2+}$ chelator, EGTA), the basal $[Ca^{2+}]_i$ declined by 0.13 ± 0.05 μM (n = 33). Following the application of AA (15 μM in the $Ca^{2+}$-free solution), $[Ca^{2+}]_i$ rose to ~1.6 μM, reflecting $Ca^{2+}$ release from intracellular stores. Despite the continued presence of AA, the AA-mediated $Ca^{2+}$ signal started to decline after it reached a peak, indicating the termination of intracellular $Ca^{2+}$ release. In ~18% of the cells challenged with 15 μM AA (4 out 22 cells), the AA-mediated $Ca^{2+}$ signal was biphasic: a small plateau elevation in $[Ca^{2+}]_i$ was followed by a rapid and larger $[Ca^{2+}]_i$ rise (e.g. Figure 4-1B). Figure 4-1C summarizes the results obtained from cells recorded with the same experimental protocol as in Figure 4-1A. In these cells, the mean amplitude of the $Ca^{2+}$ signal triggered by AA (15 μM) in the $Ca^{2+}$-free extracellular solution was 1.62 ± 0.31 μM (n = 16). At lower concentrations

(5 and 10 μM), AA could still trigger a $[Ca^{2+}]_i$ rise, though the amplitudes were smaller (0.30 ± 0.08 μM, n = 12 and 0.84 ± 0.57 μM, n = 5, respectively; Figure 4-1B). These observations suggest that the AA-mediated $Ca^{2+}$ signal includes a component of $Ca^{2+}$ release from intracellular stores, and that this component is concentration-dependent. Since the AA-induced $Ca^{2+}$ signal in the absence of extracellular $Ca^{2+}$ was more robust at 15 μM AA, this concentration was used for all subsequent experiments.

AA is rapidly metabolized in the cell into a variety of eicosanoid products. To determine whether the effect on intracellular $Ca^{2+}$ release was due to AA itself or to one of its metabolites, we examined the actions of eicosatetraynoic acid (ETYA), a non-metabolizable analog of AA that is a blocker of lipoxygenase, cyclooxygenase, and P450 pathways for AA metabolism (57;59;61). In this experiment, single islet cells were loaded with fura-2 AM and $[Ca^{2+}]_i$ was monitored with fura-2 digital imaging. Figure 4-2 shows that the mean increase in $[Ca^{2+}]_i$ evoked by 15 or 30 μM ETYA in the absence of extracellular $Ca^{2+}$ was not significantly different from that evoked by 15 μM AA. Thus, the action of AA on intracellular $Ca^{2+}$ release does not require AA metabolism.

### *4.2.2 AA-induced intracellular $Ca^{2+}$ release is not mediated by RyRs*

We first examined the involvement of the ryanodine-sensitive store because a previous study reported that, in INS-1 cells, inhibition of RyRs could abolish the AA-induced $Ca^{2+}$ signal (both the intracellular $Ca^{2+}$ release component and extracellular $Ca^{2+}$ entry components) (59). To inhibit $Ca^{2+}$ release via RyRs, we

incubated single rat islet cells with caffeine (10 mM), a RyR activator, and ryanodine (at 100 μM, a concentration that inhibits RyRs) (19) for 1 hour at 37°C. This protocol was employed because it has been reported that ryanodine cannot bind to the RyR (and thus cannot inhibit $Ca^{2+}$ release from the RyR) unless they have been previously activated (by caffeine, for example) (62). Moreover, the same protocol has been shown to inhibit the AA-mediated $Ca^{2+}$ signal in INS-1 cells (59). In our experiment, ryanodine (100 μM) was also included in the whole-cell pipette solution. In all the following experiments, single β cells were voltage-clamped at -70 mV in a $Ca^{2+}$-free external solution before challenge with AA (15 μM). As shown in Figure 4-3, the inhibition of RyRs did not reduce the AA-mediated intracellular $Ca^{2+}$ release. The mean amplitude of the $[Ca^{2+}]_i$ rise induced by AA in cells pretreated with caffeine and ryanodine was 1.39 ± 0.26 μM (n = 9), which was not significantly different from the controls (Figure 4-3B). Thus, in contrast to INS-1 cells, there was no significant contribution of RyRs to the AA-mediated intracellular $Ca^{2+}$ release from rat β cells .

### *4.2.3 AA triggers $Ca^{2+}$ release from a non-lysosomal acidic store*

We next examined whether acidic $Ca^{2+}$ stores contribute to the effect of AA on intracellular $Ca^{2+}$ release. Bafilomycin A1 and GPN are widely used to disrupt acidic stores, and have previously been used to investigate $Ca^{2+}$ release from acidic organelles in rat (39) and mouse (30) β cells. In this experiment, cells were pretreated with bafilomycin A1 (2 μM) for 15 minutes at 37°C. Single cells were voltage-clamped at -70 mV and the same concentration of bafilomycin A1

was included in the whole-cell pipette solution. As shown by the example in Figure 4-4A, AA (15 μM) triggered a smaller $Ca^{2+}$ signal (~0.5 μM) in a bafilomycin-treated cell. In 6 cells pretreated with bafilomycin A1, the AA-induced $[Ca^{2+}]_i$ rise was 0.36 ± 0.08 μM, which was significantly smaller than the controls (Figure 4-4C). A reduction of the AA-mediated intracellular $Ca^{2+}$ release was also found in cells pretreated with GPN (e.g. Figure 4-4B). For 5 cells pretreated with GPN (50 μM) for 1 hour at 37°C , the mean amplitude of the AA-induced $[Ca^{2+}]_i$ rise was only 0.59 ± 0.26 μM, which was significantly smaller than the controls (Figure 4-4C). Since both bafilomycin A1 and GPN target organelles with acidic pH, these results indicate that the action of AA involves $Ca^{2+}$ release from an acidic store.

In the β cell, there are several organelles with an acidic pH, including the Golgi apparatus, lysosomes/endosomes, and the secretory granules (27). Bafilomycin A1 inhibits the V-type $H^+$-ATPase that acidifies several organelles, including the Golgi and the secretory granules (27), and GPN has been reported to act on both lysosomes (29) and secretory granules (30). Thus, AA may evoke $Ca^{2+}$ release from one or multiple acidic $Ca^{2+}$ stores in β cells. To investigate the possibility that AA mediates $Ca^{2+}$ release from a lysosomal compartment, we examined whether the triggering of $Ca^{2+}$ release from lysosomal $Ca^{2+}$ stores could affect the AA-mediated intracellular $Ca^{2+}$ release. Since adenosine diphosphoribose (ADPR) was reported to evoke $Ca^{2+}$ release from the lysosomal compartments of INS-1 cells via activation of TRPM2 channels (35), we applied ADPR (1 mM) to the cell interior via whole-cell dialysis. As shown in the

example in Figure 4-5A, intracellular dialysis of ADPR did not evoke any transient $[Ca^{2+}]_i$ rise and AA (15 μM) could still evoke a robust $Ca^{2+}$ response. In 6 cells examined with intracellular dialysis of ADPR, the amplitude of the AA-evoked $Ca^{2+}$ signal was not significantly different from the controls (Figure 4-5C). We also employed NAADP, which was shown to gate the TPCN2 channel in endosomal and lysosomal membranes (34) and to cause $Ca^{2+}$ release in MIN6 cells (32;37). As shown in the example in Figure 4-5B, whole-cell dialysis of NAADP (100 nM) did not cause any $[Ca^{2+}]_i$ rise and did not attenuate the AA-induced intracellular $[Ca^{2+}]_i$ release (summarized in Figure 4-5C). It is perhaps not surprising that neither ADPR nor NAADP alone had any major effect on $[Ca^{2+}]_i$, since the participation of TRPM2 or TPCN2 channels in physiological $Ca^{2+}$ signalling, and indeed even their expression levels, in rat β cells is controversial. On the other hand, it is possible that the $Ca^{2+}$ release from the lysosomal stores is small and slow with intracellular dialysis of ADPR or NAADP, such that the $Ca^{2+}$ release was balanced by cytosolic $Ca^{2+}$ removal mechanisms. Nevertheless, the failure of intracellular ADPR or NAADP to reduce the AA-mediated $Ca^{2+}$ signal suggests that the lysosomal $Ca^{2+}$ store does not contribute significantly to the AA-mediated $Ca^{2+}$ signaling.

### *4.2.4 The involvement of $IP_3$-sensitive stores in the AA response*

In both mouse (30) and rat β cells (39), the secretory granules are an important acidic $Ca^{2+}$ store. A previous study in rat β cells has suggested that extracellular ATP mobilizes $Ca^{2+}$ from an $IP_3$-sensitive store that is associated

with the secretory granules (39). Therefore, we investigated whether the emptying of the ATP-sensitive stores could attenuate the AA response. In this experiment, single β cells were bathed continuously in a $Ca^{2+}$-free bath solution and voltage-clamped at -70 mV. Individual cells were first challenged with ATP (100 μM) and then with AA (15 μM). As shown in the example in Figure 4-6A, extracellular ATP triggered a transient $[Ca^{2+}]_i$ rise, and subsequent challenge with AA to the same cell triggered only a very small $[Ca^{2+}]_i$ rise. In 10 cells examined, ATP evoked a transient $[Ca^{2+}]_i$ rise (0.34 ± 0.12 μM), and a subsequent challenge with AA only elevated $[Ca^{2+}]_i$ by 0.11 ± 0.03 μM (Figure 4-6C). Since the SERCA pump inhibitor, thapsigargin was reported to attenuate the ATP-mediated $Ca^{2+}$ response in rat β cells (39), we tested whether thapsigargin affected the AA response. An example of such an experiment is shown in Figure 4-6B. Treatment with thapsigargin (1 μM) dramatically reduced the AA-mediated $Ca^{2+}$ signal. In 12 cells examined, the AA-induced intracellular $Ca^{2+}$ release was reduced to 0.21 ± 0.07 μM (Figure 4-6C). Thus, our results show that AA and ATP trigger $Ca^{2+}$ release from the same intracellular stores, and these stores can be depleted by SERCA pump inhibitor.

In rat β cells, the ATP-triggered intracellular $Ca^{2+}$ release is mediated via $P_2Y$ receptors, which are coupled to the PLC pathway and the generation of $IP_3$. Therefore, we examined whether the depletion of $IP_3$-sensitive stores could attenuate the AA response. In this experiment, we employed adenophostin A, which is the most potent known agonist of $IP_3$Rs, and whose activity is 100-fold more potent than that of $IP_3$ (63). When adenophostin A (2 μM) was dialysed

into single rat β cell via the whole-cell pipette (e.g. Figure 4-7A), there was a transient rise in basal $[Ca^{2+}]_i$, reflecting the emptying of the $IP_3$-sensitive stores. Note that a subsequent challenge with AA (15 μM) in the same cell evoked only a small $Ca^{2+}$ response. On average, the emptying of the $IP_3$-sensitive stores by adenophostin reduced the AA-induced $Ca^{2+}$ signal to 0.14 ± 0.06 μM (Figure 4-7C). The dramatic reduction of the AA response (~90%) by adenophostin raises the possibility that the acidic store is sensitive to $IP_3$. Consistent with this notion, we found that in cells pretreated with bafilomycin (2 μM) for 15 mins at 37$^{o}$C and then whole-cell dialysed with a combination of adenophostin and bafilomycin, the inhibition in the AA-mediated $Ca^{2+}$ signal was not statistically different from that of adenophostin alone (Figure 4-7B & C). Figure 4-8 summarizes the relative inhibition of the AA (15 μM)-mediated $Ca^{2+}$ signal (in a $Ca^{2+}$-free external solution) by the various pharmacological agents. The disruption of the acidic $Ca^{2+}$ stores by bafilomycin A1 or GPN reduced the AA response by ~78% and ~63% respectively. The emptying of the $IP_3$-sensitive stores by adenophostin A or the SERCA pump inhibitor thapsigargin reduced the AA response by ~90%. Exogenous ATP, which was postulated to mobilize $Ca^{2+}$ from the $IP_3$-sensitive ER and acidic secretory granules, reduced the AA response to ~7% of the controls. The AA response was smallest in cells treated with ATP (7% of that in controls) or with bafilomycin A1 and adenophostin A (< 3% of the controls) but this value is not significantly different from either the adenophostin or thapsigargin treatment. Overall, these results support the idea that AA induces

$Ca^{2+}$ release from multiple $IP_3$-sensitive stores, including the ER and the acidic store.

### 4.3 Discussion

Our results show that low concentrations of AA (5-15 μM) can stimulate intracellular $Ca^{2+}$ release in rat β cells (Figure 4-1). This effect of AA does not require AA metabolism because it can be mimicked by ETYA, a non-metabolizable analog of AA (Figure 4-2). We found that ~70% of the AA-mediated intracellular $Ca^{2+}$ release was abolished when the acidic $Ca^{2+}$ stores were disrupted with bafilomycin A1 or GPN (Figure 4-3), suggesting that a large fraction of the AA-mediated intracellular $Ca^{2+}$ release was due to the mobilization of $Ca^{2+}$ from an acidic store. Lysosomes occupy only 0.4% of the cellular volume in β cells (64). In view of the large amplitude (~1.6 μM) of the $Ca^{2+}$ signal when triggered by AA (15 μM), it is unlikely that the lysosomal $Ca^{2+}$ store is the source of $Ca^{2+}$ for the AA response. Consistent with this, neither intracellular ADPR nor NAADP was able to attenuate the AA-mediated intracellular $Ca^{2+}$ release (Figure 4-4).

We found that the AA-mediated intracellular $Ca^{2+}$ release was essentially abolished by the depletion of $IP_3$-sensitive stores with adenophostin A (Figure 4-8). Since $Ca^{2+}$ release from the acidic stores comprised ~70% of the AA-mediated $Ca^{2+}$ signal, we proposed that the AA-sensitive acidic store was gated by $IP_3R$. We speculate that the AA-sensitive acidic $Ca^{2+}$ store is the secretory granules for the following reasons. First, the secretory granules occupy ~15% of

the cell volume (64) and their $Ca^{2+}$ content was estimated to be 30-90 μM (40). Thus, the secretory granules can release the quantities of $Ca^{2+}$ needed to elevate $[Ca^{2+}]_i$ to the μM range when challenged with AA. Second, exogenous ATP was reported to stimulate exocytosis in rat β cells by mobilizing $Ca^{2+}$ release from the secretory granules via the activation of $IP_3R$ (39). We found that the AA-mediated intracellular $Ca^{2+}$ release was largely abolished when cells were pretreated with exogenous ATP (Figure 4-8), suggesting that AA and ATP mobilize the same $Ca^{2+}$ stores. Third, $IP_3Rs$ have been detected in the secretory granules of mouse β cells (4) and activation of $IP_3Rs$ has been shown to mobilize $Ca^{2+}$ from the secretory granules of chromaffin cells (44-46) and pancreatic acinar cells (36). However, note that in permeabilized MIN6 cells, $IP_3$ failed to release $Ca^{2+}$ from aequorin-labeled secretory granules (40), but $Ca^{2+}$ release from granules could be triggered by the activation of RyRs or NAADP receptors (37;40). In contrast, our results show that neither RyRs (Figure 4-3) or NAADP receptors (Figure 4-5) contribute to the AA-mediated intracellular $Ca^{2+}$ release in rat β cells, suggesting that the secretory granules are not gated by RyRs or NAADP receptors. Consistent with our results, the application of intracellular NAADP failed to reduce $[Ca^{2+}]$ in the organelles of permeabilized mouse β cells (15) and the inhibition of RyRs also failed to reduce $Ca^{2+}$ release from the secretory granules in mouse β cells (30). One possible explanation for the discrepancy could be the differences in receptor expression and localization between the insulin-secreting cell line (MIN6) and the primary β cells. A lack of

colocalization between RyRs and insulin was reported in human β cells (14), suggesting that the secretory granules in human β cells are not gated by RyRs.

Our findings suggest that ~70% of the AA-mediated $Ca^{2+}$ signal arises from an $IP_3R$-gated acidic $Ca^{2+}$ store and the rest of the $Ca^{2+}$ comes from an $IP_3$-sensitive ER store. Since $Ca^{2+}$ can trigger release from $IP_3$-sensitive stores via a $Ca^{2+}$-induced $Ca^{2+}$ release mechanism, it is possible that the release of $Ca^{2+}$ from a population of secretory granules may act as a trigger for the neighboring granules or ER store. Alternatively, $Ca^{2+}$ release from the ER stores may act as a trigger for the release of $Ca^{2+}$ from the acidic stores. This may account for the biphasic pattern of the AA-evoked $Ca^{2+}$ signal (Figure 4-1B) observed in some cells, in which a small plateau elevation in $[Ca^{2+}]_i$ was followed by a rapid and larger $[Ca^{2+}]_i$ rise. The mechanism by which AA triggers $Ca^{2+}$ release from the two $IP_3$-sensitive stores is unclear. Since AA has been shown to increase the opening of a number of $Ca^{2+}$-permeable channels, including the ARC channels and the TRP channels (65;66), it is possible that AA modulates the opening of the $IP_3R$ channels.

We also found that the SERCA pump inhibitor, thapsigargin mostly attenuated the AA-mediated intracellular $Ca^{2+}$ release (Figure 4-8). While it is well known that the inhibition of SERCA pump causes depletion of ER $Ca^{2+}$ stores in β cells (26), it is controversial whether $Ca^{2+}$ uptake into the secretory granules can be inhibited by SERCA pump inhibitors. $Ca^{2+}$ uptake into the secretory granules could be reduced by SERCA pump inhibitors in chromaffin

and PC12 cells (52;53) but not in MIN6 cells (40). However, in mouse β cells, $Ca^{2+}$ release from the secretory granules was sensitive to thapsigargin (30).

In summary, this is a first report that in single rat β cells, AA triggers $Ca^{2+}$ release from an acidic store and an ER store, both of which are gated by $IP_3Rs$. This effect may contribute significantly to the effects of AA on glucose-stimulated insulin secretion.

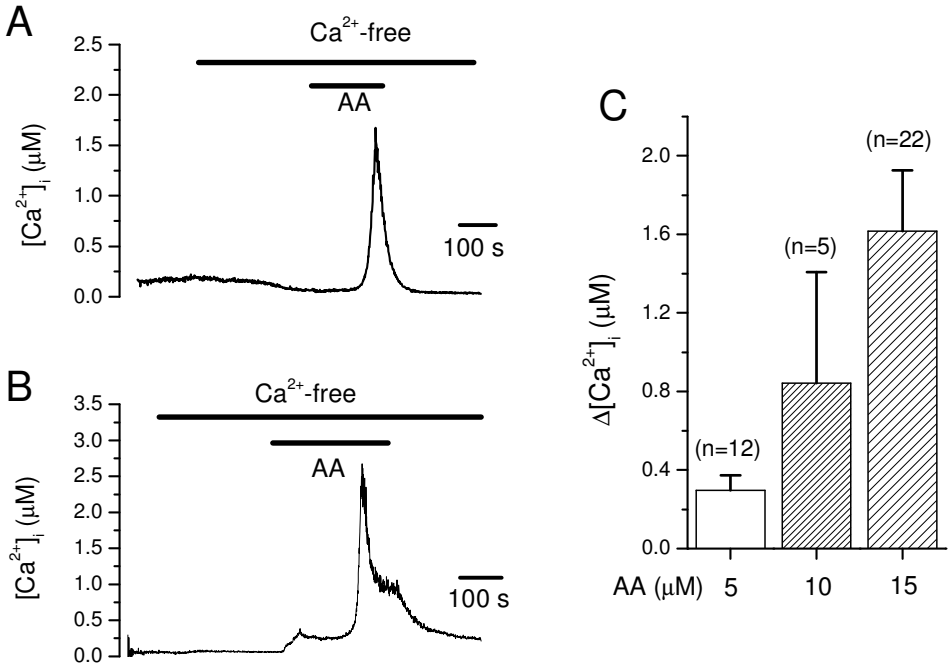


**Figure 4-1**: AA evokes intracellular $Ca^{2+}$ release from rat β cells in a dose-dependent manner. (***A***) The removal of extracellular $Ca^{2+}$ ($Ca^{2+}$-free bath solution) resulted in a decrease in basal $[Ca^{2+}]_i$. In the absence of extracellular $Ca^{2+}$, application of AA (15 μM) evoked a transient $[Ca^{2+}]_i$ rise, reflecting intracellular $Ca^{2+}$ release. The cell was voltage-clamped at -70 mV. (***B***) In some cells, the AA-mediated $Ca^{2+}$ signal was biphasic. (***C***) Summary of the mean amplitude of the $[Ca^{2+}]_i$ increase induced by AA (5, 10, and 15 μM) in the absence of extracellular $Ca^{2+}$. Recordings were from 3-5 batches of cells.

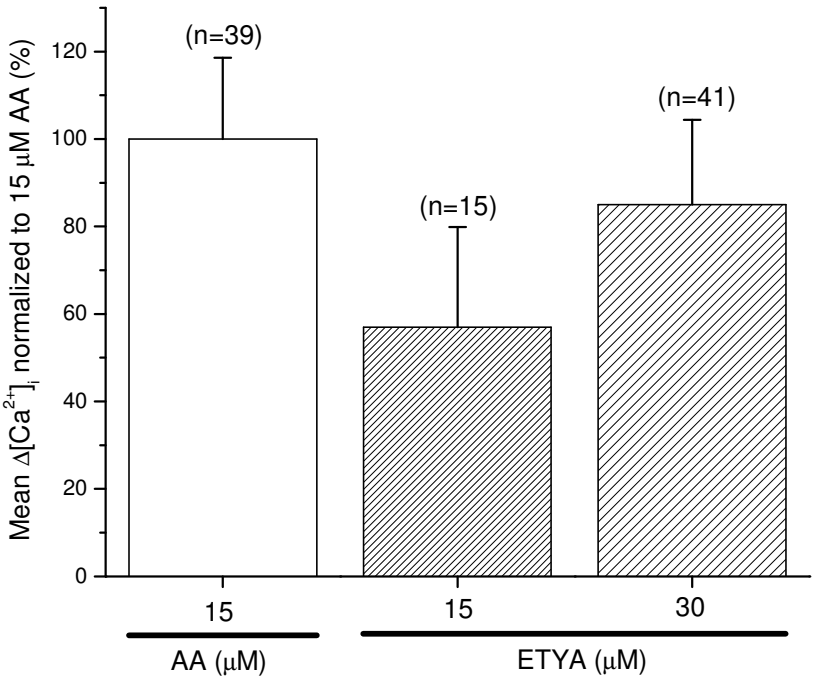


**Figure 4-2**: The AA-mediated intracellular $Ca^{2+}$ release does not require AA metabolism. The mean amplitude of the $[Ca^{2+}]_i$ increase evoked by 15 μM AA and 15 and 30 μM ETYA in the absence of extracellular $Ca^{2+}$. Values were normalized to amplitude of $[Ca^{2+}]_i$ rise mediated by 15 μM AA. In this experiment, single cells were loaded with fura-2 AM and $[Ca^{2+}]_i$ was monitored with fura-2 digital imaging. Recordings were from 3-5 batches of cells.

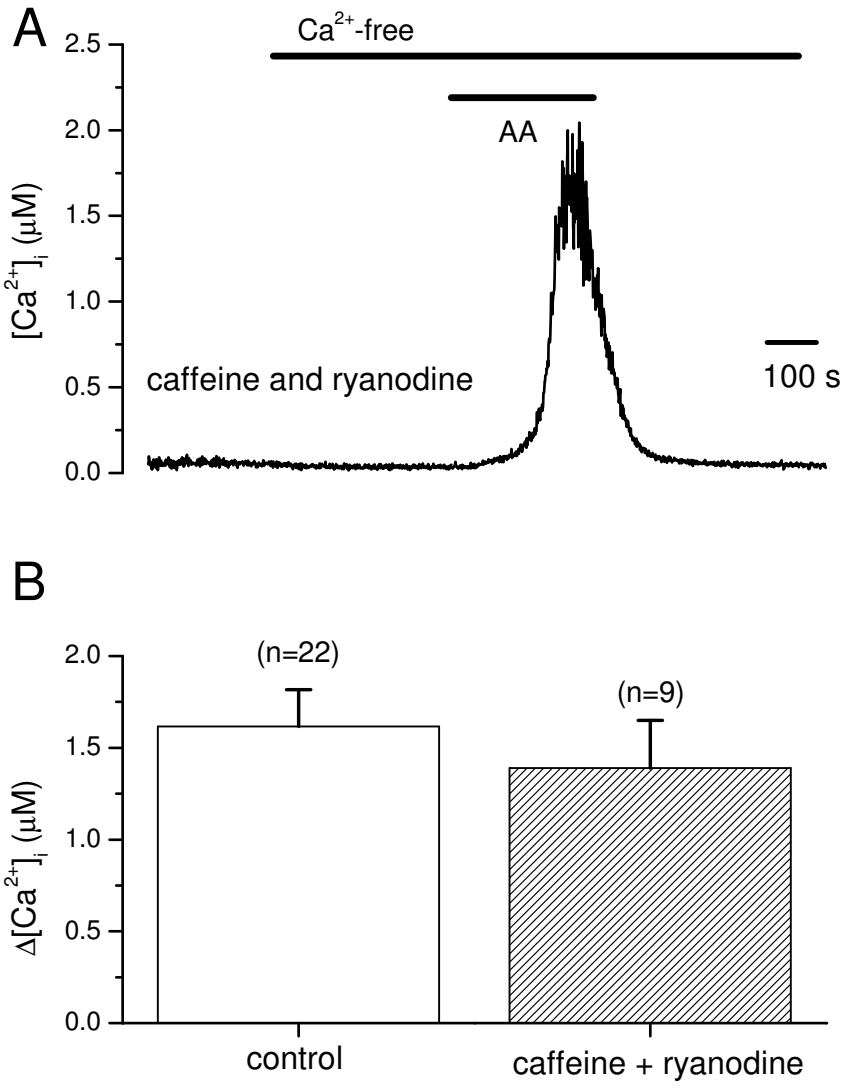


**Figure 4-3**: Inhibition of RyR did not affect the AA-mediated intracellular $Ca^{2+}$ release in rat β cells. (***A***) In a cell pretreated for 1 hour with caffeine (10 mM) and ryanodine (100 μM), AA (15 μM) could still evoke a robust $Ca^{2+}$ signal in a $Ca^{2+}$-free external solution. Ryanodine was also included in the pipette solution. The $[Ca^{2+}]_i$ trace started at ~20 s after the establishment of whole-cell. The cell was voltage-clamped at -70 mV. (***B***) Summary of the mean amplitude of the AA (15 μM)-mediated $[Ca^{2+}]_i$ rise in control cells and cells pretreated with caffeine and ryanodine. The mean $[Ca^{2+}]_i$ rise evoked by AA in the pretreated cells was not significantly different from that of controls. Recordings were from 3 batches of cells.

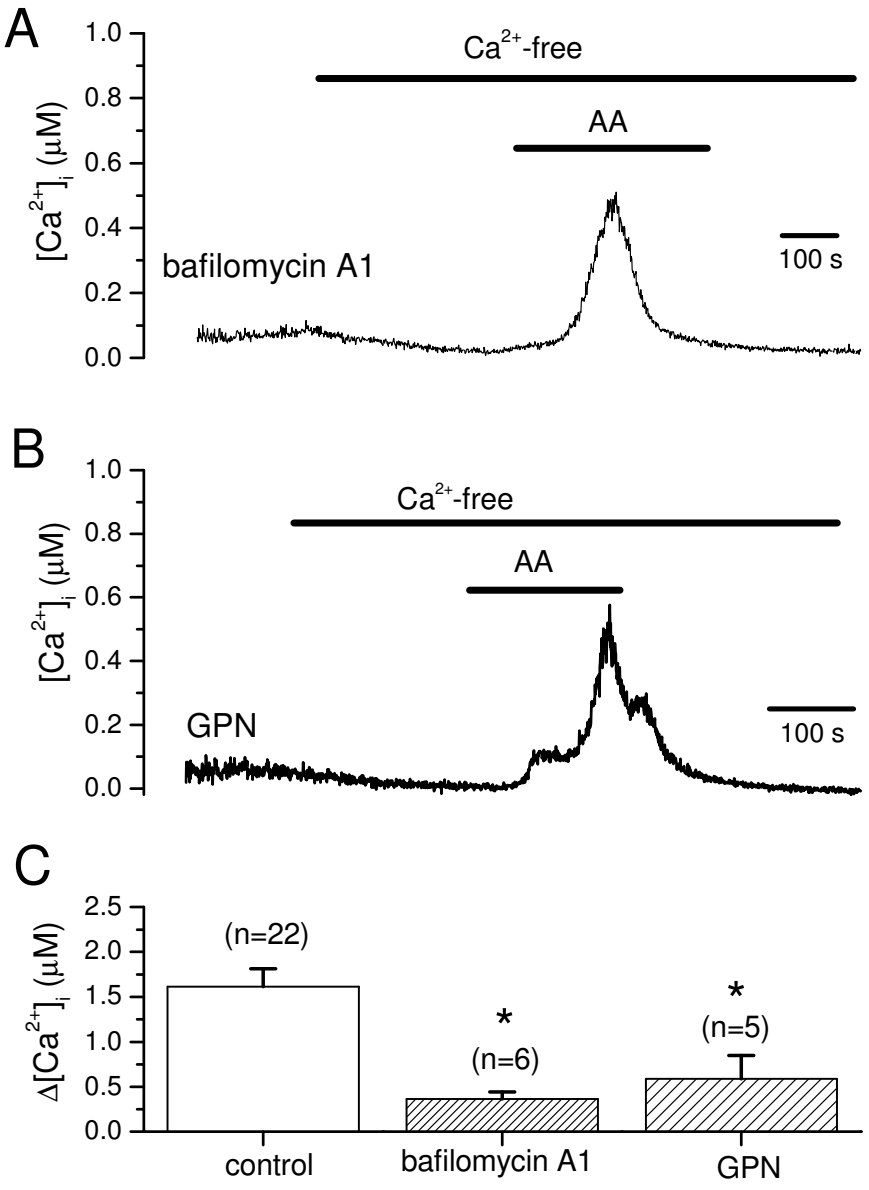


**Figure 4-4**: Pharmacological disruption of acidic stores attenuated the AA-mediated intracellular $Ca^{2+}$ release. (***A***) An example of the AA-mediated intracellular $Ca^{2+}$ release in a cell pretreated with bafilomycin A1 (2 μM) for 15 min. Bafilomycin A1 was also included in the whole-cell pipette solution. The cell was voltage-clamped at -70 mV. (***B***) An example of the AA-mediated intracellular $Ca^{2+}$ release in a cell pretreated with GPN (50 μM) for 1 hour. GPN was also included in the $Ca^{2+}$-free bath solution. The cell was voltage-clamped at -70 mV. (***C***) The mean amplitude of the AA (15 μM)-mediated $[Ca^{2+}]_i$ rise in cells pretreated with either bafilomycin A1 or GPN was significantly smaller than the controls. Recordings were from 3-5 batches of cells.

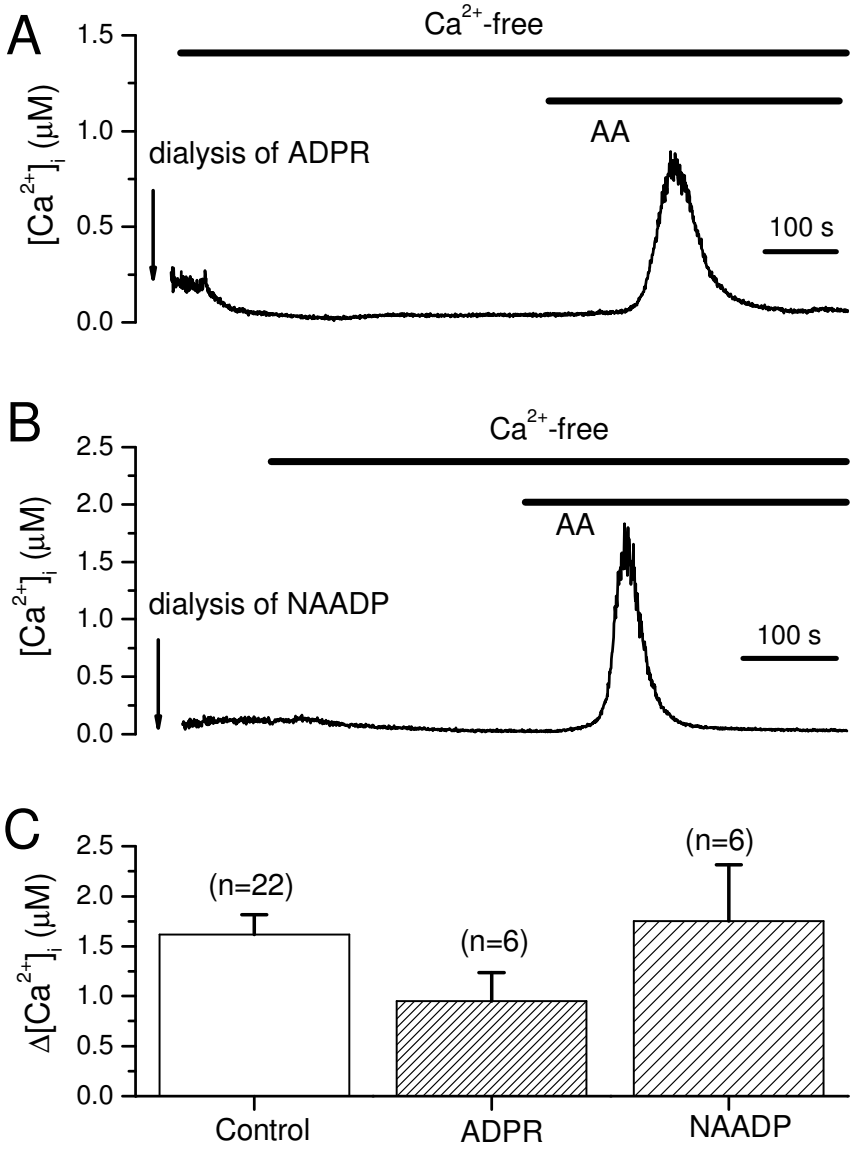


**Figure 4-5**: The depletion of the lysosomal $Ca^{2+}$ store with ADPR or NAADP did not attenuate the AA-mediated intracellular $Ca^{2+}$ release. (***A***) Whole-cell dialysis of ADPR (1 mM) did not trigger any rise in basal $[Ca^{2+}]_i$, and AA could still evoke a robust $Ca^{2+}$ response. The $[Ca^{2+}]_i$ trace started at ~20 s after the establishment of whole-cell. The cell was voltage-clamped at -70 mV. (***B***) Whole-cell dialysis of NAADP (100 nM) did not affect basal $[Ca^{2+}]_i$ or the AA response. The $[Ca^{2+}]_i$ trace started at ~20 s after the establishment of whole-cell. The cell was voltage-clamped at -70 mV. (***C***) Summary of the mean amplitude of the AA (15 μM)-mediated $[Ca^{2+}]_i$ rise in control cells and cells dialysed with either ADPR (1 mM) or NAADP (100 nM). Recordings were from 3-5 batches of cells.

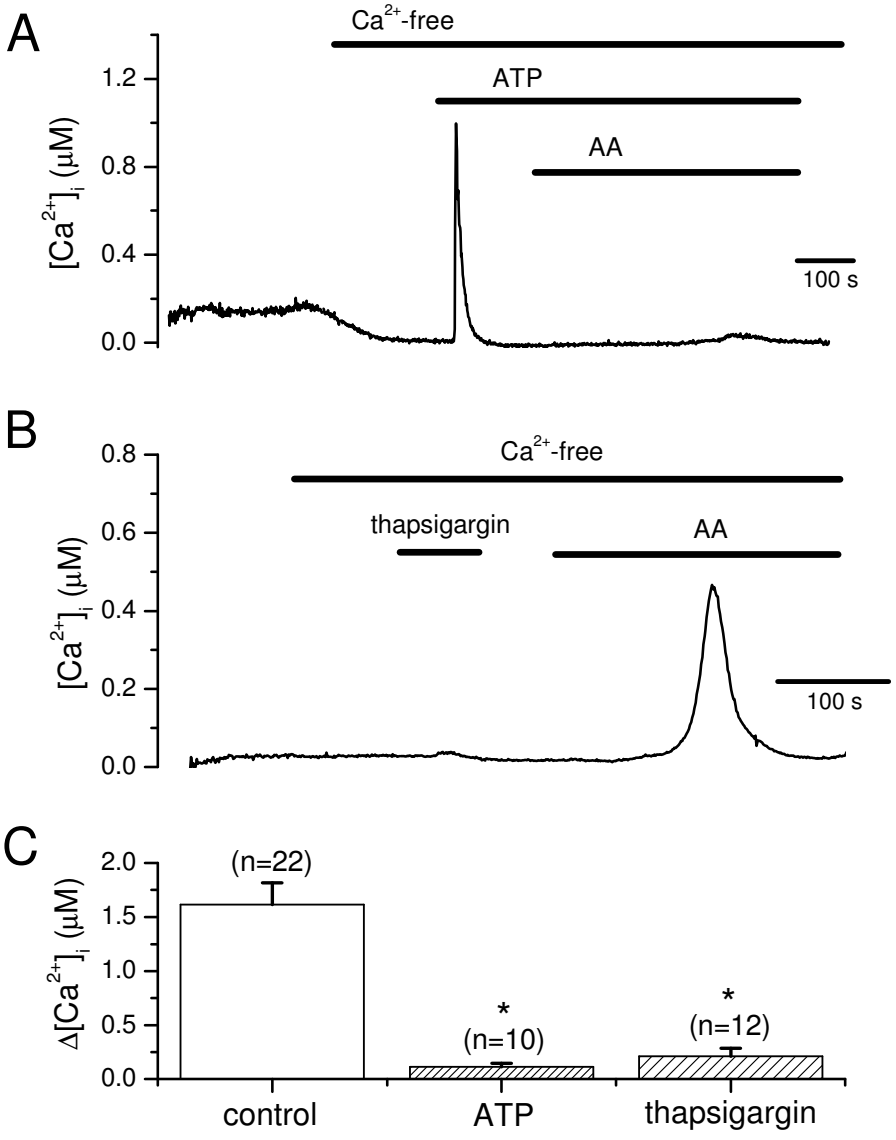


**Figure 4-6:** The AA-mediated intracellular $Ca^{2+}$ release was dramatically reduced by the emptying of the ATP-sensitive store or the inhibition of SERCA pump. (***A***) Application of ATP (100 μM) triggered a transient $[Ca^{2+}]_i$ rise but subsequent application of AA triggered only a very small response. (***B***) Treatment of the SERCA pump inhibitor, thapsigargin (1 μM) strongly attenuated the AA response. (***C***) For cells challenged with either ATP (100 μM) or thapsigargin (1 μM), the amplitude of the AA-mediated $Ca^{2+}$ signal was significantly smaller than controls. Recordings were from 3-5 batches of cells.

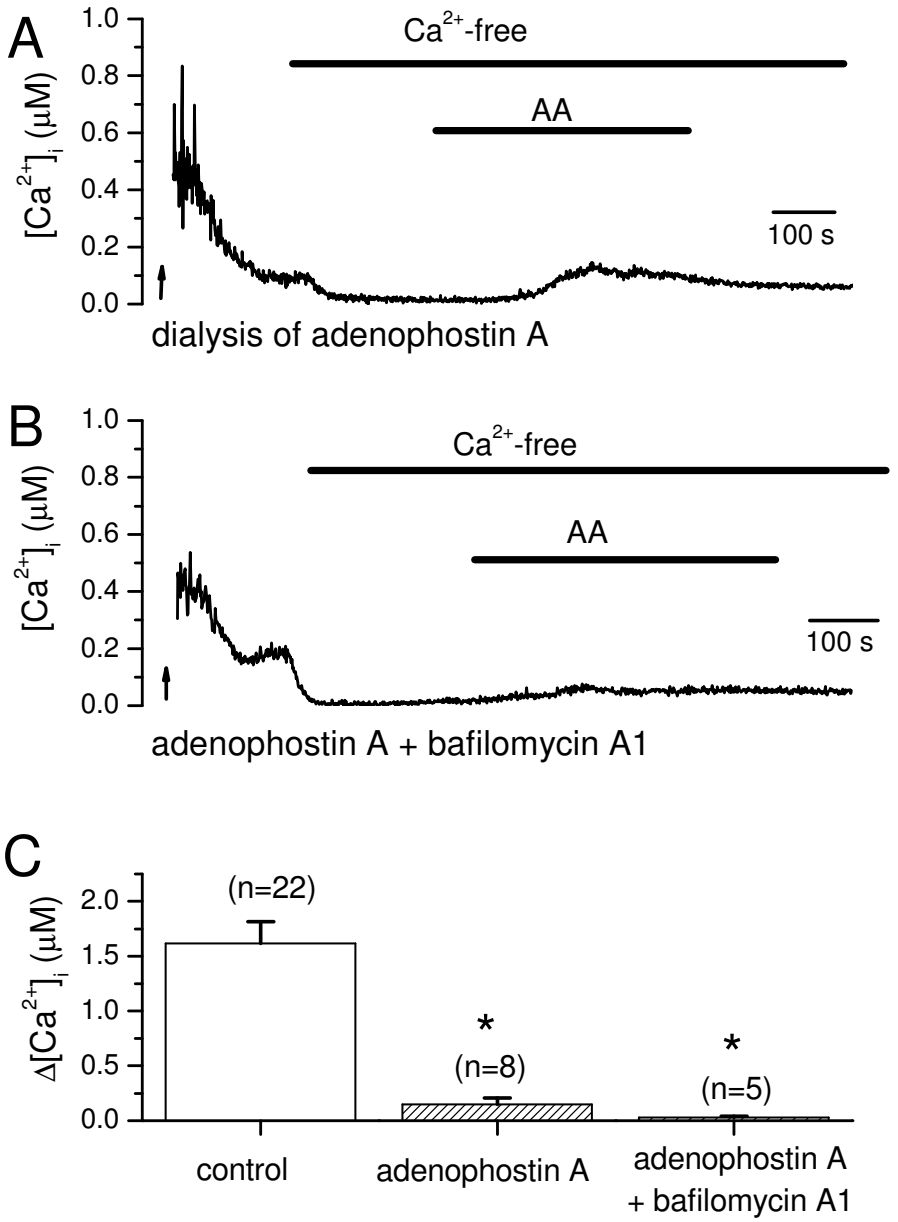


**Figure 4-7**: The emptying of the $IP_3$-sensitive stores essentially abolished the AA-mediated intracellular $Ca^{2+}$ release. (***A***) Whole-cell dialysis of adenophostin A (2 μM) triggered $Ca^{2+}$ release from $IP_3$-sensitive stores and reduced the AA response. The $[Ca^{2+}]_i$ trace started at ~20 s after the establishment of whole-cell. The cell was voltage-clamped at -70 mV. (***B***) The inhibition of AA response in a cell treated with bafilomycin A1 (2 μM), followed by whole-cell dialysis of adenophostin A (2 μM) and bafilomycin A1 (2 μM). The $[Ca^{2+}]_i$ trace started at ~20 s after the establishment of whole-cell. The cell was voltage-clamped at -70 mV. (***C***) The AA (15 μM)-mediated $[Ca^{2+}]_i$ rise was significantly reduced by intracellular adenophostin A or treatment with adenophostin A and bafilomycin A1. Recordings were from 3-5 batches of cells.

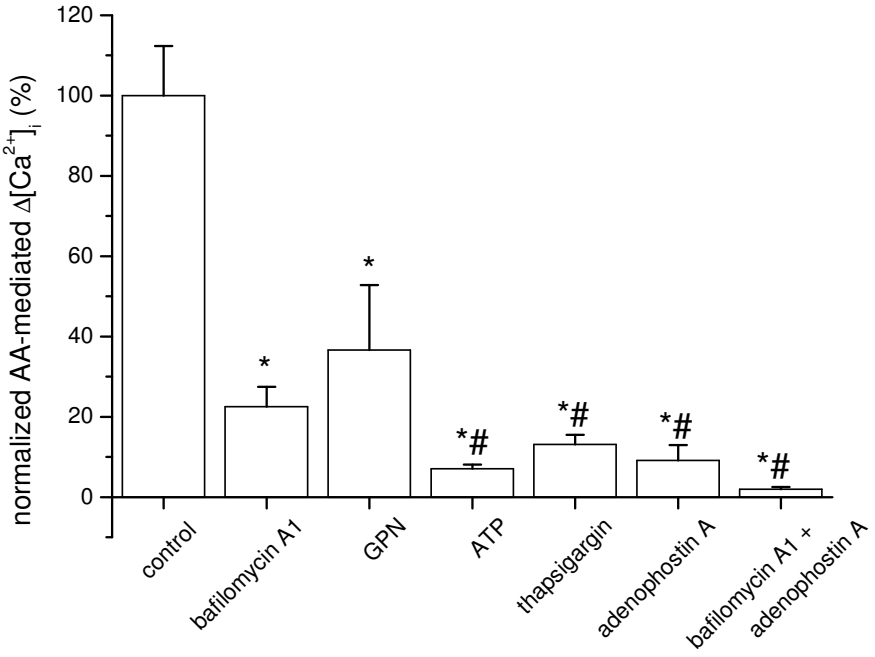


**Figure 4-8**: Summary of the effects of disruption of acidic and $IP_3$-sensitive stores on the AA-mediated intracellular $Ca^{2+}$ release. The disruption of acidic stores by bafilomycin A1 or GPN reduced the AA-mediated $Ca^{2+}$ signal to ~30% of the controls. The AA-mediated $Ca^{2+}$ signal was reduced to <10% of that of the controls following treatment with ATP, thapsigargin, adenophostin A or bafilomycin A1 plus adenophostin A. * denotes significant difference from the controls and # denotes significant differences from cells treated with bafilomycin A1 or GPN. The AA-mediated $Ca^{2+}$ signals from groups of cells treated with ATP, thapsigargin, adenophostin A, or adenophostin A plus bafilomycin A1 were not significantly different from each other.

## References


1. Iismaa,TP, Kerr,EA, Wilson,JR, Carpenter,L, Sims,N, Biden,TJ: Quantitative and functional characterization of muscarinic receptor subtypes in insulin-secreting cell lines and rat pancreatic islets. *Diabetes* 49:392-398, 2000
2. Petit,P, Lajoix,AD, Gross,R: P2 purinergic signalling in the pancreatic beta-cell: control of insulin secretion and pharmacology. *Eur J Pharm Sci* 37:67-75, 2009
3. Tu,H, Wang,Z, Nosyreva,E, De,SH, Bezprozvanny,I: Functional characterization of mammalian inositol 1,4,5-trisphosphate receptor isoforms. *Biophys J* 88:1046-1055, 2005
4. Srivastava,M, Atwater,I, Glasman,M, Leighton,X, Goping,G, Caohuy,H, Miller,G, Pichel,J, Westphal,H, Mears,D, Rojas,E, Pollard,HB: Defects in inositol 1,4,5-trisphosphate receptor expression, Ca(2+) signaling, and insulin secretion in the anx7(+/-) knockout mouse. *Proc Natl Acad Sci U S A* 96:13783-13788, 1999
5. Li,F, Zhang,ZM: Comparative identification of Ca2+ channel expression in INS-1 and rat pancreatic beta cells. *World J Gastroenterol* 15:3046-3050, 2009
6. Uhlen, M. Human Protein Atlas. 2010. Knut and Alice Wallenberg Foundation.

Ref Type: Online Source

7. Rosker,C, Meur,G, Taylor,EJ, Taylor,CW: Functional ryanodine receptors in the plasma membrane of RINm5F pancreatic beta-cells. *J Biol Chem* 284:5186-5194, 2009
8. Joseph,SK: The inositol triphosphate receptor family. *Cell Signal* 8:1-7, 1996
9. Bezprozvanny,I: The inositol 1,4,5-trisphosphate receptors. *Cell Calcium* 38:261-272, 2005
10. Hagar,RE, Ehrlich,BE: Regulation of the type III InsP3 receptor and its role in beta cell function. *Cell Mol Life Sci* 57:1938-1949, 2000
11. Islam,MS: The ryanodine receptor calcium channel of beta-cells: molecular regulation and physiological significance. *Diabetes* 51:1299-1309, 2002
12. Takasawa,S, Akiyama,T, Nata,K, Kuroki,M, Tohgo,A, Noguchi,N, Kobayashi,S, Kato,I, Katada,T, Okamoto,H: Cyclic ADP-ribose and inositol 1,4,5-trisphosphate as alternate second messengers for intracellular Ca2+ mobilization in normal and diabetic beta-cells. *J Biol Chem* 273:2497-2500, 1998
13. Holz,GG, Leech,CA, Heller,RS, Castonguay,M, Habener,JF: cAMP-dependent mobilization of intracellular Ca2+ stores by activation of ryanodine receptors in pancreatic beta-cells. A Ca2+ signaling system stimulated by the insulinotropic hormone glucagon-like peptide-1-(7-37). *J Biol Chem* 274:14147-14156, 1999
14. Johnson,JD, Kuang,S, Misler,S, Polonsky,KS: Ryanodine receptors in human pancreatic beta cells: localization and effects on insulin secretion. *FASEB J* 18:878-880, 2004
15. Tengholm,A, Hellman,B, Gylfe,E: Mobilization of Ca2+ stores in individual pancreatic beta-cells permeabilized or not with digitonin or alpha-toxin. *Cell Calcium* 27:43-51, 2000
16. Guse,AH: Second messenger function and the structure-activity relationship of cyclic adenosine diphosphoribose (cADPR). *FEBS J* 272:4590-4597, 2005
17. Zalk,R, Lehnart,SE, Marks,AR: Modulation of the ryanodine receptor and intracellular calcium. *Annu Rev Biochem* 76:367-385, 2007
18. Bezprozvanny,I, Watras,J, Ehrlich,BE: Bell-shaped calcium-response curves of Ins(1,4,5)P3- and calcium-gated channels from endoplasmic reticulum of cerebellum. *Nature* 351:751-754, 1991

19. Ehrlich,BE, Kaftan,E, Bezprozvannaya,S, Bezprozvanny,I: The pharmacology of intracellular Ca(2+)-release channels. *Trends Pharmacol Sci* 15:145-149, 1994
20. Dyachok,O, Tufveson,G, Gylfe,E: Ca2+-induced Ca2+ release by activation of inositol 1,4,5-trisphosphate receptors in primary pancreatic beta-cells. *Cell Calcium* 36:1-9, 2004
21. Roderick,HL, Berridge,MJ, Bootman,MD: Calcium-induced calcium release. *Curr Biol* 13:R425, 2003
22. Kang,G, Holz,GG: Amplification of exocytosis by Ca2+-induced Ca2+ release in INS-1 pancreatic beta cells. *J Physiol* 546:175-189, 2003
23. Varadi,A, Molnar,E, Ostenson,CG, Ashcroft,SJ: Isoforms of endoplasmic reticulum Ca(2+)-ATPase are differentially expressed in normal and diabetic islets of Langerhans. *Biochem J* 319 ( Pt 2):521-527, 1996
24. Varadi,A, Rutter,GA: Dynamic imaging of endoplasmic reticulum Ca2+ concentration in insulin-secreting MIN6 Cells using recombinant targeted cameleons: roles of sarco(endo)plasmic reticulum Ca2+-ATPase (SERCA)-2 and ryanodine receptors. *Diabetes* 51 Suppl 1:S190-S201, 2002
25. Chen,L, Koh,DS, Hille,B: Dynamics of calcium clearance in mouse pancreatic beta-cells. *Diabetes* 52:1723-1731, 2003
26. Hughes,E, Lee,AK, Tse,A: Dominant role of sarcoendoplasmic reticulum Ca2+-ATPase pump in Ca2+ homeostasis and exocytosis in rat pancreatic beta-cells. *Endocrinology* 147:1396-1407, 2006
27. Demaurex,N: pH Homeostasis of cellular organelles. *News Physiol Sci* 17:1-5, 2002
28. Camello-Almaraz,C, Pariente,JA, Salido,G, Camello,PJ: Differential involvement of vacuolar H(+)-ATPase in the refilling of thapsigargin- and agonist-mobilized Ca(2+) stores. *Biochem Biophys Res Commun* 271:311-317, 2000
29. Jadot,M, Colmant,C, Wattiaux-de,CS, Wattiaux,R: Intralysosomal hydrolysis of glycyl-L-phenylalanine 2-naphthylamide. *Biochem J* 219:965-970, 1984
30. Duman,JG, Chen,L, Palmer,AE, Hille,B: Contributions of intracellular compartments to calcium dynamics: implicating an acidic store. *Traffic* 7:859-872, 2006
31. Churchill,GC, Okada,Y, Thomas,JM, Genazzani,AA, Patel,S, Galione,A: NAADP mobilizes Ca(2+) from reserve granules, lysosome-related organelles, in sea urchin eggs. *Cell* 111:703-708, 2002
32. Masgrau,R, Churchill,GC, Morgan,AJ, Ashcroft,SJ, Galione,A: NAADP: a new second messenger for glucose-induced Ca2+ responses in clonal pancreatic beta cells. *Curr Biol* 13:247-251, 2003
33. Johnson,JD, Misler,S: Nicotinic acid-adenine dinucleotide phosphate-sensitive calcium stores initiate insulin signaling in human beta cells. *Proc Natl Acad Sci U S A* 99:14566-14571, 2002
34. Calcraft,PJ, Ruas,M, Pan,Z, Cheng,X, Arredouani,A, Hao,X, Tang,J, Rietdorf,K, Teboul,L, Chuang,KT, Lin,P, Xiao,R, Wang,C, Zhu,Y, Lin,Y, Wyatt,CN, Parrington,J, Ma,J, Evans,AM, Galione,A, Zhu,MX: NAADP mobilizes calcium from acidic organelles through two-pore channels. *Nature* 459:596-600, 2009
35. Lange,I, Yamamoto,S, Partida-Sanchez,S, Mori,Y, Fleig,A, Penner,R: TRPM2 functions as a lysosomal Ca2+-release channel in beta cells. *Sci Signal* 2:ra23, 2009
36. Gerasimenko,JV, Sherwood,M, Tepikin,AV, Petersen,OH, Gerasimenko,OV: NAADP, cADPR and IP3 all release Ca2+ from the endoplasmic reticulum and an acidic store in the secretory granule area. *J Cell Sci* 119:226-238, 2006

37. Mitchell,KJ, Lai,FA, Rutter,GA: Ryanodine receptor type I and nicotinic acid adenine dinucleotide phosphate receptors mediate Ca2+ release from insulin-containing vesicles in living pancreatic beta-cells (MIN6). *J Biol Chem* 278:11057-11064, 2003
38. Kim,BJ, Park,KH, Yim,CY, Takasawa,S, Okamoto,H, Im,MJ, Kim,UH: Generation of nicotinic acid adenine dinucleotide phosphate and cyclic ADP-ribose by glucagon-like peptide-1 evokes Ca2+ signal that is essential for insulin secretion in mouse pancreatic islets. *Diabetes* 57:868-878, 2008
39. Xie,L, Zhang,M, Zhou,W, Wu,Z, Ding,J, Chen,L, Xu,T: Extracellular ATP stimulates exocytosis via localized Ca(2+) release from acidic stores in rat pancreatic beta cells. *Traffic* 7:429-439, 2006
40. Mitchell,KJ, Pinton,P, Varadi,A, Tacchetti,C, Ainscow,EK, Pozzan,T, Rizzuto,R, Rutter,GA: Dense core secretory vesicles revealed as a dynamic Ca(2+) store in neuroendocrine cells with a vesicle-associated membrane protein aequorin chimaera. *J Cell Biol* 155:41-51, 2001
41. Howell,SL, Tyhurst,M, Duvefelt,H, Andersson,A, Hellerstrom,C: Role of zinc and calcium in the formation and storage of insulin in the pancreatic beta-cell. *Cell Tissue Res* 188:107-118, 1978
42. Austin,CD, Shields,D: Prosomatostatin processing in permeabilized cells. Calcium is required for prohormone cleavage but not formation of nascent secretory vesicles. *J Biol Chem* 271:1194-1199, 1996
43. Lang,T: SNARE proteins and 'membrane rafts'. *J Physiol* 585:693-698, 2007
44. Gerasimenko,OV, Gerasimenko,JV, Belan,PV, Petersen,OH: Inositol trisphosphate and cyclic ADP-ribose-mediated release of Ca2+ from single isolated pancreatic zymogen granules. *Cell* 84:473-480, 1996
45. Yoo,SH, Albanesi,JP: Inositol 1,4,5-trisphosphate-triggered Ca2+ release from bovine adrenal medullary secretory vesicles. *J Biol Chem* 265:13446-13448, 1990
46. Yoo,SH: Secretory granules in inositol 1,4,5-trisphosphate-dependent Ca2+ signaling in the cytoplasm of neuroendocrine cells. *FASEB J* 24:653-664, 2010
47. Blondel,O, Bell,GI, Moody,M, Miller,RJ, Gibbons,SJ: Creation of an inositol 1,4,5-trisphosphate-sensitive Ca2+ store in secretory granules of insulin-producing cells. *J Biol Chem* 269:27167-27170, 1994
48. Blondel,O, Moody,MM, Depaoli,AM, Sharp,AH, Ross,CA, Swift,H, Bell,GI: Localization of inositol trisphosphate receptor subtype 3 to insulin and somatostatin secretory granules and regulation of expression in islets and insulinoma cells. *Proc Natl Acad Sci U S A* 91:7777-7781, 1994
49. Ravazzola,M, Halban,PA, Orci,L: Inositol 1,4,5-trisphosphate receptor subtype 3 in pancreatic islet cell secretory granules revisited. *Proc Natl Acad Sci U S A* 93:2745-2748, 1996
50. Missiaen,L, Dode,L, Vanoevelen,J, Raeymaekers,L, Wuytack,F: Calcium in the Golgi apparatus. *Cell Calcium* 41:405-416, 2007
51. Mitchell,KJ, Tsuboi,T, Rutter,GA: Role for plasma membrane-related Ca2+-ATPase-1 (ATP2C1) in pancreatic beta-cell Ca2+ homeostasis revealed by RNA silencing. *Diabetes* 53:393-400, 2004
52. Santodomingo,J, Vay,L, Camacho,M, Hernandez-Sanmiguel,E, Fonteriz,RI, Lobaton,CD, Montero,M, Moreno,A, Alvarez,J: Calcium dynamics in bovine adrenal medulla chromaffin cell secretory granules. *Eur J Neurosci* 28:1265-1274, 2008
53. Mahapatra,NR, Mahata,M, Hazra,PP, McDonough,PM, O'Connor,DT, Mahata,SK: A dynamic pool of calcium in catecholamine storage vesicles.

Exploration in living cells by a novel vesicle-targeted chromogranin A-aequorin chimeric photoprotein. *J Biol Chem* 279:51107-51121, 2004
54. Metz,SA, Draznin,B, Sussman,KE, Leitner,JW: Unmasking of arachidonate-induced insulin release by removal of extracellular calcium. Arachidonic acid mobilizes cellular calcium in rat islets of Langerhans. *Biochem Biophys Res Commun* 142:251-258, 1987
55. Metz,SA: Exogenous arachidonic acid promotes insulin release from intact or permeabilized rat islets by dual mechanisms. Putative activation of Ca2+ mobilization and protein kinase C. *Diabetes* 37:1453-1469, 1988
56. Band,AM, Jones,PM, Howell,SL: Arachidonic acid-induced insulin secretion from rat islets of Langerhans. *J Mol Endocrinol* 8:95-101, 1992
57. Wolf,BA, Turk,J, Sherman,WR, McDaniel,ML: Intracellular Ca2+ mobilization by arachidonic acid. Comparison with myo-inositol 1,4,5-trisphosphate in isolated pancreatic islets. *J Biol Chem* 261:3501-3511, 1986
58. Dettbarn,C, Palade,P: Arachidonic acid-induced Ca2+ release from isolated sarcoplasmic reticulum. *Biochem Pharmacol* 45:1301-1309, 1993
59. Woolcott,OO, Gustafsson,AJ, Dzabic,M, Pierro,C, Tedeschi,P, Sandgren,J, Bari,MR, Nguyen,KH, Bianchi,M, Rakonjac,M, Radmark,O, Ostenson,CG, Islam,MS: Arachidonic acid is a physiological activator of the ryanodine receptor in pancreatic beta-cells. *Cell Calcium* 39:529-537, 2006
60. Gustafsson,AJ, Ingelman-Sundberg,H, Dzabic,M, Awasum,J, Nguyen,KH, Ostenson,CG, Pierro,C, Tedeschi,P, Woolcott,O, Chiounan,S, Lund,PE, Larsson,O, Islam,MS: Ryanodine receptor-operated activation of TRP-like channels can trigger critical Ca2+ signaling events in pancreatic beta-cells. *FASEB J* 19:301-303, 2005
61. Tobias,LD, Hamilton,JG: The effect of 5,8,11,14-eicosatetraynoic acid on lipid metabolism. *Lipids* 14:181-193, 1979
62. Chen,TH, Lee,B, Yang,C, Hsu,WH: Effects of caffeine on intracellular calcium release and calcium influx in a clonal beta-cell line RINm5F. *Life Sci* 58:983-990, 1996
63. Takahashi,M, Tanzawa,K, Takahashi,S: Adenophostins, newly discovered metabolites of Penicillium brevicompactum, act as potent agonists of the inositol 1,4,5-trisphosphate receptor. *J Biol Chem* 269:369-372, 1994
64. Schnell Landstrom,AH, Andersson,A, Borg,LA: Lysosomes and pancreatic islet function: adaptation of beta-cell lysosomes to various metabolic demands. *Metabolism* 40:399-405, 1991
65. Watanabe,H, Vriens,J, Prenen,J, Droogmans,G, Voets,T, Nilius,B: Anandamide and arachidonic acid use epoxyeicosatrienoic acids to activate TRPV4 channels. *Nature* 424:434-438, 2003
66. Chyb,S, Raghu,P, Hardie,RC: Polyunsaturated fatty acids activate the Drosophila light-sensitive channels TRP and TRPL. *Nature* 397:255-259, 1999

# Chapter 5

## Cholesterol overload impairs glucose-mediated $Ca^{2+}$ signaling in mouse pancreatic β cells

## 5.1 Introduction

### *5.1.1 Regulation of cellular cholesterol*

Cellular cholesterol level is tightly controlled by a balance between intracellular cholesterol synthesis and uptake of cholesterol from plasma, on one hand, and cholesterol sequestration and efflux, on the other. Cholesterol synthesis takes place in the ER and the rate-limiting enzyme is 3-hydroxy-3-methyl-glutaryl-CoA (HMG CoA) reductase, which catalyzes the conversion of HMG CoA to mevalonate. The other major source of cellular cholesterol is uptake from the plasma, via low-density lipoprotein (LDL) receptors. LDLs bound to LDL receptors undergo endocytic uptake into the cell, and the cholesteryl esters contained in the LDLs are hydrolyzed in late endosomes and lysosomes and delivered throughout the cell. To eliminate cholesterol temporarily, the cell can esterify excess cholesterol through the action of acyl-coenzymeA: acyltransferase (ACAT), an ER enzyme (1). The esterified cholesterol is stored in cytoplasmic lipid droplets, where it can be hydrolyzed by cholesterol ester hydrolases. Cholesterol efflux mechanisms, however, such as the ATP-binding cassette transporter subfamily A member 1 (ABCA1), can eliminate cholesterol from the cell entirely (2). ABCA1, which is found in the plasma membrane, is a key mediator of the reverse cholesterol transport pathway, in which excess cholesterol from peripheral tissues is transported to the liver. Cholesterol is delivered by ABCA1 to extracellular HDLs and their associated lipoprotein, apolipoprotein A-I (apoA-I) (3).

The expression of a number of genes related to cholesterol metabolism is under the control of transcription factors such as sterol-regulatory-element binding protein 2 (SREBP-2) and liver X receptor β (LXRβ). The SREBP family of transcription factors regulates expression of genes related to fatty acid synthesis, and SREBP-2 is a major regulator of cholesterol-synthesis-related genes, in particular ABCA1 and HMG CoA reductase. When cellular cholesterol is normal/high, SREBP-2 is retained in the ER, but when cellular cholesterol is low, SREBP-2 is cleaved and then translocates to the nucleus, where it activates gene transcription (4). LXRβ, a nuclear hormone receptor that is widely expressed, regulates the expression of genes that mediate reverse cholesterol transport, including ABCA1. LXRβ is activated by binding to oxysterols, which are cholesterol metabolites, and thus serves as a cholesterol sensor in the cell (5).

### *5.1.2 Lipid rafts and manipulation of membrane cholesterol*

Lipid rafts have long been defined by their resistance to detergents, conferred by the presence of cholesterol in rafts, which ensures tight packing of raft lipids. However, growing evidence indicates that, due to the complex actions of detergents and the variability in isolation techniques, the detergent-resistant fraction may not necessarily correspond to the membrane raft fraction (6). Therefore, the term "membrane rafts" is now used rather than "lipid rafts," and membrane rafts are defined as "small (10-200 nm), heterogeneous, highly dynamic, sterol- and sphingolipid-enriched domains that compartmentalize cellular processes" (7). Membrane rafts spatially organize signaling molecules to

promote specific cellular signal transduction. In β cells, proteins that participate in stimulus-secretion coupling are postulated to be dependent on membrane organization by rafts. For example, members of the soluble N-ethylmaleimide-sensitive factor (NSF) attachment protein (SNAP) receptor (or SNARE) superfamily of proteins, which are involved in exocytosis, are associated with membrane rafts (8). Alteration of subcellular distribution of SNAP-25 (a member of the SNARE superfamily) can induce changes in exocytosis (9). One widely used method of disrupting rafts is treatment with methyl-β-cyclodextrin (MβCD), a cholesterol extractor. MβCD is a water-soluble ring-shaped molecule with a hydrophobic cavity that is optimally sized for cholesterol. Due to its weak affinity for cholesterol, it can be used an a cholesterol acceptor (to extract cellular cholesterol) or, when saturated with cholesterol, as a cholesterol donor (10). Extraction of membrane cholesterol is thought to disrupt membrane rafts, redistributing proteins out of the raft fraction and thus affecting their function. For example, MβCD treatment was reported to impair the activity of Kv2.1 in HIT-T15 cells (11), as well as $Ca^{2+}$ channels in mouse β cells (9), and these effects were attributed to the disruption of membrane rafts. However, other than membrane raft disruption, a reduction in the level of plasma membrane cholesterol can affect membrane fluidity, which may in turn modulate the functions of membrane proteins. Moreover, cholesterol in plasma membranes does not reside exclusively in membrane rafts, and MβCD may not affect raft and non-raft populations of cholesterol equally (10).

### *5.1.3 Cholesterol overload may impair β cell function*

Type II diabetes is characterized by the development of insulin resistance, followed by β cell dysfunction and a reduction in β cell mass, which leads to insulin deficiency. These processes are often accompanied by dyslipidemia: in humans, the major changes that occur are hypertriglyceridemia, a decrease in HDL cholesterol in plasma, and alterations in LDL composition (12). Although the elevation in plasma triglycerides is thought to contribute to the development of β cell dysfunction and, eventually, to cell death (13), there is emerging evidence that changes in cellular cholesterol have a strong impact on glucose-stimulated insulin secretion.

Cholesterol homeostasis in cells is tightly regulated and is under the control of a complex network. Disrupting any component of that network can lead to drastic changes in cellular cholesterol levels, and this in turn affect cellular functions. In whole animals, transgenic mice have demonstrated the importance of cholesterol in the maintenance of normal insulin secretion. One such model is the ABCA1 knockout mouse. Mice with global deletion of ABCA1 gene have an inability to eliminate excess cellular cholesterol, and display impaired glucose tolerance but normal insulin sensitivity, implying a dysfunction in insulin secretion (14). Mice with selective deletion of ABCA1 gene in β cells have high islet cholesterol (but normal plasma cholesterol) and impaired glucose-stimulated insulin secretion (14). As described above, the expression of ABCA1 and other genes related to cholesterol metabolism is regulated by transcription factors such as SREBP-2 and LXRβ. Isolated islets from transgenic mice overexpressing SREBP-2 in β cells

display high islet cholesterol and impaired glucose-stimulated insulin secretion (15). On the other hand, glucose-stimulated insulin secretion was enhanced by activation of LXRβ in MIN6 cells (16), but reduced in islets from *LXRβ*$^{-/-}$ mice (17). Another factor that is important for cholesterol homeostasis is apolipoprotein E (apoE). ApoE is a constituent of chylomicrons, very-low-density lipoproteins (VLDLs), and HDLs, and it binds to LDL receptors on peripheral cells. Mice deficient in apoE showed elevated levels of cholesterol in plasma (but no change in the level of free fatty acids in plasma) and islets, and impairment of glucose-stimulated insulin response (18). Together, these observations indicate that cholesterol accumulation in islets may be harmful to β cells.

While the evidence discussed above suggests that glucose-stimulated insulin secretion is impaired when cholesterol homeostasis is disrupted, little is known about the cellular mechanisms underlying this impairment. One way to investigate the cellular mechanisms regulated by membrane cholesterol is to manipulate cholesterol in cells or islets in culture. As described below, studies looking at the effects of cholesterol on insulin-secreting cells have shown that while reducing cellular cholesterol from normal levels has variable effects on insulin secretion (9;11;18-20), increasing cellular cholesterol impairs glucose-induced insulin secretion (18;20).

Several studies have examined the effects of lowering cellular cholesterol from normal levels on glucose-induced insulin secretion. Extraction of cellular cholesterol in mouse pancreatic islets with MβCD enhanced glucose-stimulated

insulin secretion, and these effects were thought to arise from an increase in glucokinase activity, because treatment of INS-1 cells with MβCD increased the translocation of glucokinase from the membrane-bound fraction to the cytoplasmic fraction (18). However, in a later study by the same author, the enhancement of glucose-stimulated insulin secretion by MβCD in INS-1 cells was attributed to an increase in glucose-stimulated depolarization, possibly due to a reduction in plasma membrane $PIP_2$ (20). Other studies have associated changes in β cell function with disruption of membrane rafts by cholesterol extraction. Mouse islets exposed to a low concentration of MβCD (0.1 mM) had reduced glucose-stimulated insulin secretion, and this effect was accompanied by a reduction in the $Ca^{2+}$ sensitivity of exocytosis, as well as a redistribution of SNAP-25 from the granular to the cytosolic fraction (9). It was concluded that cholesterol extraction may induce mobilization of SNAP-25 out of cholesterol-rich plasma domains, thus impairing the $Ca^{2+}$ sensitivity of the exocytotic machinery. In HIT-T15 cells treated with MβCD, however, redistribution of some membrane proteins, including Kv2.1, Cav1.2, and SNARE family members syntaxin-1A, SNAP-25, and vesicle-associated membrane protein (VAMP), out of the detergent-resistant fraction, actually resulted in enhancement of glucose-induced insulin secretion (11). This was accompanied by inhibition of delayed rectifier currents, though no change in whole-cell $Ca^{2+}$ currents was observed. Conversely, mouse islet cells in which cholesterol was reduced with NB598, a squalene epoxidase inhibitor (squalene epoxidase catalyzes a late step in cholesterol biosynthesis), displayed a decrease in insulin secretion, and inhibition

of whole-cell delayed rectifier and $Ca^{2+}$ currents, as well as a reduction of granule mobilization (19). In MIN6 cells, NB598 also caused redistribution of membrane proteins, including Kv2.1, Cav1.2, syntaxin-1A, SNAP-25, and VAMP, out of the detergent-resistant fraction (19), and so the impairments in function seen in mouse β cells could be due to disruption of membrane rafts induced by cholesterol depletion. Based on these studies, it is not clear whether the effects of lowering cellular cholesterol from normal levels are beneficial or detrimental for insulin-secreting cells. However, overloading cells with cholesterol seems to have negative effects on glucose-stimulated insulin secretion. INS-1 cells overloaded with cholesterol displayed a reduced ability to secrete insulin in response to glucose, possibly due to a reduction in glucokinase activity (18) or glucose-induced depolarization (20). Thus, the actions of cholesterol on glucose-stimulated insulin secretion are complex, and cholesterol may affect multiple steps in the stimulus-secretion coupling machinery. In this chapter, I study the effects of cholesterol overload on glucose-stimulated $Ca^{2+}$ signaling.

## 5.2 Results

### *5.2.1 Cholesterol overload reduced the glucose-mediated $Ca^{2+}$ response in mouse β cells*

Hypercholesterolemia in humans is defined as a total plasma cholesterol level > 200 mg/dL (21), which is equivalent to 2 mg/mL. Therefore, in our experiments, we treated single islet cells with 1 mg/mL of soluble cholesterol (as described in Chapter 2) to elevate cellular cholesterol. To examine the effects of

our treatment, which is designed to elevate cellular cholesterol, on the glucose-mediated $Ca^{2+}$ signal, single mouse islet cells were loaded with fura-2/AM and $[Ca^{2+}]_i$ of individual islet cells was recorded with digital imaging. A representative example of the $Ca^{2+}$ response in a control cell is shown in Figure 5-1A. In this example, glucose elevation (from 3 to 20 mM) triggered a robust $[Ca^{2+}]_i$ rise, and a subsequent challenge with the $K_{ATP}$ channel inhibitor, tolbutamide (100 μM), also evoked a robust $[Ca^{2+}]_i$ rise (Figure 5-1A). As shown in Figure 5-1D, ~90% of the control β cells (identified by their $Ca^{2+}$ response to tolbutamide) exhibited a rise in $[Ca^{2+}]_i$ when challenged with glucose. However, for islet cells incubated with cholesterol, tolbutamide could still trigger a $Ca^{2+}$ response, but glucose failed to cause any $[Ca^{2+}]_i$ rise in most of the β cells (e.g. Figure 5-1B). Since the soluble cholesterol contained MβCD (saturated with cholesterol), I tested whether the reduction in glucose response was due to elevation of cholesterol or of MβCD. In this experiment, islet cells were treated with the same concentration of soluble cholesterol (1 mg/mL), but 10 or 20 mM MβCD was added to reduce the amount of cholesterol delivered to the cells. Under these conditions, both glucose and tolbutamide could evoke robust $Ca^{2+}$ responses (e.g. Figure 5-1C). As shown in Figure 5-1D, the fraction of β cells that exhibited a $Ca^{2+}$ response to glucose was dramatically reduced in cholesterol-treated cells (~19%, as compared to ~90% in controls) but not in cells treated with cholesterol plus excessive MβCD (~90%).

In the small fraction of cholesterol-treated β cells that exhibited a glucose-evoked $Ca^{2+}$ response, the amplitude (Figure 5-2A) as well as the time integral

(Figure 5-2C) of the glucose-mediated $Ca^{2+}$ signal were significantly reduced. Cholesterol treatment also reduced the amplitude (Figure 5-2B) and time integral (Figure 5-2D) of the tolbutamide-induced $[Ca^{2+}]_i$ rise. Therefore, cholesterol treatment reduced both glucose- and tolbutamide-mediated $Ca^{2+}$ entry. For cells treated with cholesterol plus MβCD (10 or 20 mM), both the amplitude and time integral of the glucose- and tolbutamide-mediated $Ca^{2+}$ signals were similar to that of controls, confirming that excessive MβCD did not reduce $Ca^{2+}$ response to glucose or tolbutamide.

### *5.2.2 Glucose-stimulated $[Ca^{2+}]_i$ rise was also reduced in whole animals with elevated plasma and islet cholesterol*

We investigated whether chronic cholesterol elevation in whole animals would have similar effects to our shorter-term treatment. Traditionally, plasma cholesterol in animals is elevated by feeding a high-fat diet. However, this approach also results in an increase in plasma triglycerides, which can itself have negative effects on β cell function (13). To avoid this problem, we used apolipoprotein E (apoE)-deficient mice (*ApoE*$^{-/-}$), which develop elevated plasma cholesterol with no significant change in plasma free fatty acids (22). The cholesterol in islets from *ApoE*$^{-/-}$ mice is reported to be ~2-fold higher than that in wild-type mice and, importantly, islets from *ApoE*$^{-/-}$ mice display ~40% reduction in glucose-stimulated insulin secretion (18). We examined the $[Ca^{2+}]_i$ rise in single islet cells from *ApoE*$^{-/-}$ mice when challenged with 20 mM glucose. As described above, the $Ca^{2+}$ response to tolbutamide (100 μM) was used to identify

β cells from *ApoE*$^{-/-}$ mice. Figure 5-3A shows an example of a β cell from an *ApoE*$^{-/-}$ mouse that failed to respond to glucose. The proportion of glucose-responding β cells was reduced to ~48% in *ApoE*$^{-/-}$ mice, as compared to ~90% in wild-type controls (Figure 5-3C). Furthermore, the amplitudes of both the glucose-induced and tolbutamide-induced $[Ca^{2+}]_i$ rise in the β cells of *ApoE*$^{-/-}$ mice were reduced when compared to the wild-type controls (Figure 5-3D & E). To determine whether the reduction in glucose-stimulated $[Ca^{2+}]_i$ rise in the β cells of *ApoE*$^{-/-}$ mice was related to excessive cellular cholesterol, we incubated single islet cells from *ApoE*$^{-/-}$ mice overnight with lovastatin (5 μM), an inhibitor of cholesterol synthesis, and then for 1 hour with MβCD (10 mM). Under these conditions, which were designed to decrease cellular cholesterol in cells of *ApoE*$^{-/-}$ mice, glucose was able to evoke a $Ca^{2+}$ responses (e.g. Figure 5-3B), and the proportion of β cells responding to glucose increased to ~79% (Figure 5-3C), indicating that conditions designed to decrease cellular cholesterol could at least partially rescue the phenotype. However, there was no increase in the amplitude of the glucose or tolbutamide-stimulated $[Ca^{2+}]_i$ rise in β cells of *ApoE*$^{-/-}$ mice with cholesterol reduction (Figure 5-3D & E), suggesting that some chronic defects in the stimulus-secretion coupling machinery (e.g. downregulation of VGCCs) of the *ApoE*$^{-/-}$ mice β cells cannot be rescued by an acute treatment with cholesterol-lowering agents (lovastatin and MβCD).

### *5.2.3 Cholesterol overload reduced glucose uptake and glucose-mediated ATP production in mouse β cells*

As described previously (Figure 1-1), glucose stimulates VGCC activation via the closure of $K_{ATP}$ channels, which in turn causes membrane depolarization. Using perforated patch clamp recording, Dr. A. Lee in my laboratory found that cholesterol treatment reduced the amplitude of the glucose-evoked depolarization (2 ± 1 mV versus 46 ± 4 mV in the controls; data not shown) but tolbutamide could still evoke a robust depolarization (~46 mV). The reduction in glucose-evoked depolarization in the cholesterol-treated cells is not due to an increase in $K_{ATP}$ current density, since there is actually a reduction in the $K_{ATP}$ current density in the cholesterol-treated cells (unpublished finding from A. Lee). Since the generation of cytosolic ATP during glucose stimulation is responsible for the closure of $K_{ATP}$ channels, I investigated whether the glucose-stimulated ATP production was affected by cholesterol. In this experiment, I compared the cellular ATP level among the three groups of islet cells (control, cholesterol-treated, and cells treated with cholesterol plus excessive MβCD). Cells were incubated with either 3 or 20 mM glucose for 40 minutes before lysing, and their ATP level was measured immediately using a luciferin-luciferase assay in a tube luminometer. The results are summarized in Figure 5-4. Under basal conditions (incubation with 3 mM glucose), there was no significant difference between controls and cells treated either with cholesterol or with cholesterol plus MβCD. In the presence of 20 mM glucose, the cellular ATP increased by 1.6-fold (n = 5) over basal in control cells. Note that for the cholesterol-treated cells, the cellular

ATP level after treatment with high glucose was significantly smaller than that of the control or cells treated with cholesterol plus excessive MβCD. Thus, incubation with cholesterol is associated with a significant reduction of glucose-stimulated increase in cellular ATP. The resultant reduction in ATP level may account for the reduction in glucose-evoked depolarization in cholesterol-treated cells.

Glucose must be first transported into the β cells before it can be metabolized by the mitochondria to produce cellular ATP. Therefore, I investigated whether glucose uptake through the glucose transporters was impaired by cholesterol treatment. The fluorescent glucose analogue, 2-[*N*-(7-nitrobenz-2-oxa-1,3-diazol-4-yl) amino]-2-deoxy-d-glucose (2-NBDG) has been employed to monitor glucose uptake in single living β cells (23;24). In this experiment, I incubated the islet cells with 2-NBDG (200 μM) and fura-2/AM in the presence of 20 mM glucose for 10 minutes at 37$^{o}$C. Cells were then washed with the standard bath solution (containing 3 mM glucose) for 5 minutes before recording. A fluorescence image of the islet cells in the optical field was obtained, and the same cells were subsequently challenged with tolbutamide. Individual islet cells that exhibited a $Ca^{2+}$ response to tolbutamide were identified as β cells. This identification procedure is important because it has been shown that all islet cells will take up 2-NBDG following a 10 min incubation (23). For example, all the islet cells shown in the bright-field image of Figure 5-5A exhibited some 2-NBDG fluorescence (Figure 5-5B), but one cell did not exhibit any $Ca^{2+}$ response to tolbutamide. In my analysis, only the 2-NBDG fluorescence of

identified β cells was included. As shown in Figure 5-5C, there was a significant reduction in the mean 2-NBDG fluorescence in the cholesterol-treated cells in comparison to the controls or cells treated with cholesterol plus MβCD. This finding suggests that glucose uptake is reduced in the cholesterol-treated cells and that such impairment contributes to the reduction in the glucose-evoked ATP production in these cells.

### *5.2.4 Cholesterol overload reduced the density of voltage-gated $Ca^{2+}$ current*

In cholesterol-treated cells, the amplitude of the tolbutamide-induced $[Ca^{2+}]_i$ rise was significantly smaller than controls (Figure 5-2C&D). Since tolbutamide directly depolarizes β cells by closing $K_{ATP}$ channels, and does not require glucose metabolism or ATP production, the reduction in glucose uptake or ATP production cannot account for the decrease in the amplitude of the tolbutamide-mediated $[Ca^{2+}]_i$ rise. Therefore, incubation with cholesterol may impair a step in the tolbutamide-stimulated $[Ca^{2+}]_i$ increase pathway downstream of depolarization. Activation of VGCCs is a crucial step prior to the tolbutamide-mediated $Ca^{2+}$ elevation. To test whether cholesterol treatment had any effect on VGCCs, inward $Ca^{2+}$ currents ($I_{Ca}$) were elicited from single cells voltage-clamped in the whole-cell configuration. Cells were held at -80 mV and depolarized to potentials between -70 to +60 mV. To reduce voltage-gated $Ca^{2+}$ current rundown, cells in this experiment were recorded at 25°C, with 10 mM EGTA in the pipette. As shown by the examples of $I_{Ca}$ in Figure 5-6A, the amplitude of $I_{Ca}$ in cholesterol-treated cells was smaller, but there was no apparent

change in the time course of current decay during the voltage step. Cholesterol treatment reduced $I_{Ca}$ density at a wide range of potentials, as shown in the I-V plots of control cells versus those treated with cholesterol or cholesterol plus MβCD (Figure 5-6B). The peak $I_{Ca}$ amplitude (normalized to individual cell capacitance) measured at +10 mV was ~12 pA/pF (n=13) in control cells, ~6 pA/pF (n=8) in cells treated with cholesterol, and ~13 pA/pF (n=7) in cells treated with cholesterol plus MβCD. To further examine whether cholesterol treatment affected the time course of $I_{Ca}$ inactivation, an exponential was fitted to the time course of decay of the current evoked at +10 mV. Figure 5-6C shows that there was no significant difference in the mean decay rate (τ) of $I_{Ca}$ at +10 mV among the three groups of cells. This finding suggests that the reduction in glucose or tolbutamide-mediated $Ca^{2+}$ signals in cholesterol-treated cells is in part due to a reduction of voltage-gated $Ca^{2+}$ current density.

### *5.2.5 Cholesterol overload reduced the current density of delayed rectifier $K^+$ channels*

In insulin-secreting cells, delayed rectifier $K^+$ channels mediate membrane repolarization (25) and thus regulate $Ca^{2+}$ signaling in β cells. To investigate whether the delayed rectifier $K^+$ current ($I_{K(DR)}$) was affected by incubation with cholesterol, outward $K^+$ currents were elicited from single cells voltage-clamped in the whole-cell configuration. Cells were held at -80 mV and depolarized to potentials between -70 to +60 mV at 25°C (Figure 5-7A). The whole-cell pipette contained 10 mM EGTA and the bath contained the VGCC blocker $Cd^{2+}$ and the

$K_{ATP}$ inhibitor tolbutamide. Under this condition, $K_{Ca}$ and $K_{ATP}$ channels were inhibited and the outward currents evoked were predominantly due to $I_{K(DR)}$ (confirmed by its inhibition by TEA; data not shown). As shown in Figure 5-7A, the $I_{K(DR)}$ evoked from cholesterol-treated cells was typically smaller than that in control cells, but there was no apparent change in the time course of the current during the voltage step. For example, the time course of $I_{K(DR)}$ evoked at +30 mV in control was similar to that of the cholesterol-treated cell (scaled to matching amplitude; Figure 5-7A, inset). As shown in Figure 5-7B, over a wide range of potentials, the density of $I_{K(DR)}$ in the cholesterol-treated cells was significantly smaller than that in controls or cells treated with cholesterol plus MβCD.

### 5.3 Discussion

Recent studies have suggested that high islet cholesterol impairs β cell function and glucose-stimulated insulin secretion (14;18;20;26). Our results show that even a relatively brief exposure (1 hour) to a high level of cholesterol can impair glucose-mediated $Ca^{2+}$ signaling in β cells (Figure 5-1 & 2). The detrimental effect of elevated cholesterol on β cell $Ca^{2+}$ signaling is further supported by our observations from *ApoE* $^{-/-}$ mice, which have chronic elevation of plasma cholesterol, and whose β cells also exhibited a reduction in glucose-stimulated $Ca^{2+}$ response (Figure 5-3).

Given that cholesterol is ubiquitously present in the cell and may regulate numerous cellular processes, it is unlikely that a single mechanism is responsible for the observed effects on glucose-stimulated insulin secretion. In fact, we

demonstrate here that cholesterol treatment reduced glucose-stimulated $[Ca^{2+}]_i$ increase via multiple mechanisms. We report here for the first time that conditions designed to elevate cellular cholesterol impair glucose-stimulated $Ca^{2+}$ signaling via two mechanisms. The first mechanism is the reduction of glucose-stimulated ATP production (Figure 5-4), which leads to less closure of $K_{ATP}$ channels, resulting in a smaller glucose-evoked depolarization and thus less VGCC activation. Our data also shows that the reduction in glucose-evoked ATP production in cholesterol-treated cells is in part due to a decrease in glucose uptake via the glucose transporters (Figure 5-5). Since glucose metabolism is also regulated by glucokinase and cholesterol overload was shown to cause a significant reduction of the glucokinase activities in INS-1 cells (18), it is possible that a decrease in glucokinase activities may also contribute to the reduction in glucose-evoked ATP production in the cholesterol-treated mouse β cells. The second mechanism is a decrease in the density of VGCCs with cholesterol treatment; the VGCC density at +10 mV was reduced by ~50% (Figure 5-6). The reduction in $Ca^{2+}$ entry via VGCC further impairs glucose-mediated $Ca^{2+}$ signaling in β cells with cholesterol treatment. Since insulin secretion is $Ca^{2+}$-dependent, the above mechanisms have major roles in the impairment of glucose-stimulated insulin secretion observed in cholesterol-elevated islets.

Our study shows that cholesterol overload is associated with a decrease in the current density of delayed rectifier channels (Figure 5-7) as well as the $K_{ATP}$ channels (findings from Dr. A. Lee). The resting membrane potential of the β cells is primarily regulated by the activities of the $K_{ATP}$ channels. Although

there was a reduction in density of $K_{ATP}$ channels in the cholesterol-treated cells, their resting membrane potential was similar to the controls (~-80 mV; finding from Dr. Lee). This is probably due to the high input resistance of β cells, such that the opening of only a fraction of $K_{ATP}$ channels is sufficient to maintain the resting membrane potential. Despite the reduction in $K_{ATP}$ channel density, glucose triggered only a very small depolarization (~ 2 mV; findings from Dr. Lee) in the cholesterol-treated cells, probably because there is very little increase in cellular ATP in these cells. Since the delayed rectifier is voltage-dependent and significant activation of the delayed rectifier occurred at potentials more positive than -20 mV (Figure 5-7), this current has little contribution to the resting membrane potential but contributes to membrane repolarization in control β cells. In the cholesterol-overloaded cells, however, the delayed rectifier is not expected to be significantly activated because of the small glucose-evoked depolarization in these cells.

Cholesterol elevation may impair function of membrane proteins (including ion channels) through a number of different mechanisms. Our finding that our treatment designed to elevate cellular cholesterol resulted in general reduction of currents through VGCCs, $K_{ATP}$ channels, and delayed rectifier channels, without affecting the voltage dependence or inactivation kinetics of these currents, suggests that perhaps the mechanism of cholesterol elevation-mediated inhibition of the different channels is related to general changes in membrane properties, rather than specific changes in channel protein function. For example, cholesterol is known to increase lipid ordering in membranes, resulting in increased

membrane viscosity and stiffness, which may affect channel function. This issue is further discussed in Section 6.2.2.

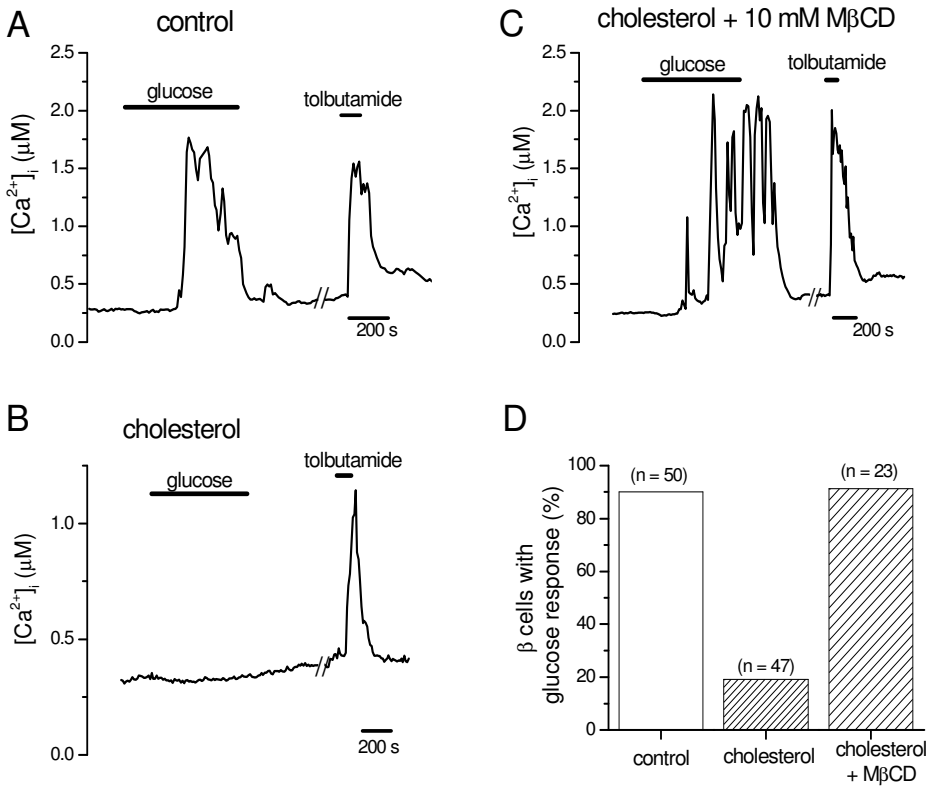


**Figure 5-1**: Cholesterol overload reduced the fraction of mouse β cells that exhibited a glucose-mediated $[Ca^{2+}]_i$ rise. (***A***) Glucose elevation (from 3 to 20 mM) triggered a robust $[Ca^{2+}]_i$ rise in a control cell. Subsequent challenge with tolbutamide (100 μM) also evoked a robust $Ca^{2+}$ response. In these and all subsequent experiments, β cells were identified by their $Ca^{2+}$ response to tolbutamide. (***B***) In most cholesterol-overload cells, glucose failed to evoke any $Ca^{2+}$ response but tolbutamide could still evoke a $[Ca^{2+}]_i$ rise. (***C***) In a cell treated with cholesterol plus 10 mM MβCD, glucose triggered a robust $Ca^{2+}$ response. (***D***) The fraction of β cells responding to glucose was dramatically reduced in cells treated with cholesterol but not in cells treated with cholesterol plus MβCD (10 or 20 mM). Recordings were obtained from 3 batches of cells.

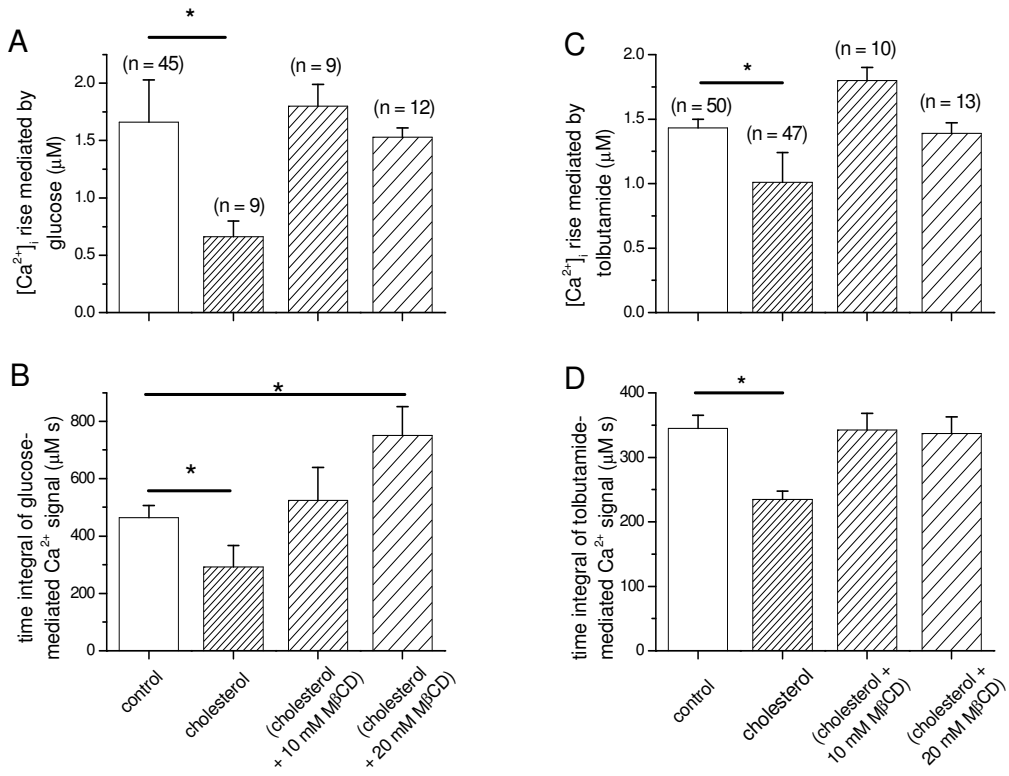


**Figure 5-2**: Both the amplitude and time integral of the glucose- or tolbutamide-triggered $Ca^{2+}$ signals were reduced in cells treated with cholesterol. For β cells overloaded with cholesterol that exhibited a $Ca^{2+}$ response when challenged with glucose, the amplitude (***A***) as well as the time integral (***B***) of the glucose-mediated $Ca^{2+}$ signal were significantly reduced. Cholesterol overload also reduced the amplitude (***C***) and time integral (***D***) of the tolbutamide-induced $[Ca^{2+}]_i$ rise. For cells treated with cholesterol plus MβCD, the glucose- and tolbutamide-mediated $Ca^{2+}$ signals were similar to controls. Recordings were obtained from 3 batches of cells.

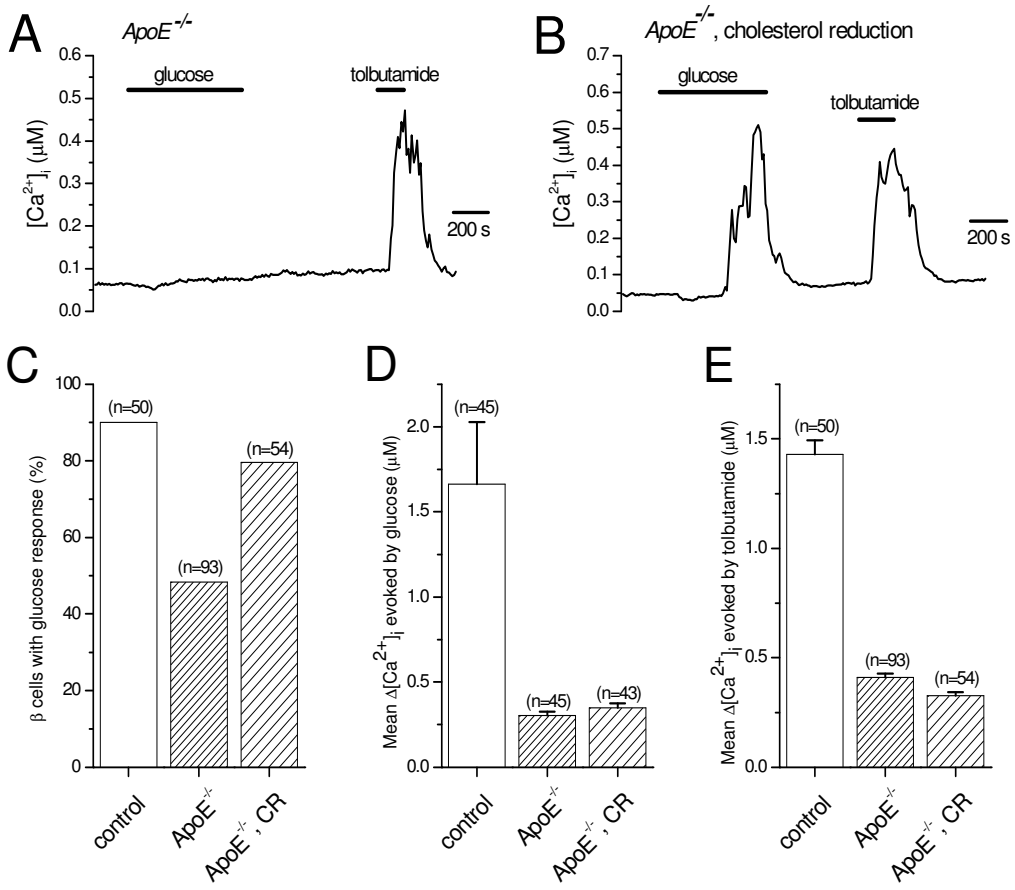


**Figure 5-3**: In comparison to the controls, β cells from *ApoE*$^{-/-}$ mice had impaired $Ca^{2+}$ response to glucose and tolbutamide. (***A***) An example of an *ApoE*$^{-/-}$ mouse β cell (identified by its response to tolbutamide) that failed to respond to glucose. (***B***) Reduction of cholesterol in *ApoE*$^{-/-}$ mouse β cells rescued their $Ca^{2+}$ response to glucose. (***C***) The fraction of β cells responding to glucose was dramatically reduced in *ApoE*$^{-/-}$ mice but was restored by cholesterol reduction (CR). (***D***) & (***E***) The amplitude of the $[Ca^{2+}]_i$ rise evoked by glucose (***D***) or tolbutamide (***E***) was reduced in of *ApoE*$^{-/-}$ mouse β cells, and this effect could not be rescued by cholesterol reduction (CR). Recordings were obtained from 3 batches of cells.

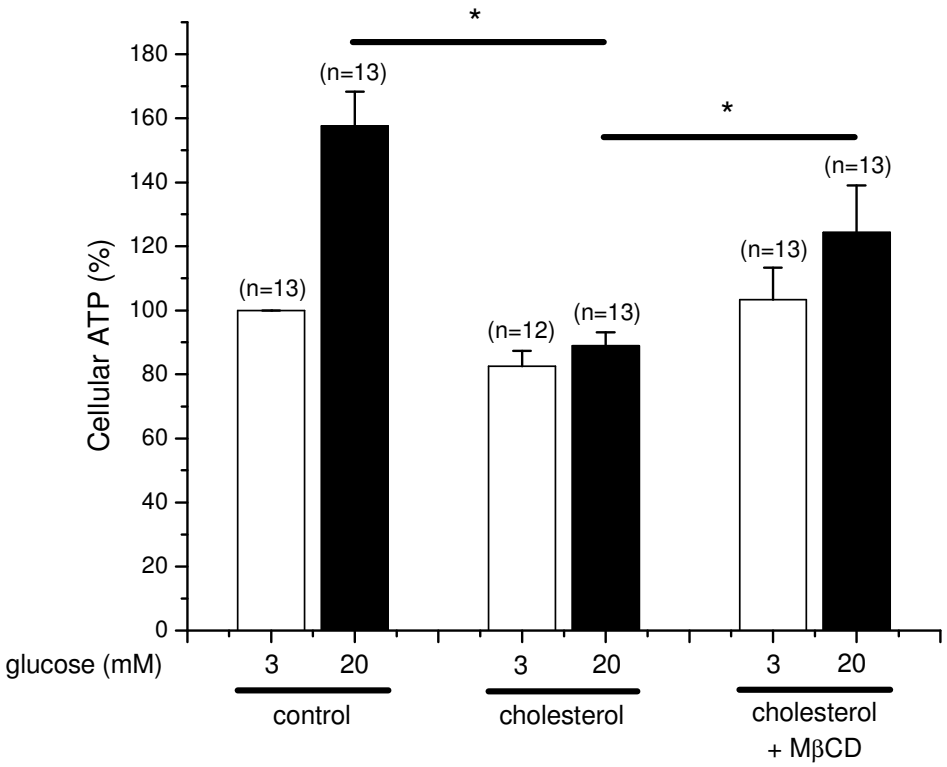


**Figure 5-4**: Glucose-stimulated ATP production was reduced in cells overloaded with cholesterol. Cellular ATP was measured using the luciferin-luciferase assay and all values were normalized to control cells in 3 mM glucose. Measurements were obtained from 5 experiments (4 batches of cells).

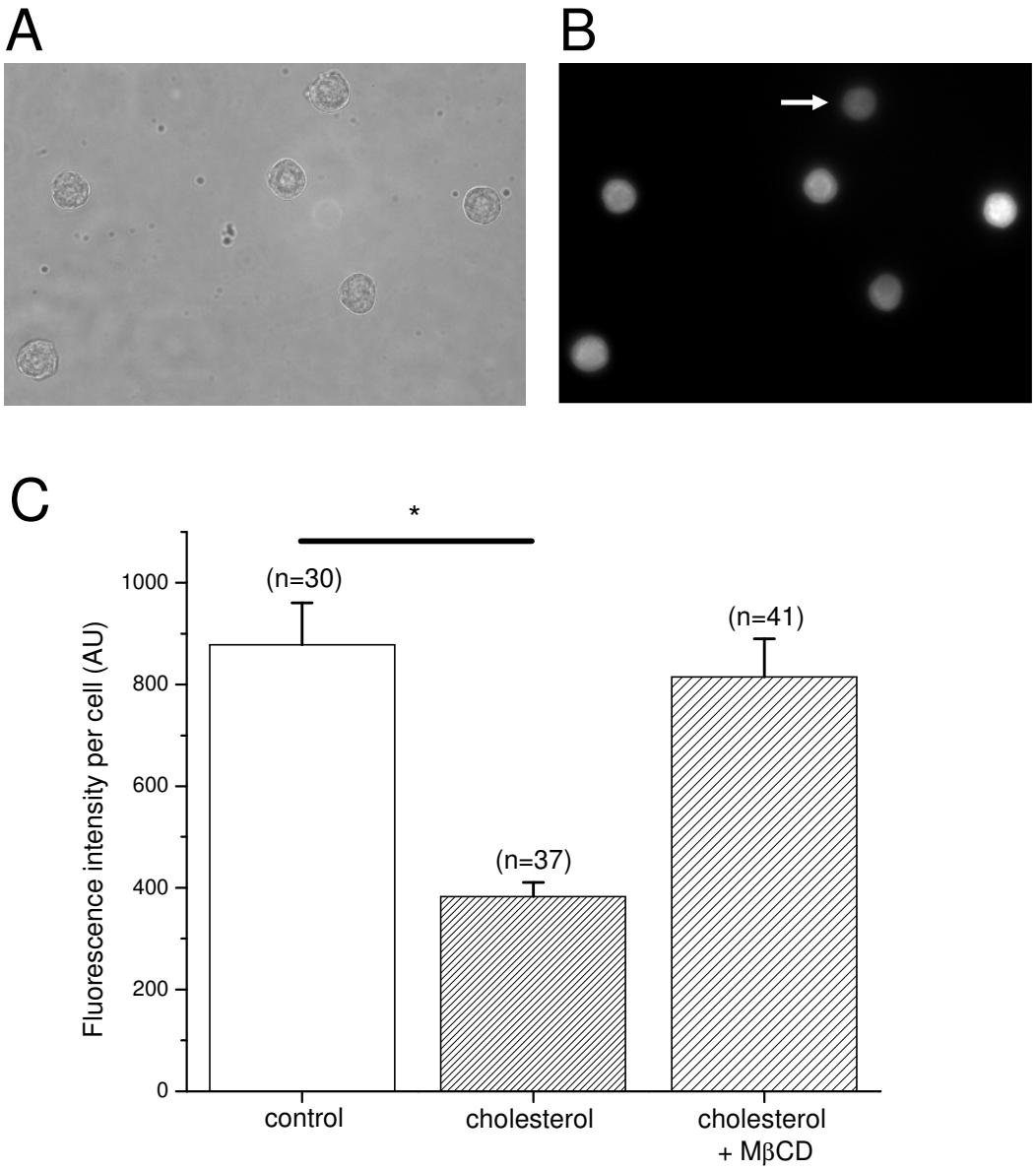


**Figure 5-5**: Glucose uptake into β cells (measured by 2-NBDG fluorescence) was reduced in cholesterol-overloaded cells. (***A***) Bright-field image of single islet cells (x400 magnification). (***B***) Fluorescent image of the same cells after incubation with 2-NBDG for 10 mins. White arrow indicates a cell that failed to exhibit a $Ca^{2+}$ response during a subsequent challenge with tolbutamide. (***C***) The mean fluorescence of 2-NBDG (expressed as arbitrary units (AU)) in individual β cells in the cholesterol-overloaded group was significantly smaller than that in cells in the control group. Images and recordings were obtained from 3 batches of islet cells.

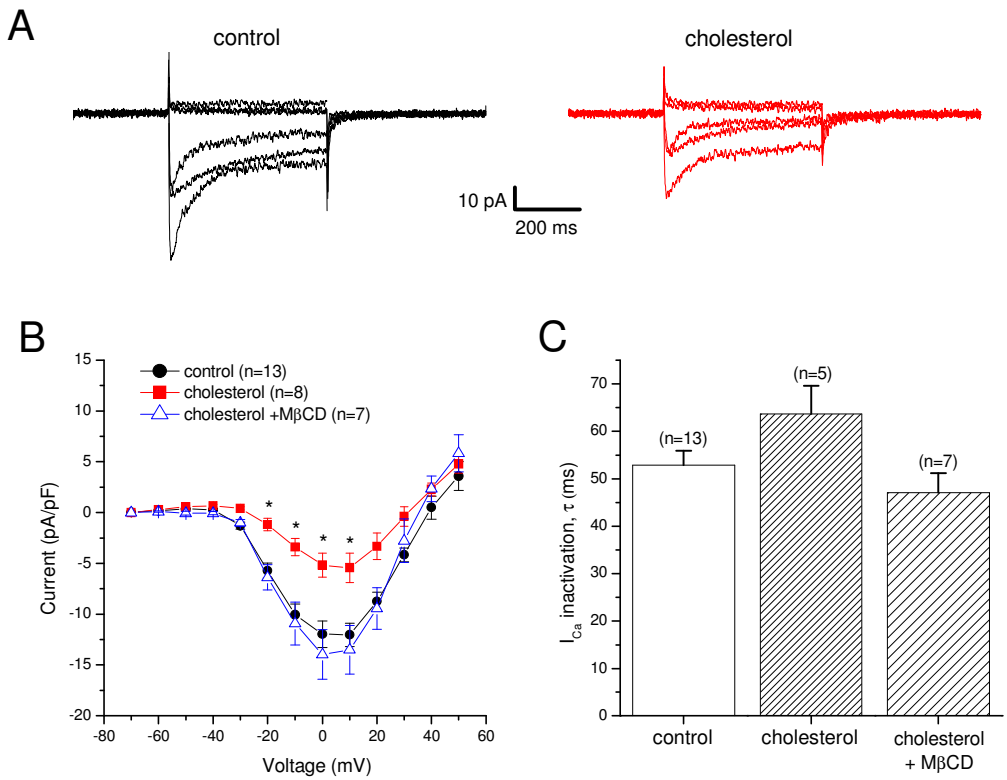


**Figure 5-6**: Cholesterol overload reduced $I_{Ca}$ density at a wide range of potentials but had no effect on $I_{Ca}$ inactivation kinetics. (***A***) Families of $I_{Ca}$ recorded from a control cell and a cell treated with cholesterol. Cells were held at -80 mV and depolarized to potentials between -70 to +50 mV at 25 $^{o}$C. $K^+$ currents were blocked by including $Cs^+$ and $TEA^+$ in the whole-cell pipette solution and tolbutamide in the bath. (***B***) I-V plots of cells treated with cholesterol, cholesterol plus MβCD or controls. The current density was obtained by normalizing the peak amplitude of $I_{Ca}$ to individual cell capacitance. (***C***) Cholesterol overload did not significantly alter the time course of $I_{Ca}$ inactivation. τ was obtained from the exponential fit to the time course of decay of $I_{Ca}$ at +10 mV. Recordings were obtained from 4 batches of islet cells.

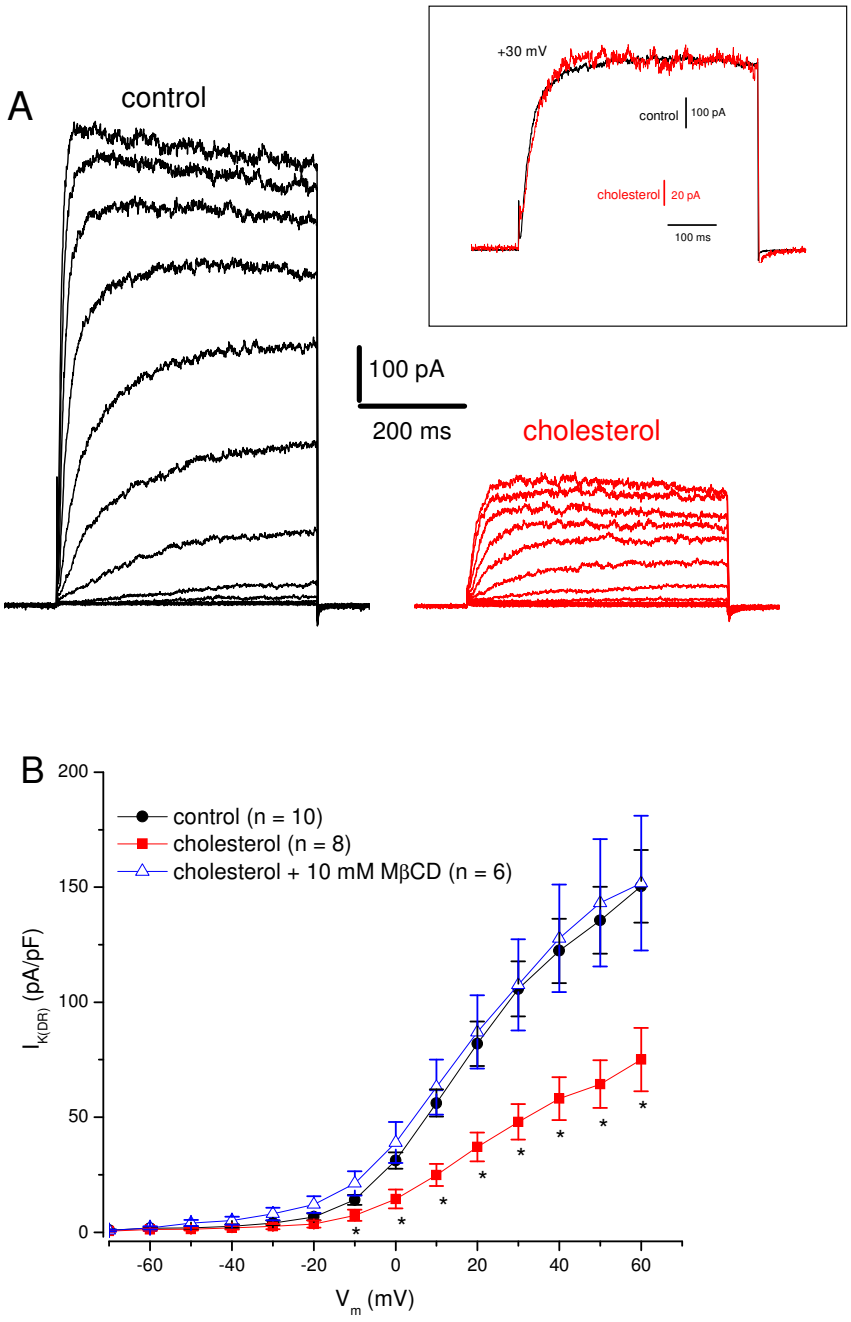


**Figure 5-7**: Cholesterol overload reduced $I_{K(DR)}$ density. (***A***) Families of $I_{K(DR)}$ recorded from a control cell and a cell treated with cholesterol. Cells were held at -80 mV and depolarized to potentials between -70 to +60 mV at 25 $^{o}$C. The inset shows that the time course of $I_{K(DR)}$ evoked at +30 mV in control is similar to that of the cholesterol overload cell (scaled to matching amplitude). The whole-cell pipette contained 10 mM EGTA and the bath contained tolbutamide and $Cd^{2+}$. (***B***) Cholesterol overload reduced the density of $I_{K(DR)}$ over a wide range of potentials. Recordings were obtained from 4 batches of islet cells.

## References


1. Chang,TY, Li,BL, Chang,CC, Urano,Y: Acyl-coenzyme A:cholesterol acyltransferases. *Am J Physiol Endocrinol Metab* 297:E1-E9, 2009
2. Oram,JF, Lawn,RM: ABCA1. The gatekeeper for eliminating excess tissue cholesterol. *J Lipid Res* 42:1173-1179, 2001
3. Tall,AR, Costet,P, Wang,N: Regulation and mechanisms of macrophage cholesterol efflux. *J Clin Invest* 110:899-904, 2002
4. Shimano,H: Sterol regulatory element-binding proteins (SREBPs): transcriptional regulators of lipid synthetic genes. *Prog Lipid Res* 40:439-452, 2001
5. Zelcer,N, Tontonoz,P: Liver X receptors as integrators of metabolic and inflammatory signaling. *J Clin Invest* 116:607-614, 2006
6. Lichtenberg,D, Goni,FM, Heerklotz,H: Detergent-resistant membranes should not be identified with membrane rafts. *Trends Biochem Sci* 30:430-436, 2005
7. Pike,LJ: Rafts defined: a report on the Keystone Symposium on Lipid Rafts and Cell Function. *J Lipid Res* 47:1597-1598, 2006
8. Lang,T: SNARE proteins and 'membrane rafts'. *J Physiol* 585:693-698, 2007
9. Vikman,J, Jimenez-Feltstrom,J, Nyman,P, Thelin,J, Eliasson,L: Insulin secretion is highly sensitive to desorption of plasma membrane cholesterol. *FASEB J* 23:58-67, 2009
10. Zidovetzki,R, Levitan,I: Use of cyclodextrins to manipulate plasma membrane cholesterol content: evidence, misconceptions and control strategies. *Biochim Biophys Acta* 1768:1311-1324, 2007
11. Xia,F, Gao,X, Kwan,E, Lam,PP, Chan,L, Sy,K, Sheu,L, Wheeler,MB, Gaisano,HY, Tsushima,RG: Disruption of pancreatic beta-cell lipid rafts modifies Kv2.1 channel gating and insulin exocytosis. *J Biol Chem* 279:24685-24691, 2004
12. Howard,BV: Insulin resistance and lipid metabolism. *Am J Cardiol* 84:28J-32J, 1999
13. Cnop,M: Fatty acids and glucolipotoxicity in the pathogenesis of Type 2 diabetes. *Biochem Soc Trans* 36:348-352, 2008
14. Brunham,LR, Kruit,JK, Pape,TD, Timmins,JM, Reuwer,AQ, Vasanji,Z, Marsh,BJ, Rodrigues,B, Johnson,JD, Parks,JS, Verchere,CB, Hayden,MR: Beta-cell ABCA1 influences insulin secretion, glucose homeostasis and response to thiazolidinedione treatment. *Nat Med* 13:340-347, 2007
15. Takahashi,A, Motomura,K, Kato,T, Yoshikawa,T, Nakagawa,Y, Yahagi,N, Sone,H, Suzuki,H, Toyoshima,H, Yamada,N, Shimano,H: Transgenic mice overexpressing nuclear SREBP-1c in pancreatic beta-cells. *Diabetes* 54:492-499, 2005
16. Efanov,AM, Sewing,S, Bokvist,K, Gromada,J: Liver X receptor activation stimulates insulin secretion via modulation of glucose and lipid metabolism in pancreatic beta-cells. *Diabetes* 53 Suppl 3:S75-S78, 2004
17. Gerin,I, Dolinsky,VW, Shackman,JG, Kennedy,RT, Chiang,SH, Burant,CF, Steffensen,KR, Gustafsson,JA, Macdougald,OA: LXRbeta is required for adipocyte growth, glucose homeostasis, and beta cell function. *J Biol Chem* 280:23024-23031, 2005
18. Hao,M, Head,WS, Gunawardana,SC, Hasty,AH, Piston,DW: Direct effect of cholesterol on insulin secretion: a novel mechanism for pancreatic beta-cell dysfunction. *Diabetes* 56:2328-2338, 2007
19. Xia,F, Xie,L, Mihic,A, Gao,X, Chen,Y, Gaisano,HY, Tsushima,RG: Inhibition of cholesterol biosynthesis impairs insulin secretion and voltage-gated calcium channel function in pancreatic beta-cells. *Endocrinology* 149:5136-5145, 2008

20. Hao,M, Bogan,JS: Cholesterol regulates glucose-stimulated insulin secretion through phosphatidylinositol 4,5-bisphosphate. *J Biol Chem* 284:29489-29498, 2009
21. Executive Summary of The Third Report of The National Cholesterol Education Program (NCEP) Expert Panel on Detection, Evaluation, And Treatment of High Blood Cholesterol In Adults (Adult Treatment Panel III). *JAMA* 285:2486-2497, 2001
22. Jawien,J, Nastalek,P, Korbut,R: Mouse models of experimental atherosclerosis. *J Physiol Pharmacol* 55:503-517, 2004
23. Yamada,K, Nakata,M, Horimoto,N, Saito,M, Matsuoka,H, Inagaki,N: Measurement of glucose uptake and intracellular calcium concentration in single, living pancreatic beta-cells. *J Biol Chem* 275:22278-22283, 2000
24. Yamada,K, Saito,M, Matsuoka,H, Inagaki,N: A real-time method of imaging glucose uptake in single, living mammalian cells. *Nat Protoc* 2:753-762, 2007
25. MacDonald,PE, Sewing,S, Wang,J, Joseph,JW, Smukler,SR, Sakellaropoulos,G, Wang,J, Saleh,MC, Chan,CB, Tsushima,RG, Salapatek,AM, Wheeler,MB: Inhibition of Kv2.1 voltage-dependent K+ channels in pancreatic beta-cells enhances glucose-dependent insulin secretion. *J Biol Chem* 277:44938-44945, 2002
26. Bonfleur,ML, Vanzela,EC, Ribeiro,RA, de Gabriel,DG, de Franca Carvalho,CP, Collares-Buzato,CB, Carneiro,EM, Boschero,AC, de Oliveira,HC: Primary hypercholesterolaemia impairs glucose homeostasis and insulin secretion in low-density lipoprotein receptor knockout mice independently of high-fat diet and obesity. *Biochim Biophys Acta* 1801:183-190, 2010

# Chapter 6

# General discussion

All the experiments described in this thesis were performed in single pancreatic islet cells of rat or mouse. Since lipids play an integral role in the regulation of β cell functions, we examined the actions of two different lipids (AA and cholesterol), using primarily a combination of $[Ca^{2+}]_i$ measurement and electrophysiological techniques. This chapter will summarize the findings presented in the preceding chapters and address important issues arising from our findings.

## 6.1 Actions of AA on rat pancreatic β cells (Chapters 3 & 4)

### *6.1.1 Actions of AA on extracellular $Ca^{2+}$ entry*

AA is produced upon stimulation of pancreatic islets with secretagogues such as glucose (1) or ACh (2). Exogenous AA, in the presence of a substimulatory concentration of glucose, has been shown to cause an increase in $[Ca^{2+}]_i$ that is dependent on both extracellular $Ca^{2+}$ entry and intracellular $Ca^{2+}$ release (3). Part of the AA-mediated extracellular $Ca^{2+}$ entry is dependent on the activation of VGCCs, which is possibly mediated by a reduction of $K_{ATP}$ channels (4) and or delayed rectifiers (5). Our results revealed that AA also mediates extracellular $Ca^{2+}$ entry via a VGCC-independent pathway. We found that, in rat pancreatic β cells, AA mediates $Ca^{2+}$ entry through the ARC channels. Although the ARC current density in rat β cells is small (~1. 7 pA/pF at -70 mV), the ARC channels are highly $Ca^{2+}$ permeable since, as shown in Figure 3-3, the activation of ARC channels by a low concentration of AA (5 μM) was able to elevate $[Ca^{2+}]_i$ to the μM range. In our experiments, the membrane potential of the rat β cells was

voltage-clamped at -70 mV. Since ARC channels are not voltage-activated, the negative membrane potential will result in a larger extracellular $Ca^{2+}$ influx under our experimental conditions. During glucose stimulation, the closure of $K_{ATP}$ channels causes membrane depolarization in β cells and there will be less contribution from the ARC-mediated $Ca^{2+}$ entry. However, upon stimulation by ACh or cholecystokinin, the membrane potential of the β cells is near the resting membrane potential (~-70 mV). Under this condition, there will be a significant contribution from the ARC-mediated $Ca^{2+}$ entry. The ARC-mediated $Ca^{2+}$ signal is also much larger than that triggered by the activation of CCE in the same cells (~0.1 μM) (6). Most importantly, elevation of $[Ca^{2+}]_i$ to the μM range could trigger robust exocytosis in rat β cells (6). Consistent with this, Dr. Andy Lee has found that the AA-mediated $[Ca^{2+}]_i$ rise in single rat β cells was accompanied by an increase in cell membrane capacitance, reflecting exocytosis (unpublished finding). Thus, the ARC-mediated $Ca^{2+}$ signal may account for the ability of AA to trigger insulin secretion from islets at low glucose level (7). During glucose stimulation, the accumulation of AA in rat pancreatic islets can be as high as 35 μM (8). Therefore, it is likely that there is significant activation of ARC channels during glucose stimulation and that the resultant $Ca^{2+}$ influx via ARC channels may amplify secretagogue-induced $Ca^{2+}$ signals and potentiate insulin secretion. Consistent with this notion, the inhibition of arachidonate release by inhibitors of $PLA_2$ also suppressed the glucose-evoked insulin secretion from rat islets (8).

In summary, this is a novel report on the presence of functional ARC channels in an electrically excitable primary cell. Prior to our study, ARC channels have

been described mainly in non-excitable cells such as the parotid and pancreatic acinar cells (9), and they have been primarily associated with regulation of the frequency of agonist-stimulated $Ca^{2+}$ signals. Our study has revealed that in rat β cells, the extracellular $Ca^{2+}$ entry via ARC channels can trigger robust $[Ca^{2+}]_i$ rise. Thus, in electrically excitable cells such as β cells, the activation of ARC channels may represent an important source of extracellular $Ca^{2+}$ entry in addition to VGCCs.

### *6.1.2 Physiological role of AA-mediated intracellular $Ca^{2+}$ release in β cells*

In addition to $Ca^{2+}$ entry through ARC channels, AA has also been reported to induce intracellular $Ca^{2+}$ release from the ER (7). We found that the AA-induced intracellular $Ca^{2+}$ release was abolished by the prior emptying of the $IP_3$-sensitive stores with the $IP_3R$ agonist adenophostin A (Figure 4-7). However, we found that bafilomycin A1 and GPN, which ablate the acidic $Ca^{2+}$ store, reduced AA-stimulated intracellular $Ca^{2+}$ release by ~70%. Although GPN is typically employed to disrupt lysosomes, we found that activators of the lysosomal $Ca^{2+}$ release (such as ADPR or NAADP) failed to reduce the AA-mediated intracellular $Ca^{2+}$ release. Since the secretory granules are acidic stores that have a high $Ca^{2+}$ content, and since GPN has been shown to lyse secretory granules (10), we speculate that the bafilomycin- or GPN-sensitive component of the AA-mediated intracellular $Ca^{2+}$ release is due to $Ca^{2+}$ release from secretory granules. A local release of $Ca^{2+}$ from the secretory granules (when triggered by exogenous ATP) in rat β cells was reported to trigger robust exocytosis (11).

In summary, this is a novel report on the ability of AA to release $Ca^{2+}$ from an $IP_3$-sensitive acidic store in rat pancreatic β cells. Since AA is produced upon stimulation of pancreatic islets with either glucose or ACh, AA-mediated intracellular $Ca^{2+}$ release may amplify global $Ca^{2+}$ signals and enhance insulin release.

### *6.1.3 Future directions*

We have determined that AA activates extracellular $Ca^{2+}$ entry through the ARC channel. To obtain further evidence to confirm our findings, we can conduct experiments that interfere with expression of the proteins that make up the ARC channel. It has been reported that the pore of the ARC channel is composed of Orai1 and Orai3 proteins (12;13), and that its activity is regulated by the accessory protein STIM1 (14). Although antibodies against these proteins are commercially available, Orai1 and STIM1 proteins are also components of the CCE channels (15). Therefore, examining protein expression (with a Western blot or with *in situ* immunohistochemistry) will not reveal whether ARC channels are present in rat β cells. One possible experiment is to reduce the expression of STIM1, Orai1, or Orai3 (or a combination thereof) using small interfering RNA (siRNA) against these proteins, and examine whether this manipulation reduces AA-induced $Ca^{2+}$ entry. Using the same strategy, we can also examine the contribution of the ARC channels to the glucose or ACh-evoked $Ca^{2+}$ signals or insulin secretion from the β cells.

We also found that AA can induce intracellular $Ca^{2+}$ release from two $IP_3$-sensitive stores, including the ER and an acidic $Ca^{2+}$ store. However, it is unclear how AA stimulates $Ca^{2+}$ release from these stores. One possible mechanism is modulation of the $IP_3$Rs by AA such that there is an increase in the opening probability of these $Ca^{2+}$ permeable channels. This possibility can be addressed by employing $IP_3$R inhibitors, such as heparin or 2-APB, which are known to block $Ca^{2+}$ release via $IP_3$R channels. If whole-cell dialysis of heparin or bath application of 2-APB can attenuate the effects of AA on intracellular $Ca^{2+}$ release, it will suggest that the site of action of AA is on the $IP_3$R channels.

We have speculated that AA releases $Ca^{2+}$ from the secretory granules. To confirm this, we can examine whether $IP_3$Rs colocalize with a secretory granule marker (such as VAMP, which is a vesicle-specific SNARE) in rat β cells. It may also be important to use antibodies specific for each of the three different isoforms of $IP_3$R, since is has been suggested by Blondel *et al*. that $IP_3$R3 alone may mediate $Ca^{2+}$ release from secretory vesicles (16;17). Different $IP_3$R isoforms may be localized to different intracellular stores, and this may account for differential regulation of the stores (18). Another important experiment is to investigate the effects of AA on the $[Ca^{2+}]$ of secretory granules directly. One approach would be to use a bioluminescent probe such as aequorin, which is derived from *Aequorea victoria*. In the presence of the cofactor coelenterazine, aequorin binds $Ca^{2+}$, undergoes an irreversible reaction, and emits a photon. Previously, it was only possible to study cytosolic $[Ca^{2+}]$ with aequorin. However, the isolation of aequorin's cDNA sequence permitted the engineering

of chimeric aequorins that can be targeted to specific subcellular locations. For example, MIN6 cells have been transfected with chimeric cDNA encoding a fusion protein between VAMP2 and aequorin (VAMP.Aq), to enable the monitoring of intravesicular [$Ca^{2+}$] (19;20). Some of the drawbacks with aequorins are that the spatial resolution is low and the signal (number of photons emitted) is much lower than with other methods. Another approach is the use of cameleons. Cameleons are genetically encoded fluorescent $Ca^{2+}$ indicators that consist of a short-wavelength mutant of green fluorescent protein (GFP) and a long-wavelength mutant of GFP, separated by calmodulin (a $Ca^{2+}$-binding protein). Upon binding of $Ca^{2+}$ to calmodulin, the cameleon protein changes from an extended to a more compact conformation. This leads to a change in the efficiency of fluorescent resonance energy transfer (FRET) between the two mutant GFPs, which is reflected as a change in emission ratio. Cameleons can also be targeted to specific subcellular locations through the addition of localization sequences, and have previously been used to visualize [$Ca^{2+}$] in the ER of MIN6 cells (21). Although older cameleons are quenched by acidification, newer versions are less sensitive to low pH and may therefore be useful in measuring [$Ca^{2+}$] in an acidic compartment.

## 6.2 Effects of cholesterol overload on glucose-stimulated $Ca^{2+}$ signaling in mouse pancreatic β cells

### *6.2.1 Multiple steps in the glucose-stimulated $[Ca^{2+}]_i$ increase are impaired by cholesterol overload*

Studies from transgenic mouse models (22-26) and INS-1 cells (22;27) have demonstrated that accumulation of cellular cholesterol have detrimental effects on glucose-stimulated insulin secretion. Our results have shown that even an acute elevation of cellular cholesterol can dramatically reduce glucose-stimulated $[Ca^{2+}]_i$ rise in mouse β cells. This inhibitory action is mediated through two major mechanisms. The first mechanism is a reduction in glucose-stimulated ATP production, which leads to less closure of $K_{ATP}$ channels, resulting in a smaller glucose-evoked depolarization, and thus less VGCC activation. We found that the reduction in glucose-evoked ATP production in cholesterol overload cells is due in part to a decrease in glucose uptake via the glucose transporters. The second mechanism is a decrease in the current density of VGCCs with cholesterol overload. The reduction in $Ca^{2+}$ entry via VGCCs with cholesterol overload further impairs glucose-mediated $Ca^{2+}$ signaling in β cells. Since insulin secretion is $Ca^{2+}$-dependent, the above mechanisms have major roles in the impairment of glucose-stimulated insulin secretion observed in islets with elevated cholesterol.

Our results with the *ApoE*$^{-/-}$ mice indicate that chronic elevation of plasma cholesterol also results in similar reduction in the glucose-mediated $Ca^{2+}$ signaling in the β cells (Figure 5-3). Interestingly, an overnight incubation with a HMG CoA reductase inhibitor in conjunction with a 1-hour treatment with MβCD to

lower cellular cholesterol was able to restore the ability of the β cells from *ApoE*$^{-/-}$ mice to respond to glucose (Figure 5-3C). These findings suggest that cholesterol level in the plasma membrane can be altered rapidly by the level of extracellular cholesterol or the presence of a cholesterol extractor such as MβCD. Our results also indicate that elevation of plasma membrane cholesterol can have strong impact on ion channels. We have shown that cholesterol overload reduced the current density of the three major ion channels in β cells: $K_{ATP}$ channels, VGCCs, and delayed rectifier channels. In contrast, in INS-1 cells, cholesterol extraction with MβCD, which disrupted lipid rafts, reduced the delayed rectifier current density without affecting $K_{ATP}$ channels or VGCCs (28). Thus, based on current findings, the disruption of lipid rafts (with MβCD) in insulin-secreting cells has a smaller impact on ion channel function in comparison to the elevation of plasma membrane cholesterol.

In summary, this is a novel report on the ability of cholesterol overload to impair multiple steps in the stimulus-secretion coupling pathway in mouse pancreatic β cells. Since type II diabetes is associated with high plasma cholesterol and high islet cholesterol, these defects may impair the ability of the islets to secrete insulin in response to glucose elevation, thus further aggravating glucose intolerance in diabetic patients and accelerating progression of the disease.

### *6.2.2 Future directions: mechanism of inhibition of glucose-stimulated $[Ca^{2+}]_i$ rise by cholesterol*

In our experiments, the islet cells were exposed to elevated cholesterol for only 1 hour. Thus, it is unlikely that the reduction in glucose uptake and current density is due to a change in the expression of GLUT2 and ion channels. Instead, we speculate that there is a reduction in the function of the glucose transporters or ion channels when the plasma membrane cholesterol is elevated. As mentioned in Section 5.3, there are several possible mechanisms by which cholesterol overload may exert an inhibitory effect on membrane proteins. This section will explore the different possible mechanisms of cholesterol overload-mediated inhibition of channel or transporter function, of which three are more likely. First, cholesterol may directly inhibit ion channels through protein-lipid interactions. Second, cholesterol may indirectly inhibit ion channels by changing membrane properties such as fluidity and stiffness, which can influence channel function. Third, cholesterol may act indirectly via $PIP_2$, which is known to interact with and alter channel function.

Since we observed a common inhibitory effect of cholesterol overload on different families of membrane proteins, including glucose transporters, VGCCs, $K_{ATP}$ channels, and delayed rectifiers, it is possible that the effects arise from some cholesterol-mediated change in the biophysical properties of the membrane. For example, the ratio of cholesterol to phospholipids in a plasma membrane is an important factor in determining membrane fluidity. Within the plasma membrane, cholesterol increases the order of phospholipid hydrocarbon chains in

the membrane, and increases the tightness of their packing (29). Therefore, an elevation of cholesterol level in the plasma membrane is associated with a decrease in the fluidity (30), as well as increase in the stiffness (31), of the plasma membrane. The fluidity of a plasma membrane refers to the ability of proteins to move around within a lipid bilayer (rotation, flexion, lateral diffusion, etc.), and its inverse is viscosity. Membrane stiffness, on the other hand, is a reflection of the bending modulus of the plasma membrane. It has been suggested that the increase in stiffness and viscosity may increase the energy requirement for transitions between conformational states of membrane proteins (31). Consistent with this, a cholesterol-induced increase in viscosity or stiffness has been suggested to reduce the function of integral membrane proteins, including the adenine nucleotide transporter in mitochondrial membrane (30), the SERCA pump in microsomes isolated from macrophages (32), and N-type VGCCs in a lipid bilayer (31). Additionally, MβCD-mediated lowering of membrane cholesterol led to increased activity of the volume-regulated anion current in aortic endothelial cells (33).

On the other hand, the inhibitory effects of cholesterol overload may be attributed to the modulation of specific relationships between membrane proteins and membrane lipids. For example, the suppression of Kir2 channel function in endothelial cells by cholesterol elevation is regulated by a specific interaction between cholesterol and the channel (34); cholesterol binds to a specific region of the C terminus of the channel's cytosolic domain (35). Cholesterol is also known to interact directly with serotonin receptors and nicotinic receptors: both

serotonin and nicotinic receptors have specific putative binding sites for cholesterol, and receptor function is altered by the binding of cholesterol to those sites (36;37). Whether VGCCs containing similar binding sites remains to be seen; however, since a C-terminal domain conferring cholesterol sensitivity to Kir2.1 has been identified (35), and a putative cholesterol-binding sequence has been reported in serotonin receptors (37), it may be useful to screen for similar sequences in VGCCs.

To differentiate between the effects of cholesterol that are related to changes in the biophysical properties of membranes, and those that are due to specific interactions between cholesterol and proteins, one possible approach is to examine the effects of different cholesterol analogs. For example, epicholesterol, an epimer of cholesterol, has similar effects as cholesterol on the biophysical properties of plasma membranes, but cannot mimic the specific interactions between cholesterol and proteins in the regulation of Kir2 channels (38). The effects can be confirmed by using coprostanol. Coprostanol is a naturally occurring product of cholesterol metabolism that does not have any appreciable effect on membrane stiffness or viscosity, but can mimic the specific interactions between cholesterol and proteins. Therefore, if the effects of cholesterol are mimicked by epicholesterol, then it is likely that the alterations in membrane protein function that we observed are due to the increase in membrane stiffness. If, however, only coprostanol mimics the effects of cholesterol, then we may conclude that the cholesterol forms specific interactions with a variety of membrane proteins. It must also be noted that even if cholesterol's effects are

mimicked by coprostanol, this does not mean that cholesterol necessarily interacts directly with the channel or transporter; it may actually interact with a modulatory protein that in turn regulates channel or transporter function.

There is also the possibility that the effects of cholesterol on membrane proteins are actually mediated by phosphatidylinositol 4,5-bisphosphate ($PIP_2$). $PIP_2$ is necessary for the function of many ion channels and ion transporters (39). Altering $PIP_2$ concentration can alter the function of many membrane proteins, including Kir channels, VGCCs, $Na^{2+}/Ca^{2+}$ exchanger (NCX), plasma membrane $Ca^{2+}$-ATPase (PMCA) (39), and $K_{ATP}$ channels (40). Most of the cellular $PIP_2$ is in the plasma membrane, and it accounts for ~1% of membrane lipids. Although $PIP_2$ is unlikely to interact directly with cholesterol, there may still be a relationship between $PIP_2$ and cholesterol; one suggested model is that $PIP_2$ associates with $PIP_2$-interacting proteins, such as growth-associated protein of 43 kDa (GAP-43) (41), that are localized to cholesterol-enriched domains in the plasma membrane. This association results in sequestration of $PIP_2$ in a cholesterol-dependent fashion (42). Increasing membrane cholesterol may therefore increase availability of $PIP_2$ in the membrane, leading to changes in function of proteins modulated by $PIP_2$. However, it is unclear whether $PIP_2$ modulates channel function through direct specific interactions with membrane proteins, or whether its effects are mediated by downstream proteins. For example, increased interaction between Kir6.2 and $PIP_2$ can decrease the sensitivity of $K_{ATP}$ channels to ATP (40). On the other hand, cholesterol-stimulated increase in $PIP_2$ in INS-1 cells is associated with increased actin

polymerization, which may mediate cholesterol-associated decrease in glucose-stimulated insulin secretion (27). Involvement of $PIP_2$ in the effects of cholesterol overload may be probed by using agents that hydrolyze $PIP_2$ (e.g. PLC activator, such as 2,4,6-trimethyl-*N*-(*meta*-3-trifluoromethylphenyl)-benzenesulfonamide (*m*-3M3FBS) (43)). Alternatively, one can examine whether the effects of cholesterol overload are mimicked by $PIP_2$ mimics (e.g. dioctanoyl $PIP_2$).

Finally, it is possible that cholesterol overload may interfere with membrane protein trafficking, such that there are fewer transporters or channels available on the plasma membrane. One way to address this possibility would be to examine the cell surface expression of GLUT2, VGCCs, delayed rectifiers, and $K_{ATP}$ channels. This can be achieved by *in situ* immunohistochemistry in intact cells, using specific antibodies against the extracellular domain of the various proteins being studied.

## References


1. Wolf,BA, Pasquale,SM, Turk,J: Free fatty acid accumulation in secretagogue-stimulated pancreatic islets and effects of arachidonate on depolarization-induced insulin secretion. *Biochemistry* 30:6372-6379, 1991
2. Konrad,RJ, Jolly,YC, Major,C, Wolf,BA: Carbachol stimulation of phospholipase A2 and insulin secretion in pancreatic islets. *Biochem J* 287 ( Pt 1):283-290, 1992
3. Ramanadham,S, Gross,R, Turk,J: Arachidonic acid induces an increase in the cytosolic calcium concentration in single pancreatic islet beta cells. *Biochem Biophys Res Commun* 184:647-653, 1992
4. Eddlestone,GT: ATP-sensitive K channel modulation by products of PLA2 action in the insulin-secreting HIT cell line. *Am J Physiol* 268:C181-C190, 1995
5. Jacobson,DA, Weber,CR, Bao,S, Turk,J, Philipson,LH: Modulation of the pancreatic islet beta-cell-delayed rectifier potassium channel Kv2.1 by the polyunsaturated fatty acid arachidonate. *J Biol Chem* 282:7442-7449, 2007
6. Hughes,E, Lee,AK, Tse,A: Dominant role of sarcoendoplasmic reticulum Ca2+-ATPase pump in Ca2+ homeostasis and exocytosis in rat pancreatic beta-cells. *Endocrinology* 147:1396-1407, 2006
7. Wolf,BA, Turk,J, Sherman,WR, McDaniel,ML: Intracellular Ca2+ mobilization by arachidonic acid. Comparison with myo-inositol 1,4,5-trisphosphate in isolated pancreatic islets. *J Biol Chem* 261:3501-3511, 1986
8. Ramanadham,S, Gross,RW, Han,X, Turk,J: Inhibition of arachidonate release by secretagogue-stimulated pancreatic islets suppresses both insulin secretion and the rise in beta-cell cytosolic calcium ion concentration. *Biochemistry* 32:337-346, 1993
9. Mignen,O, Thompson,JL, Yule,DI, Shuttleworth,TJ: Agonist activation of arachidonate-regulated Ca2+-selective (ARC) channels in murine parotid and pancreatic acinar cells. *J Physiol* 564:791-801, 2005
10. Duman,JG, Chen,L, Palmer,AE, Hille,B: Contributions of intracellular compartments to calcium dynamics: implicating an acidic store. *Traffic* 7:859-872, 2006
11. Xie,L, Zhang,M, Zhou,W, Wu,Z, Ding,J, Chen,L, Xu,T: Extracellular ATP stimulates exocytosis via localized Ca(2+) release from acidic stores in rat pancreatic beta cells. *Traffic* 7:429-439, 2006
12. Mignen,O, Thompson,JL, Shuttleworth,TJ: Both Orai1 and Orai3 are essential components of the arachidonate-regulated Ca2+-selective (ARC) channels. *J Physiol* 586:185-195, 2008
13. Mignen,O, Thompson,JL, Shuttleworth,TJ: The molecular architecture of the arachidonate-regulated Ca2+-selective ARC channel is a pentameric assembly of Orai1 and Orai3 subunits. *J Physiol* 587:4181-4197, 2009
14. Mignen,O, Thompson,JL, Shuttleworth,TJ: STIM1 regulates Ca2+ entry via arachidonate-regulated Ca2+-selective (ARC) channels without store depletion or translocation to the plasma membrane. *J Physiol* 579:703-715, 2007
15. Roos,J, DiGregorio,PJ, Yeromin,AV, Ohlsen,K, Lioudyno,M, Zhang,S, Safrina,O, Kozak,JA, Wagner,SL, Cahalan,MD, Velicelebi,G, Stauderman,KA: STIM1, an essential and conserved component of store-operated Ca2+ channel function. *J Cell Biol* 169:435-445, 2005
16. Blondel,O, Moody,MM, Depaoli,AM, Sharp,AH, Ross,CA, Swift,H, Bell,GI: Localization of inositol trisphosphate receptor subtype 3 to insulin and somatostatin secretory granules and regulation of expression in islets and insulinoma cells. *Proc Natl Acad Sci U S A* 91:7777-7781, 1994

17. Blondel,O, Bell,GI, Moody,M, Miller,RJ, Gibbons,SJ: Creation of an inositol 1,4,5-trisphosphate-sensitive Ca2+ store in secretory granules of insulin-producing cells. *J Biol Chem* 269:27167-27170, 1994
18. Ehrlich,BE, Kaftan,E, Bezprozvannaya,S, Bezprozvanny,I: The pharmacology of intracellular Ca(2+)-release channels. *Trends Pharmacol Sci* 15:145-149, 1994
19. Mitchell,KJ, Pinton,P, Varadi,A, Tacchetti,C, Ainscow,EK, Pozzan,T, Rizzuto,R, Rutter,GA: Dense core secretory vesicles revealed as a dynamic Ca(2+) store in neuroendocrine cells with a vesicle-associated membrane protein aequorin chimaera. *J Cell Biol* 155:41-51, 2001
20. Mitchell,KJ, Lai,FA, Rutter,GA: Ryanodine receptor type I and nicotinic acid adenine dinucleotide phosphate receptors mediate Ca2+ release from insulin-containing vesicles in living pancreatic beta-cells (MIN6). *J Biol Chem* 278:11057-11064, 2003
21. Varadi,A, Rutter,GA: Dynamic imaging of endoplasmic reticulum Ca2+ concentration in insulin-secreting MIN6 Cells using recombinant targeted cameleons: roles of sarco(endo)plasmic reticulum Ca2+-ATPase (SERCA)-2 and ryanodine receptors. *Diabetes* 51 Suppl 1:S190-S201, 2002
22. Hao,M, Head,WS, Gunawardana,SC, Hasty,AH, Piston,DW: Direct effect of cholesterol on insulin secretion: a novel mechanism for pancreatic beta-cell dysfunction. *Diabetes* 56:2328-2338, 2007
23. Bonfleur,ML, Vanzela,EC, Ribeiro,RA, de Gabriel,DG, de Franca Carvalho,CP, Collares-Buzato,CB, Carneiro,EM, Boschero,AC, de Oliveira,HC: Primary hypercholesterolaemia impairs glucose homeostasis and insulin secretion in low-density lipoprotein receptor knockout mice independently of high-fat diet and obesity. *Biochim Biophys Acta* 1801:183-190, 2010
24. Brunham,LR, Kruit,JK, Pape,TD, Timmins,JM, Reuwer,AQ, Vasanji,Z, Marsh,BJ, Rodrigues,B, Johnson,JD, Parks,JS, Verchere,CB, Hayden,MR: Beta-cell ABCA1 influences insulin secretion, glucose homeostasis and response to thiazolidinedione treatment. *Nat Med* 13:340-347, 2007
25. Gerin,I, Dolinsky,VW, Shackman,JG, Kennedy,RT, Chiang,SH, Burant,CF, Steffensen,KR, Gustafsson,JA, Macdougald,OA: LXRbeta is required for adipocyte growth, glucose homeostasis, and beta cell function. *J Biol Chem* 280:23024-23031, 2005
26. Ishikawa,M, Iwasaki,Y, Yatoh,S, Kato,T, Kumadaki,S, Inoue,N, Yamamoto,T, Matsuzaka,T, Nakagawa,Y, Yahagi,N, Kobayashi,K, Takahashi,A, Yamada,N, Shimano,H: Cholesterol accumulation and diabetes in pancreatic beta-cell-specific SREBP-2 transgenic mice: a new model for lipotoxicity. *J Lipid Res* 49:2524-2534, 2008
27. Hao,M, Bogan,JS: Cholesterol regulates glucose-stimulated insulin secretion through phosphatidylinositol 4,5-bisphosphate. *J Biol Chem* 284:29489-29498, 2009
28. Xia,F, Gao,X, Kwan,E, Lam,PP, Chan,L, Sy,K, Sheu,L, Wheeler,MB, Gaisano,HY, Tsushima,RG: Disruption of pancreatic beta-cell lipid rafts modifies Kv2.1 channel gating and insulin exocytosis. *J Biol Chem* 279:24685-24691, 2004
29. Rog,T, Pasenkiewicz-Gierula,M: Effects of epicholesterol on the phosphatidylcholine bilayer: a molecular simulation study. *Biophys J* 84:1818-1826, 2003
30. Colell,A, Garcia-Ruiz,C, Lluis,JM, Coll,O, Mari,M, Fernandez-Checa,JC: Cholesterol impairs the adenine nucleotide translocator-mediated mitochondrial permeability transition through altered membrane fluidity. *J Biol Chem* 278:33928-33935, 2003

31. Lundbaek,JA, Birn,P, Girshman,J, Hansen,AJ, Andersen,OS: Membrane stiffness and channel function. *Biochemistry* 35:3825-3830, 1996
32. Li,Y, Ge,M, Ciani,L, Kuriakose,G, Westover,EJ, Dura,M, Covey,DF, Freed,JH, Maxfield,FR, Lytton,J, Tabas,I: Enrichment of endoplasmic reticulum with cholesterol inhibits sarcoplasmic-endoplasmic reticulum calcium ATPase-2b activity in parallel with increased order of membrane lipids: implications for depletion of endoplasmic reticulum calcium stores and apoptosis in cholesterol-loaded macrophages. *J Biol Chem* 279:37030-37039, 2004
33. Romanenko,VG, Rothblat,GH, Levitan,I: Sensitivity of volume-regulated anion current to cholesterol structural analogues. *J Gen Physiol* 123:77-87, 2004
34. Levitan,I: Cholesterol and Kir channels. *IUBMB Life* 61:781-790, 2009
35. Epshtein,Y, Chopra,AP, Rosenhouse-Dantsker,A, Kowalsky,GB, Logothetis,DE, Levitan,I: Identification of a C-terminus domain critical for the sensitivity of Kir2.1 to cholesterol. *Proc Natl Acad Sci U S A* 106:8055-8060, 2009
36. Barrantes,FJ: Cholesterol effects on nicotinic acetylcholine receptor. *J Neurochem* 103 Suppl 1:72-80, 2007
37. Fantini,J, Barrantes,FJ: Sphingolipid/cholesterol regulation of neurotransmitter receptor conformation and function. *Biochim Biophys Acta* 1788:2345-2361, 2009
38. Levitan,I: Cholesterol and Kir channels. *IUBMB Life* 61:781-790, 2009
39. Suh,BC, Hille,B: PIP2 is a necessary cofactor for ion channel function: how and why? *Annu Rev Biophys* 37:175-195, 2008
40. Lin,CW, Yan,F, Shimamura,S, Barg,S, Shyng,SL: Membrane phosphoinositides control insulin secretion through their effects on ATP-sensitive K+ channel activity. *Diabetes* 54:2852-2858, 2005
41. Tong,J, Nguyen,L, Vidal,A, Simon,SA, Skene,JH, McIntosh,TJ: Role of GAP-43 in sequestering phosphatidylinositol 4,5-bisphosphate to Raft bilayers. *Biophys J* 94:125-133, 2008
42. Epand,RM: Proteins and cholesterol-rich domains. *Biochim Biophys Acta* 1778:1576-1582, 2008
43. Bae,YS, Lee,TG, Park,JC, Hur,JH, Kim,Y, Heo,K, Kwak,JY, Suh,PG, Ryu,SH: Identification of a compound that directly stimulates phospholipase C activity. *Mol Pharmacol* 63:1043-1050, 2003